

**Characterization of the processivity of the fast fungal kinesin,
NKin, from *Neurospora crassa*, on the level of single molecules**

Vom dem Fachbereich Chemie
der Universität Hannover

zur Erlangung des Grades eines
Doktors der Naturwissenschaften
Dr.rer.nat.
genehmigte Dissertation
von

Dipl. Biochem. Stefan Lakämper
geboren am 02.02.1974, in Gütersloh

2003

Referent: Prof. Dr. Dietmar Manstein
1. Koreferent: Prof. Dr. Manfred Schliwa
2. Koreferent: Prof. Dr. Edgar Meyhöfer

Tag der Promotion: 12. Dezember 2003

Abstract

Molecular motors generate directed motion on all levels of organization in living organisms. They transduce chemical energy from binding and hydrolysis of ATP to mechanical work and produce movement along protein filaments. The dimeric motor kinesin is responsible for driving long range anterograde transport of vesicles and small particles along microtubules in the cell. The most prominent adaptation to this cellular function is the ability of single kinesin molecules to move for μm -long distances along the microtubule, taking hundreds of 8 nm-steps while producing forces of $\sim 5\text{pN}$. The chemo-mechanical processes underlying such processive movement have been studied extensively in animal conventional kinesins. The description and isolation of the fungal conventional kinesins, NKin from *Neurospora crassa*, which moves considerably faster than its animal counterparts, has sparked intensive investigations aiming at the dissection of this fast movement. As the non-processive motor myosin generates comparably fast movement, it was of crucial importance to resolve whether fast NKin movement is processive or non-processive. While several reports supported that NKin is processive, it was necessary to confirm these findings with independent, direct methods. Furthermore, unusual structural features of the neck domain of NKin suggested unique opportunities to compare mechanisms possibly regulating processive movement.

Using TIRF-microscopy, the processive movement of single fluorescently labeled NKin motors was confirmed by direct evidence. Furthermore, a quantitative comparison of the processive movement revealed that NKin is able to move twice as processive as human kinesin (HKin) while maintaining high gliding speeds. An electrostatic interaction between the negatively charged flexible C-terminus of tubulin (E-hook) and the positively charged neck of conventional kinesin is implicated in maintaining highly processive movement of conventional kinesins. Removing the E-hook by partial proteolysis allowed to reveal that the E-hook not only reduces the number of steps NKin can take during processive runs, but also the speed of NKin during processive movement. However, the unusual properties of the neck domain of NKin, above all the reduced charge as compared to animal kinesins, suggest additional mechanisms determining processivity. Results from single molecule trapping measurements presented here rule out an influence of the E-hook on the strong binding state of NKin, which might have explained effects on processivity and speed.

In a short mutational study aimed at dissecting the increased speed of NKin motors, residues in the neck-linker of HKin were substituted by lysines strongly conserved at homologous positions in fast fungal kinesins. Initial gliding assays of these mutant motors, although highly preliminary, show increased gliding speeds.

Keywords: kinesin; processivity; single molecule assay

Zusammenfassung

Gerichtete Bewegung wird auf allen Ebenen zellulärer Organisation durch Motormoleküle erzeugt. Indem sie ATP binden und nachfolgend hydrolysieren, wandeln diese Proteine chemische Energie in mechanische Arbeit um und bewerkstelligen so Fortbewegung und Transportprozesse entlang von Strukturproteinen. Der dimerische Motor Kinesin ist für den intrazellulären, anterograden Transport von Vesikeln und kleinen Protein-Partikeln entlang von Mikrotubuli verantwortlich. Eine hervorstechende Anpassung an diese zelluläre Aufgabe ist die Fähigkeit einzelner Motoren, sich mehrere μm entlang des Microtubulus zu bewegen, indem mehrere hundert, 8 nm große Schritte ausgeführt werden während substantielle Kräfte von ~ 5 pN ausgeübt werden können. Die Prozesse, die die Grundlage dieser prozessiven Bewegung bilden, sind ausführlich an konventionellen tierischen Kinesinen untersucht worden. Die Beschreibung und Isolation eines schnellen Pilz-Kinesins, NKin aus dem rosa Brotschimmel *Neurospora crassa*, hat intensive Forschung angeregt, die darauf zielt, die Erzeugung der schnelle Bewegung dieser Motoren zu verstehen. Da der nicht-prozessive Motor Myosin ähnlich schnelle Bewegung von Aktin-Filamenten erzeugen kann, war es von überragender Bedeutung, zu ermitteln, ob sich NKin prozessiv entlang von Mikrotubuli bewegen kann. Obschon Hinweise auf Prozessivität von NKin veröffentlicht wurden, war es notwendig, diese mit unabhängigen direkten Methoden zu bestätigen. Weiterhin legten ungewöhnliche Eigenschaften der Hals-Domäne einzigartige Möglichkeiten nahe, Prozesse zu untersuchen, die prozessive Bewegung regulieren könnten.

Durch Verwendung TIRF-Mikroskopie konnte die prozessive Bewegung von einzelnen, fluoreszenzmarkierten NKin Molekülen eindeutig bestätigt werden. Weiterhin konnte durch einen direkten Vergleich gezeigt werden, daß NKin in der Lage ist, unter Beibehaltung der hohen Gleitgeschwindigkeit, doppelt so viele Schritte wie humanes Kinesin (HKin) auszuführen. Die prozessive Bewegung tierischer Kinesine scheint durch eine Interaktion zwischen dem negativ geladenen C-Terminus (E-hook) der Tubulin-Monomere des Mikrotubulus' und dem positiv geladenen Hals bestimmt zu werden. Teilweiser enzymatischer Verdau des Tubulins erlaubte es, den E-hook zu entfernen und so zu zeigen, daß der E-hook nicht nur die Prozessivität sondern auch maßgeblich die Geschwindigkeit der prozessiven Bewegung von NKin beeinflusst. Die ungewöhnlichen Eigenschaften, vor allem die in Vergleich zu HKin stark reduzierte Ladung in der Hals-Domäne von NKin, deuten darauf hin, daß zusätzliche Mechanismen Prozessivität und Geschwindigkeit von NKin beeinflussen. Resultate von Kraftmessungen am Eizelmolekül, schließen aus, daß der E-hook einen Einfluß auf die starke Bindung des Kopfes an den Mikrotubulus hat.

In einer kurze Studie, die darauf abzielte, die erhöhte Gleitgeschwindigkeit von NKin zu untersuchen, wurden Aminosäuren im Neck-Linker von HKin durch Lysin-Reste ersetzt, die in Pilz-Kinesinen stark konserviert sind. Obgleich die Ergebnisse nur sehr vorläufige Schlussfolgerungen erlauben, zeigen erste Gleitassays eine erhöhte Gleitgeschwindigkeit.

Schlagerworte: Kinesin, Prozessivität; Einzelmolekülassays

Table of contents

Abstract	1
Zusammenfassung	2
Table of contents	3
Abbreviations	5
Chapter I: Introduction	6
Directed Motion is a criteria of life	6
Directed Motion is generated by motor molecules	6
The Eukaryotic Cytoskeleton	7
Linear Motor Molecules of the Eukaryotic Cytoskeleton	7
Kinesin motors	8
Conventional Kinesin	8
Processivity of kinesin	9
Hand over hand-model of movement and the concept of alternating head catalysis	10
Strain communicates nucleotide states between the two heads	12
Crystal structure of dimeric kinesin	13
Processivity requires two heads – KIF1A discussion	15
Fast fungal kinesins	16
Specific questions	16
Chapter II : Comparison of the processive movement of HKin and NKin in single molecule fluorescence assays	18
Introduction	18
RESULTS	20
Multiple motor gliding assays	20
Single molecule gliding assays	20
Single molecule fluorescence assays	22
DISCUSSION	27
In vitro gliding assays	27
TIRF microscopy-based processivity assays	29
Physiological basis of fast, processive movement	32
Chapter III: The E-hook of the microtubule strongly influences processivity and speed of kinesin motors	36
Introduction	36
Results	41
Partial Digestion of Microtubules with subtilisin removes the E-hook of tubulin	41
Removal of the E-hook leads to reduced processivity and speed of NK433cys	42
Digested microtubules are transported at lower speeds in multiple motor gliding assays	44
ATPase measurements of dimeric NKin motors on dMT show decreased k_{cat} -values	45
Dimeric NK433cys binds at a reduced rate to digested microtubules	46
The E-hook does neither affect ATPase nor $k_{bi,ADP}$ of monomeric construct NK343cys.	50
Discussion	51
Chapter IV: NKin generates 5 pN force on both digested and undigested microtubules	56
Introduction	56
Results	58
Cloning and Purification of motors	58
Laser trapping nanometry	59
Biotinylation of HKin and Nkin motors.	60
Bead assays	60
HKin generates ~5 pN force on undigested microtubules	63

NKin generates ~5 pN force on undigested microtubules.	64
NKin motors generate ~5 pN on digested microtubules.	65
Discussion	68
<i>Chapter V: Do conserved Lysine residues in the Neck-linker region of NKin confer fast motility to HKin? – a short analysis of point mutants</i>	71
Introduction	71
Results	73
Discussion	75
<i>Summary and outlook</i>	77
<i>Appendices</i>	79
Methods	79
Molecular biology methods	79
Biochemical Methods	88
Protein purifications	90
Instrumentation	98
Biophysical Methods	99
List of Figures	105
List of Tables	106
Curriculum vitae	107
Abstracts and Publications	109
Literature	110
<i>Acknowledgements</i>	115

Abbreviations

k_B	Boltzmanns constants
ADP	Adenosindiphosphate
ATP	Adenosintriphosphate
BME	B-mercaptoethanol
bp	Base pair
AA	Amino acid
MT	microtubule
dMT	Digested microtubule
BSA	Bovine serum albumin
DMSO	Dimethylsulfoxide
mant-ADP	N-mathylanthranoyl-ADP
dMT	(subtilisin) digested Microtubule
DNA	Desoyribonucleic acid
DTT	Di-thiothreitol
EDTA	Ethylene-diamine-tetra-acetic acid
EGTA	Bis-(aminoethyl) glycoleter-N,N,N'N'.tetra-acetate
EPR	Electron paramagnetic resonance
FRET	Fluorescence resonant energy transfer
GndHCl	Guanidinium-Hydrochloride
HEPES	N-(2-Hydroxyethyl)piperazine-N'-(2-ethansulfonic acid)
KCl	Potassium Chloride
kDa	kiloDalton
KHC	Kinesin heavy chain
KLC	Kinesin light chain
KLP	kinesin like protein
MES	2-(N-Morpholino)-ethansulfonic acid
MgCl ₂	Magnesium Chloride
mRNA	messenger RNA
MT	Microtubule
NaCl	Sodium Chloride
PCR	Polymerase chain reaction
Pe	Pefabloc
P _i	Anorganic phosphate
Pi	Protease inhibitor mix
PIPES	Piperazine-N, N'-bis(2-ethanesulfonic acid)
RNA	Ribonucleic acid
TMR	Tetramethylrhodamine
K	Kelvin

Chapter I: Introduction

Directed Motion is a criteria of life

One of the defining criteria of life is directed motion, be it either motion as a whole organism or directed transport processes inside an individual cell, the minimal living unit of every organism. Directed motion appears on all levels of evolution and size, from small single cell organisms, for example an amoeba, to highly organized multi-cellular organisms, like us humans or a giant sequoia tree. Not only does motility appear on all scales it also serves a multitude of different crucial functions for the cell: uptake and transport of nutrients in vesicles as well as chromosome segregation and cell division, the amoeboid movement of single cell organisms or macrophages - immune-defense cells in the human body - as well as the coordinated movement of billions of molecules in the muscles, that are necessary to let your eyes follow this text or simply to play soccer. How is all this motion generated?

Directed Motion is generated by motor molecules

In all organisms directed motion is generated by the so-called motor proteins. The defining feature of motor proteins is that they transduce chemical energy from binding and subsequent hydrolysis of ATP into mechanical work. ATP is an energy-rich nucleotide that serves as intermediate storage unit for free (i.e. usable) energy in the cell ($\Delta G' = -60\text{kJ/mol}$ ATP). While vastly diverse in structure and function, motor proteins are divided in two mayor groups, rotary motors and linear motors. Rotary motors are inserted in the membranes of cells and organelles. They confer rotary motion and regenerate ATP by dissipation of ion gradients (e.g. the F_0F_1 -ATPase of mitochondria). In the reversible process, however, the F_0 -portion of the F_0F_1 -ATPase generates rotary motion by hydrolysing ATP (Kinosita *et al.*, 1998; Masaike *et al.*, 2002; Noji *et al.*, 1997). On the contrary, linear motors are force generating enzymes that produce motility relative to the protein-filaments of eukaryotic cells, the so-called cytoskeleton. Although prokaryotic organisms express proteins that are homologous to the cytoskeletal components of eukaryotes and that clearly take on similar functions (Moller-Jensen *et al.*, 2002; van den Ent *et al.*, 1999), so far no prokaryotic linear motor could be identified (Vale, R. D., 2003). Strictly speaking, helicases, enzymes that unwind and separate DNA strands, and to a certain degree RNA- and DNA polymerases as well as the ribosome

should be included in the group of linear motors as they exercise considerably amount of work along the DNA which they unwind, separate, replicate and translate (Lohman *et al.*, 1998). However, they do not generate motility and could perhaps be termed “machines” rather than linear motors. The following chapter will give a short introduction to the cytoskeleton and its linear motors

The Eukaryotic Cytoskeleton

The cytoskeleton of eukaryotic cells is a highly dynamic structural network of three protein polymers – actin filaments, intermediate filaments and microtubuli or microtubules - and a vast number of accessory proteins that regulate and direct the networks activity (Vale, R., 2001). Actin filaments and microtubuli are polar structures with a plus (+) and a minus (-) end. The plus-end is defined as the fast-growing, more dynamic end. While the minus-end of microtubules is anchored at the microtubule-organizing center (MTOC) close to the nucleus, the plus-ends grow towards the periphery of the cell. This polar structure is well suited for long-range transport. Short-range transport processes near the cell periphery are predominantly actin-dependent. Motor proteins can be described as one group of the accessory proteins of the cytoskeleton (Vale, R., 2001). So far more than 100 different motor molecules have been identified with the help of genetic approaches within the cell (Miki *et al.*, 2003; Vale, R. D., 2003; Vale, R. D. and Milligan, 2000). Whereas for intermediate filaments no motor molecule has been identified, there are three families of motor proteins that interact with actin filaments or microtubules. Myosin-motors interact with actin filaments, dyneins and kinesin with the microtubules.

Linear Motor Molecules of the Eukaryotic Cytoskeleton

The motor molecule Myosin II, which together with its track, the actin filament, forms the major component of skeletal muscle, is the longest and best studied motor molecule (since 1864, Kühne). It is the founding member of the super-family of myosins. By now this family comprises 14 classes of myosin, the members of which all share a myosin-defining head domain (Sellers, 2000). Except Myosin VI, all myosins studied so far are plus-end directed motors (Inoue, A. *et al.*, 2002; O'Connell and Mooseker, 2003; Wells *et al.*, 1999). The founding member of the super-family of dyneins, inner arm flagellar dynein, was first

described and isolated in the 1960ies. Until recently - before the widespread use of molecular biology techniques - detailed biophysical research on dyneins in general was especially difficult due to its large overall mass (550kd or higher) and diverse subunit composition. However, all dyneins described so far are minus-end directed motors implicated in retrograde transport (towards the nucleus) (Schnapp and Reese, 1989; Vale, R. D., 2003). In stark contrast to dynein, the last motor molecule to be isolated, the microtubule-based motor kinesin, is characterized by a remarkably compact design and relatively simple subunit organization (Brady, 1985; Vale, R. D. *et al.*, 1985). This has helped to gain insight in how motor molecules are able to generate mechanical work in the relatively short period of time since its first description. As the subject of this work is a comparison of different kinesin motors the next paragraphs will give a brief overview of the current knowledge on kinesin.

Kinesin motors

Kinesins are ubiquitous microtubule-based motor molecules of eukaryotic cells. They are involved in numerous cellular processes including vesicle and organelle transport, chromosome segregation and cell signaling (Howard, 1997; Vale, R. D., 2003). The founding member of the kinesin super-family, now referred to as conventional kinesin, has been isolated from various animal tissues (Brady, 1985; Vale, R. D. *et al.*, 1985). Using genetic approaches, soon other kinesin related proteins (KRPs) could be identified. By now about 150 members have been described. They all share a homologous motor domain, that carries the microtubule binding and ATPase activity. These motors are grouped into three types based on where the motor domain resides: N-terminal, internal motors, and C-terminal motors. These types have been re-grouped into 14 phylogenetic families (Miki *et al.*, 2001). Surprisingly, both plus- and minus-end directed motility of kinesin motors was described. Interestingly, all described minus-end directed motors are C-terminal motors, whereas N-terminal kinesin motors show plus-end directed motility (Endow, 1999; Wade and Kozielski, 2000; Woehlke and Schliwa, 2000). Conventional animal kinesins are structurally and functionally the best-studied member of these motor molecules.

Conventional Kinesin

Conventional kinesins, at least those of animal species, are tetrameric proteins consisting of two identical heavy (120 kD) and two identical light chains (64 kD, (Bloom *et al.*, 1988; Scholey *et al.*, 1989). Each heavy chain possesses an N-terminal globular head, about 7 x 5 x 5nm in size, carrying microtubule-binding and ATPase-activity. The head is connected to the alpha-helical neck (Kozielski *et al.*, 1997b) via a short (~15 AA) domain, termed neck-linker. The neck domains of the heavy chains form a two-stranded coiled-coil to dimerize both chains (de Cuevas *et al.*, 1992; Tripet *et al.*, 1997). Further C-terminal the heavy chains continue in a flexible hinge region followed by a stalk and a globular tail domain (Yang *et al.*, 1989). The stalk consists of two coiled-coils which are interrupted by a second flexible hinge region. The light chains of conventional kinesin bind to the tail region (Hackney, 1992; Hirokawa *et al.*, 1989) and are thought to be involved in anchoring kinesin to vesicular cargoes and in regulating the activity of the kinesin molecule by backfolding on the motor domain (Hackney and Stock, 2000; Jiang, M. Y. and Sheetz, 1995; Seiler *et al.*, 2000; Verhey *et al.*, 1998; Verhey and Rapoport, 2001). The light chains are not required for *in vitro* motility, but are necessary for *in vivo* function (Fig. I-1). The most prominent functional adaptation to cellular function of kinesin is the ability to move processively

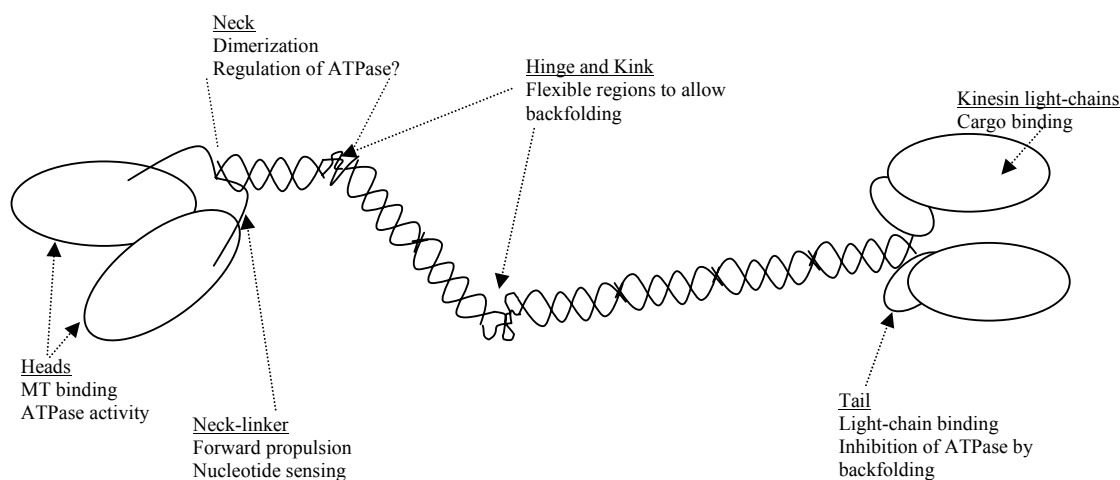


Figure I-1: Schematic domain organization of conventional kinesins

Processivity of kinesin

Conventional kinesins are microtubule based, plus-end directed motor molecules that use ATP binding and hydrolysis to drive the unidirectional transport of small vesicular organelles or particles (generally termed “cargo”) along microtubules towards the periphery

of the cell. These vesicles need to be transported over considerable, sometimes extreme distances – for example, axonal transport in nerve cells requires transport to up to meter-long distances - and against considerable resistance. Not only is the cytosol a highly viscous and crowded environment, the geometry of the cargoes only allows interaction of few or even single surface bound motor-proteins with the comparatively small cytoskeletal filaments. An adaptation to these stringent requirements is the ability of single conventional kinesin motors to move processively along the microtubule: it moves μm -long distances along the microtubule without detaching, taking hundreds of 8 nm steps per ATP molecule hydrolyzed (Hackney, 1995; Hua *et al.*, 1997; Schnitzer and Block, 1997). This remarkable ability has been first shown by single molecule gliding assays (Howard *et al.*, 1989) and was later confirmed by single molecule fluorescence assays and kinetic studies (Hackney, 1995; Vale, R. D. *et al.*, 1996). The step-sizes of individual kinesin motors was determined with nanometer-accuracy laser trapping interferometry using latex beads sparsely coated with kinesin motors (Block *et al.*, 1990). These measurements and earlier experiments using various independent approaches confirmed that during processive movement a single kinesin is able to generate up to 5-7 pN force before movement is stalled it detaches from the microtubule (Gittes *et al.*, 1996; Hunt *et al.*, 1994; Meyhofer and Howard, 1995). Therefore, the unidirectional long-distance transport against considerable loads is ensured by the high processivity of conventional kinesins. How does the motor achieve processive movement?

Hand over hand-model of movement and the concept of alternating head catalysis

The structure of dimeric conventional kinesins implies several mechanisms of how processive movement is achieved. The most straightforward model is the hand-over-hand model, initially proposed by Howard et al (Howard, 1996; Howard *et al.*, 1989): the rudimentary concept states that after the initial binding of one of the dimer's two heads to the microtubule, the motor's second head binds to the next available binding site on the same proto-filament of the microtubule (Ray *et al.*, 1993). When the leading head is strongly bound the lagging head dissociates and the cycle starts again. The affinities – and therefore binding and detachment - of the individual heads to the microtubule are predominantly determined by the nucleotide bound (Crevel, I. M. *et al.*, 1996; Romberg and Vale, 1993). The concept of the alternating catalysis (Gilbert *et al.*, 1998; Hackney, 1994a; Ma and Taylor, 1997) of the two heads describes the motor's ability to couple stepping cycles and therefore movement to the

binding and hydrolysis of ATP (Schief and Howard, 2001): While details of intermediate steps are subject of discussion, some key elements of kinesins chemo-mechanical cycle are generally agreed upon. Kinesin's head domain has the lowest affinity to the microtubule when ADP is present in the nucleotide binding pocket (Fig I-2: state 0, (Hackney, 1992; Romberg and Vale, 1993). Upon collision and binding to the microtubule the ADP of this head is rapidly released to form a nucleotide free kinesin-microtubule complex (Fig I-2 (1)). This so-called "rigor" state (in analogy to nucleotide-free myosin) has the highest affinity to microtubules (Hackney, 1992). The bound head itself is called the lagging, or rear head, in contrast to the free, leading head (also called front or tethered head). In this state conformational restrictions prevent the leading head, which still contains ADP, from binding to next available binding site (Crevel, I. *et al.*, 1999; Hackney, 2002; Hirose *et al.*, 1999; Ma and Taylor, 1997). Only after binding of ATP to the rear head (Fig I-2 (2)), can the leading head bind to the microtubule (Fig I-2 (4)) and release its ADP to form the strong-binding rigor state (Fig I-2 (5)). It is unclear, however, whether the binding of the leading head requires ATP binding alone or if the hydrolysis of ATP to ADP and Pi is necessary. In the resulting state, in which both heads are bound to the microtubule, the connection between the two heads is subjected to considerable strain (Fig I-2 (5)). Regardless of when exactly the hydrolysis of ATP to ADP and Pi in the rear head occurs, the detachment of the rear head ultimately results from the low affinity of the ADP- or the ADP- Pi-state of the rear head as compared to the leading head in the rigor state. The rear head is then propelled towards the subsequent binding site to allow the cycle to start again. Keeping the ATPase-cycles of the two heads out of phase in such a fashion requires the heads to communicate their respective nucleotide state to each other.

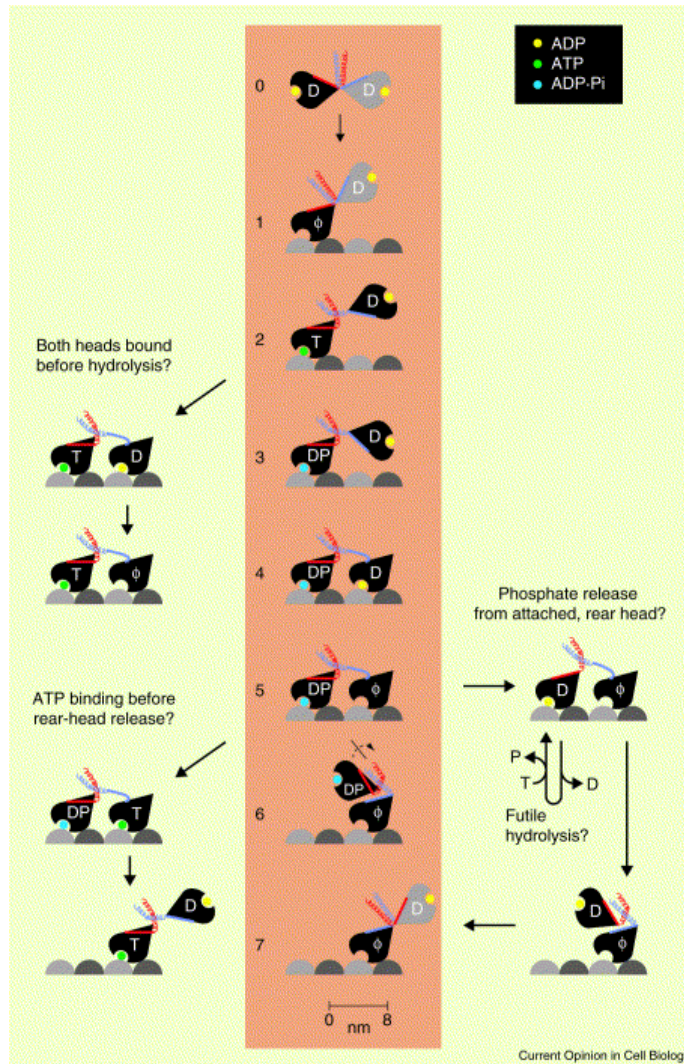


Figure I-2: Possible pathway of processive movement of conventional kinesin.

This panel schematically summarizes the nucleotide dependent conformational changes in the hand-over-hand model of kinesin movement as proposed by Schief and Howard, 2001. The favored model is highlighted in grey, alternate pathways are given in the side panels. For detailed description and discussion see text.

Strain communicates nucleotide states between the two heads

How the communication between the two heads is achieved is not yet completely understood. The crucial intermediate in this communication seems to be the state, in which the two heads of kinesin are bound in different nucleotide states. In this state the linking structures between the heads are strained (Kozielski *et al.*, 1997a; Mogilner *et al.*, 2001). Several lines of evidence suggest, that the rearward strain on the leading head prevents the

binding of ATP, trapping the forward head in the strongly bound rigor state (Hackney *et al.*, 2003; Rosenfeld *et al.*, 2001; Rosenfeld *et al.*, 2002). At the same time, the forward strain on the rear head accelerates the ATP-hydrolysis activity (Hancock and Howard, 1998; Hancock and Howard, 1999), thus accelerating dissociation of the rear head after strong binding of the leading head. Relieving the strain generated by the simultaneous binding of the two heads by increasing the length of the neck-linker severely alters the strain-mediated communication between the two heads, resulting in significantly reduced processivity as measured with biochemical methods (Hackney *et al.*, 2003). After hydrolyzing ATP the rearward head detaches and the leading head rapidly binds ATP. Binding of ATP to the leading head leads to a rapid immobilization of the otherwise highly mobile and flexible neck-linker to the motor core (Naber *et al.*, 2003; Rice *et al.*, 2003; Rice *et al.*, 1999; Sindelar *et al.*, 2002). This conformational change of the neck linker of the leading head propels the rearward head towards the subsequent binding site. The nucleotide dependent detachment and attachment of the neck-linker also provides a framework for understanding the crystal structure of dimeric rat kinesin (Kozielski *et al.*, 1997b).

Crystal structure of dimeric kinesin

The solution of the dimeric kinesin crystal structure (Fig. I-3 (Kozielski *et al.*, 1997b)) provided valuable information concerning the dimerization and conformation of kinesin dimers. Simultaneous docking the kinesin heads simultaneously to adjacent binding sites, however, is impossible, unless either the coiled-coil or the neck-linker conformations is melted. Otherwise, docking could only be achieved when disregarding information on kinesins microtubule-binding site (Woehlke *et al.*, 1997) or allowing attachment to neighboring proto-filaments as ruled out by Ray *et al.*, 1993 (Ray *et al.*, 1993). Cross-linking the coiled-coil of the neck revealed, that the coiled coil does not unwind during processive movement (Romberg *et al.*, 1998). Thus, the report on the dynamic zippering of the neck-linker provided an elegant explanation of how the two heads of kinesin can be docked simultaneously to the microtubule (Mogilner *et al.*, 2001; Rice *et al.*, 1999). Furthermore the role of the neck-linker could be confirmed by single molecule experiments: reversible cross-linking of the neck-linker to the head abolished processive movement (Mogilner *et al.*, 2001; Tomishige and Vale, 2000).

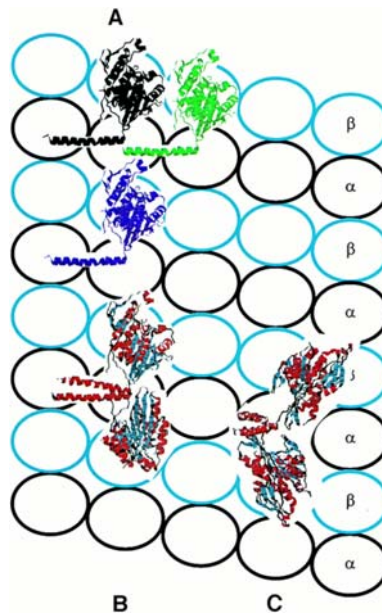


Figure I-3: Docking the crystal structure of dimeric kinesin to the microtubule-lattice

The symmetry and spacing of the two heads in the crystal structure of dimeric rat kinesin does not allow for straightforward simultaneous binding of the two heads to the microtubules as proposed in the hand-over-hand-model. Three possible models for simultaneous docking of the two heads are given: (A) Melting of the neck coiled-coil allows binding to the next binding site on the same or a neighboring protofilament. (B) detachment of the short ~10 AA neck-linker allows the motor to soace the distance to the next biding site on the same protofilament. (C) Dimers bind to different protofilaments without major conformational rearrangements. Figure adapted from Kozielski *et al.*, 1997)

Still, the symmetry of the crystal structure of dimeric kinesin poses more implications for models of kinesin motility: the motors symmetry of 120° and the orientation of the heads does not allows a purely symmetric hand-over-hand model. This structural contradiction to data that support the general hand-over-hand-model can be explained by two rivaling hypotheses: 1.) One hypothesis resolves this problem by modifying the so-far described “symmetric” hand-over-hand model to an asymmetric hand over hand model. This model implies important biophysical constraints on the stepping behavior of the motor: motors challenged by forces perpendicular to the direction of motility should display an asymmetry in stepping kinetics. Evidence for such a behavior has been gained using 2D laser trapping instruments (Block *et al.*, 2003). 2.) The second model introduces a different stepping model, the so-called “inchworm”-model. It suggests that the leading head will remain the leading head throughout a processive run. The motor advance by dissociation of the leading head, which attaches then to the binding site two tubulin dimers further to the plus end of the microtubule. Thus, intermediately the motor has to span at least 16 nm distance between the

tow heads. The lagging head then dissociates, but instead of passing the leading head and binding to the next binding site it attaches to the binding site previously occupied by the leading head. This model of motion implies that the cargo attached to kinesin does not rotate. Although highly controversial, reports supporting this view have been published (Hua *et al.*, 2002). Single molecule fluorescence assays, similar to assays for Myosin V, which unequivocally proved a hand-hand stepping mechanism for this actin based processive motor (Yildiz *et al.*, 2003), will allow to resolve this question.

Processivity requires two heads – KIF1A discussion

All the models for processive movement involve two heads. Furthermore, specific studies have confirmed that processive movement as described above requires two motor domains joined by more or less stable coiled-coil interactions (Hancock and Howard, 1998). Reports of single monomeric kinesin related proteins (MmKif1A) and myosins moving processively (Inoue, A. *et al.*, 2002; Okada and Hirokawa, 1999; Okada and Hirokawa, 2000) probably reflect interesting mechanisms of interactions between motor heads and the filament rather than explaining processive movement relevant in the cellular context. Furthermore, native full length constructs of a homolog motor (Unc104) reportedly formed transient coiled-coil interactions at high local concentrations. The local concentrations are due to lipid rafts, which contain phospho-inositol-phosphates specifically recognized by the PH domains in the tail domain of the Unc104 motor studied. Thus, Unc104 and Kif1A are likely to form processive dimers *in vivo* (Klopfenstein *et al.*, 2002a; Klopfenstein *et al.*, 2002b). Single molecule fluorescence studies using stable dimeric chimera of Unc104 and HKin further supported this conclusion (Tomishige *et al.*, 2002). In all, the processive movement of conventional and probably most unconventional kinesins requires the two heads to be stably linked by coiled coil interactions of the neck-region of the heavy chain. The use of variant kinesins with uniquely different properties from different natural sources provides a valuable source of information to further dissect the mechanisms involved in the generation for processive movement.

Fast fungal kinesins

Kinesin motors homologous to conventional animal kinesin have first been isolated from *Neurospora crassa* (NKin), and subsequently other fungi (Grummt *et al.*, 1998a; Lehmler *et al.*, 1997; Schoch *et al.*, 2003; Steinberg and Schliwa, 1995; Steinberg and Schliwa, 1996). These fungal kinesin can be sub-grouped into the family of fungal conventional kinesins, because - compared to animal conventional kinesins - they show high sequence identity/similarity and the same overall domain organization (Kirchner *et al.*, 1999b). Despite the similarities, NKin displays distinct structural and functional properties: 1.) NKin shows unusually high gliding speeds in multiple molecules gliding assays (Steinberg and Schliwa, 1995). The crystal structure of the head of NKin shows a considerably widened ATP-binding pocket, which might be one of the reasons for accelerated motor activity (Song *et al.*, 2001). 2.) So far it has not been possible to isolate kinesin light chains, indicating interesting new mechanisms of cargo attachment (Seiler *et al.*, 2000; Steinberg and Schliwa, 1996; Verhey *et al.*, 2001). 3.) The neck-domain of NKin shows unique fungal specific sequence patterns. They lead to reduced coiled-coil forming propensities of the neck-domain (Kallipolitou *et al.*, 2001). Furthermore a tyrosine residue, strikingly conserved in fungal kinesins, inhibits motor activity and is crucial for dimerization of shortened constructs (Schafer *et al.*, 2003). Especially the latter characteristics – together with the high gliding speed of Nkin motors - sparked a row of interesting questions that were addressed in this work.

Specific questions

The highly unusual properties of the neck domain (Kallipolitou *et al.*, 2001) and the extremely fast gliding speed (Steinberg and Schliwa, 1996) of NKin led to several important questions: (i) It was necessary to unequivocally determine if NKin was capable of moving processively along a microtubule: high gliding speeds could also be explained by the interaction of many non processive motors, like in myosin. Although earlier reports indicated that NKin is capable of processive movement (Crevel, I. *et al.*, 1999; Kallipolitou *et al.*, 2001), processivity of NKin had to be confirmed using single molecule fluorescence assays. (ii) Furthermore, it was necessary to compare the extent of processivity to other kinesin motors, to determine if the NKin's increase in gliding speed is achieved by trading processivity. (iii) To determine if the processivity is influenced by the an interaction between the neck of the motor and the negatively charged E-hook of tubulin, as has been reported for

animal conventional kinesins, the processivity of NKin on digested microtubules was assayed using single molecule fluorescence, bulk biochemical measurements and single molecule force measurements. (iv) In an attempt to determine structural features that might confer NKins fast motility, a pair of strictly conserved lysine residues in the neck-linker region of fungal kinesins was genetically engineered in a human kinesin.

Chapter II : Comparison of the processive movement of HKin and NKin in single molecule fluorescence assays

Introduction

Conventional kinesin has received considerable attention as a model system for dissecting the molecular mechanism of motility. This interest in the kinesin system is to a large part due to the ability of single kinesin molecules to move processively micrometer-long distances along microtubules without detaching. Initial evidence for this remarkable ability came from *in vitro* microtubule gliding (Howard *et al.*, 1989) and bead assays (Block *et al.*, 1990). At low kinesin densities microtubule gliding movement characteristically differed from that at higher densities and was suggestive of movement driven by a single motor molecule: microtubules pivoted about a single nodal point and often moved several micrometers until the trailing end of the microtubule was reached. More importantly, the observed rates of attachment and detachment of moving microtubules (landing rate) as a function of the kinesin density confirmed that the microtubule gliding at low kinesin densities was indeed due to single kinesin molecules (Howard *et al.*, 1989). Additional support in favor of the processivity of single molecules came from laser trapping experiments showing that silica beads coated on average with less than one kinesin molecule also moved micrometer-long distances when placed on microtubules or axonemes (Block *et al.*, 1990). Moreover, later work showed that single conventional kinesin molecules are even capable of moving processively, albeit slower, when challenged by substantial elastic force up to 5 – 7 pN ((Hunt *et al.*, 1994; Kojima *et al.*, 1997; Meyhofer and Howard, 1995; Svoboda *et al.*, 1993; Visscher *et al.*, 1999))

One qualm of these processivity experiments was that the motors might preferentially aggregate when adsorbing onto glass or bead surfaces. This uncertainty was dispelled by directly recording the movement of single kinesin molecules. By using low-background total internal reflection fluorescence (TIRF) microscopy Vale *et al.* (1996) were able to observe single, fluorescently-labeled kinesin molecules while trans-locating along microtubules, and from the bleaching behavior they could deduce that the fluorescing spots indeed represented single, labeled kinesin molecules. Taken together, the evidence for conventional kinesin being a processive motor is overwhelming.

Recently, a fungal counterpart to conventional kinesin from animal cells has been isolated from the ascomycete *Neurospora crassa* ((Steinberg and Schliwa, 1995; Steinberg and Schliwa, 1996). Sequence comparison indicates that *Neurospora* kinesin (NKin) is a distant relative to conventional animal kinesins, consistent with the phylogenetic relation between fungi and animals. NKin shares the same overall molecular design plan with conventional kinesins and seems to have analogous cellular functions, despite the apparent lack of light chains. Surprisingly, however, NKin translocates microtubules in *in vitro* gliding assays more than 3-times faster than conventional animal kinesins (Steinberg and Schliwa, 1995; Steinberg and Schliwa, 1996). Because of the functional and sequence difference to conventional animal kinesins NKin offers unique opportunities to analyze the molecular mechanisms underlying the movement of kinesins by combining, for example, domains from fungal and animal kinesins (Grummt *et al.*, 1998a; Grummt *et al.*, 1998b; Henningsen and Schliwa, 1997). As a prerequisite for such studies it is critical to determine whether NKin is processive.

First experiments with NKin presented by Crevel *et al.* (1999) demonstrated a swiveling behavior of microtubules in gliding assays and runs of consecutive 8 nm steps in laser trapping experiments typical for the motile behavior of a processive kinesin. However, in contrast to *in vitro* assays with animal kinesins, the concentrations of NKin required for these motility assays were so high that based on the calculated surface density of motors multiple, not single, molecule interactions are to be expected. Furthermore, observations of Inoue *et al.* (Inoue, Y. *et al.*, 1997) also showed that multiple kinesins power beads in a stepwise fashion along microtubules. Therefore, despite the findings by Crevel *et al.* (Crevel, I. *et al.*, 1999), it is possible that NKin, like Ncd or Eg5, is not processive (Crevel, I. M. *et al.*, 1997; Foster and Gilbert, 2000). Alternatively, NKin might just adsorb poorly to glass surfaces or small latex beads. Therefore, an important control experiment was to determine whether NKin is indeed processive by using a method that does not depend upon the adsorption of the motor to the substrate.

Following the approach of Vale and Yanagida, we sought to directly track the movements of single motors to quantitatively determine the processivity of *Neurospora crassa* kinesin (Vale, R. D. *et al.*, 1996). Proteins were cloned and in part also purified by Dr. Athina Kallipolitou in the Institute for Cell Biology at the Ludwig-Maximilians-Universität, Munich, Germany, in the group of Dr. Günther Woehlke. She cloned a truncated *Neurospora* motor construct (NKin483), and, for comparative purposes, a human kinesin (HKin560) which consisted of the N-terminal 483 and 560 amino acid residues, respectively. Both motor

molecules were engineered to carry a reactive cysteine residue at the C-terminus (Kallipolitou *et al.*, 2001). Purified proteins were labeled with the fluorescent dye Cy3, using a monofunctional succinimidyl-ester that had been transformed to a maleimide-ester using PEM. To determine if NKin motors are processive, we first recorded the movement of single motor molecules Hkin motors in single molecule gliding assays and a low background total internal reflection fluorescence (TIRF) microscope, and subsequently compared their behavior to NKin motors under the same conditions. Our results not only show that NKin is capable of processive movement, but also demonstrate that Nkin483 is significantly more processive than Hkin560.

RESULTS

Multiple motor gliding assays

Multiple motor *in vitro* gliding assays of a wild-type mammalian kinesin (porcine kinesin) and wt-NKin using high motor densities showed gliding speeds of $0.60 \mu\text{m/s}$ ($\pm 0.07 \mu\text{m/s}$, $N = 24$) and $1.72 \mu\text{m/s}$ ($\pm 0.03 \mu\text{m/s}$, $N = 48$) respectively. All errors are stated as SEM. Truncated constructs of human (HKin560) *Neurospora* (NKin483) kinesin used for the single molecule fluorescence assays transported microtubules in multiple molecule gliding assays with the same velocities as wt-motors (HKin: $0.78 \pm 0.09 \mu\text{m/s}$, $N=101$, NKin: $1.95 \pm 0.05 \mu\text{m/s}$, $N=20$). NKin gliding velocities were susceptible to the ionic strength of the buffer solution; microtubule gliding speeds increased from about 1.40 ± 0.07 ($N=25$) to $2.43 \pm 0.07 \mu\text{m/s}$ ($N = 25$) in P12 without salt and BRB80 with additional 400 mM KCl, respectively. Microtubule gliding assays using more than 400 mM KCl in BRB80 showed no microtubule binding to glass surfaces coated with NKin.

Single molecule gliding assays

One strategy to demonstrate processive movement of single HKin and NKin molecules was to reduce the motor density in the gliding assays until the transport of microtubules by a single kinesin molecule could be observed (Howard *et al.*, 1989). Reduction of the HKin560 densities on the glass-surface to less than $500 \text{ molecules}/\mu\text{m}^2$ (calculation based on the assumption that all motor protein adsorbed in a functional manner) allowed observations of

events where short (2 - 5 μm long) microtubules bound to the surface and pivoted around a nodal point while being transported with wt-speed ($0.77 \mu\text{m}$, $\pm 0.03 \mu\text{m/s}$ $N=49$, Figure II-1a). The density of Nkin483 at which single molecule gliding events could be identified was calculated to be about $5000 \text{ molecules}/\mu\text{m}^2$, much higher than for Hkin560 (Figure II-1b). To address the possibility that the adsorption of NKin483 is impaired, we also attempted dilution experiments with two additional constructs that offer improved surface adsorption as compared to Nkin483: Full length NKin, and a NKin construct in which the C-terminal portion of the motor (amino acid residues 434 – 483) was exchanged for the slightly longer C-terminus of HKin560 (amino acid residues 430-560). We observed single molecule gliding experiments with both constructs, but the densities that were required to effectively observe events were basically identical to those reported for NKin483.

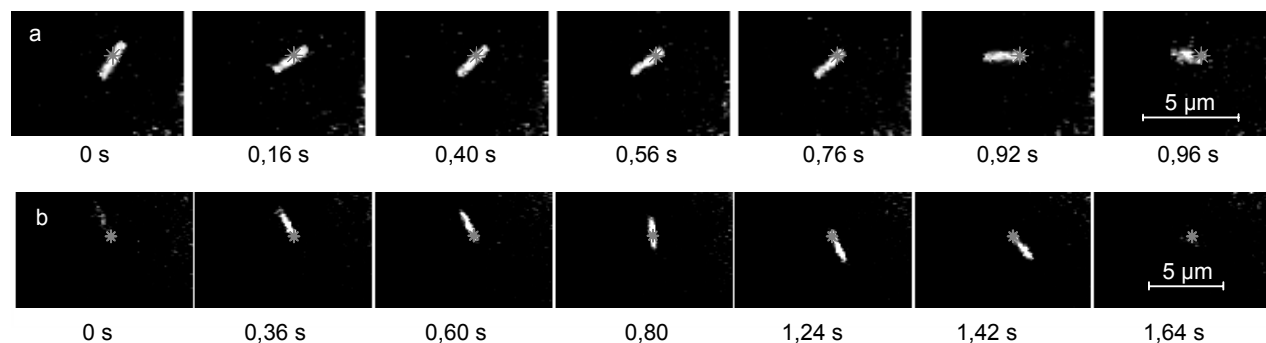


Fig. II-1: Single molecule gliding assays of Hkin and NKin

The panels show typical events for the truncated constructs of Hkin (a) and NKin (b). MT bound to the surface and were transported unidirectionally at wt-speed ($\sim 0.8 \mu\text{m/s}$ and $\sim 1.7 \mu\text{m/s}$, respectively) while pivoting around a single point. Calculated densities of truncated motors on the casein pre-treated glass surface were $500/\mu\text{m}^2$ and $5000/\mu\text{m}^2$ for Hkin and NKin, respectively. For animal conventional kinesin (porcine kinesin) we could detect such events at motor densities as low as $5/\mu\text{m}^2$.

Nonetheless, the observed motile behavior of individual NKin events was consistent with single motor events: microtubules pivoted about a single point, the rotation of the microtubule was random (diffusive) covering angular ranges up 45 degrees in one second, and microtubules moved with wildtype-speed relative to the nodal point ($2.31 \mu\text{m/s} \pm 0.07 \mu\text{m/s}$, $N=46$, BRB80 with additional 200mM KCl, Figure II-1b), suggesting that a single motor molecule is located at the nodal point. During most single motor events microtubules abruptly dissociated from the motor before the end of the microtubule was reached ($> 80\%$). Motile events running to the end of the microtubules, which could be spatially resolved to about 0.4

μm , were excluded from the analysis. For HKin and NKin assays no tethering of microtubules was observed at the end of motile events, independent of whether the end of the microtubule was reached or not. Given the similar length distribution of microtubules used for the in single molecule gliding assays, the estimate of the average run length of NKin is more susceptible to a slight underestimation because of NKin's longer average run length. Altogether, the motile behavior shown in Fig. II-1 is consistent with the hypothesis that both Hkin560 and Nkin483 are capable of processive movement. The calculated mean run-lengths for Hkin and NKin from these single molecule *in vitro* gliding assays are $1.09 \pm 0.10 \mu\text{m}$ and $2.14 \pm 0.29 \mu\text{m}$, respectively.

Single molecule fluorescence assays

To circumvent potential problems involving aggregation and adsorption, and to address the finding of unexpectedly high densities of motor molecule at which we observed single molecule microtubule gliding events, we sought to directly assay the processive movement of single, fluorescently marked motor molecules. We first quantified the bleaching behavior of our Cy3-labeled, truncated Hkin560 and Nkin483 motors in the TIRF-microscope. We attached a large number of labeled motor molecules either by nonspecific adsorption or by binding microtubules decorated with labeled motor molecules to the surface of a quartz slide and recorded the TIRF signal. The fluorescence intensity was quantified over time using an Argus image processor. In agreement with previous observations the decay of the fluorescence intensity could be fitted to a single exponential function (Pierce *et al.*, 1997; Pierce and Vale, 1998; Vale *et al.*, 1996). From the exponential rate constants we determined the average times for bleaching fluorescently labeled NKin and HKin molecules, which were $15.9 \pm 2.2\text{s}$ and $18.6 \pm 2.7\text{s}$, respectively (Figure II-2). In addition, we recorded the fluorescence under conditions where the fluorescently-labeled motor molecules were diluted to a surface concentration below $0.1 \text{ molecules}/\mu\text{m}^2$. Under these conditions we observed individual spots; a frame-by-frame analysis of the fluorescence intensities of these spots showed an incremental bleaching behavior, either in one or two steps, for both HKin and NKin molecules (Fig. II-3 c, and Fig II-4 c, d). A one - or two step bleaching behavior of dimeric motor molecules is consistent with the labeling ratio of reactive cysteines of about 0.8. Roughly, we observed twice as many molecules bleaching in two steps compared to motors bleaching in one step. These observations confirm that we can resolve single molecules and that the motors do not aggregate under the conditions used in this study.

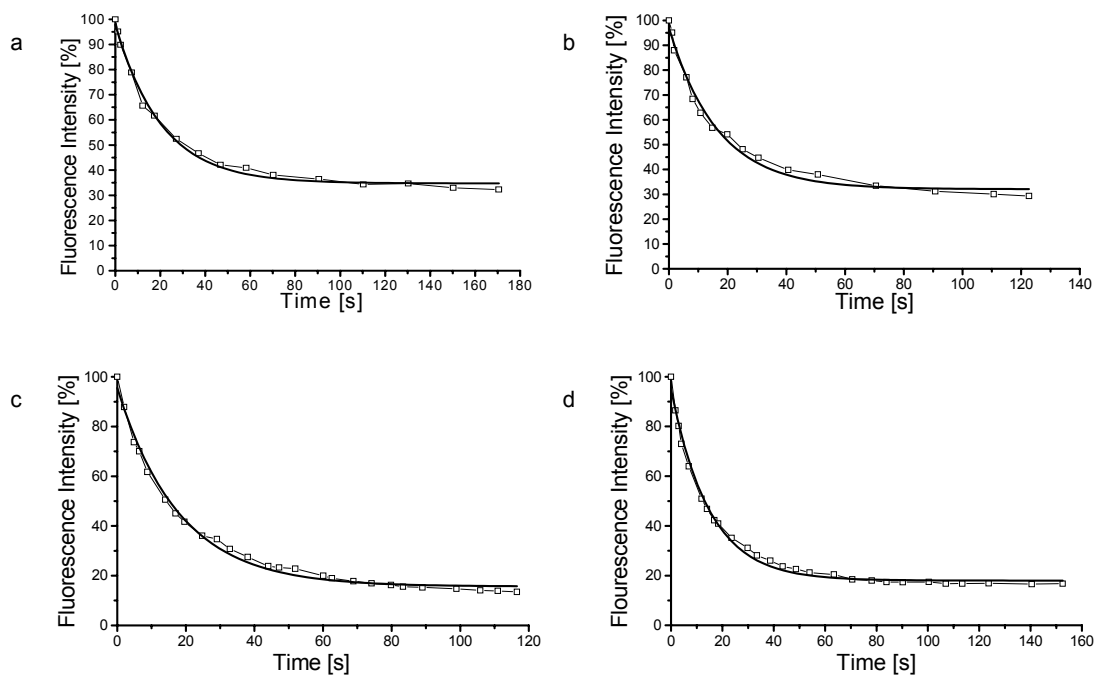


Fig. II-2: Global bleaching behavior of Cy3 marked HKin and NKin motors

The global fluorescence lifetime of the fluorophores covalently linked to the motor protein constructs was determined by observing several hundred fluorophores in a designated area over time, and plotting the overall intensity of the signal against time. The resulting bleaching were 15.6 ± 2.2 s (a and b) and 18.6 ± 2.7 s (c and d) for NKin and HKin, respectively (two independent preparations each).

When we combined Cy5-labelled microtubules with Cy3-labelled HKin in the TIRF setup, association and movement of fluorescent spots could be observed. The spots moved with an average velocity of 0.81 ± 0.01 $\mu\text{m/s}$ (N=229), which is in very good agreement with

the wt-speed and the velocity of the truncated HKin constructs in both multiple ($0.78 \pm 0.01 \mu\text{m/s}$) and single ($0.77 \pm 0.03 \mu\text{m/s}$) molecule gliding experiments.

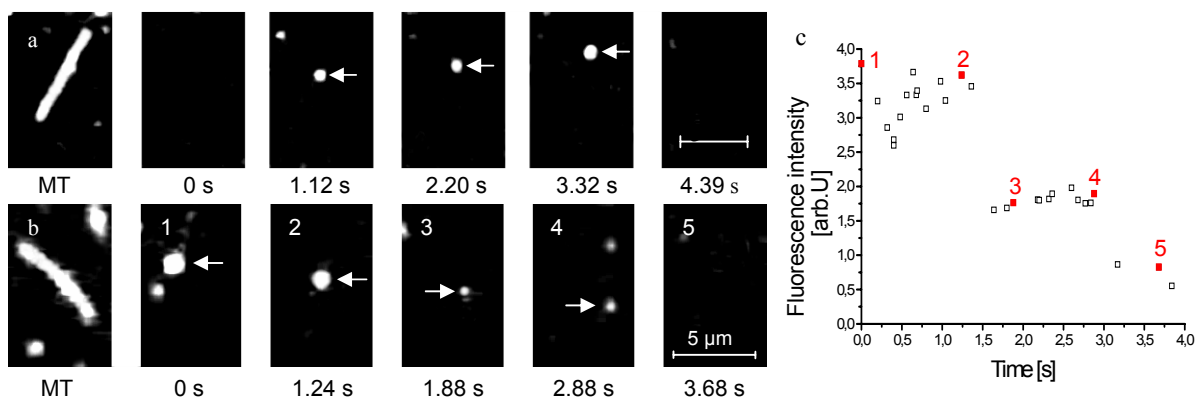


Fig. II-3: Single molecule fluorescence processivity assays for HKin

Fluorescently labeled HKin molecules were observed to bind to and move along a Cy5 marked MT (a,b). The gliding speed of the motor molecules ($0.8 \mu\text{m/s}$) corresponded well to the speed observed in multiple molecule gliding assays and single molecule gliding assays. Both surface adsorbed (c) and moving (d) HKin motor molecules bleached in an incremental fashion. Panel b shows a gliding HKin molecule bleaching in a two-step fashion. The intensity of this moving fluorescent spot in (b) is shown in d. Numbered intensities in (d) correspond to the numbered frames in b.

While we also observed the same behavior for Cy3-labeled NKin483, this approach proved to be experimentally impractical as NKin associates with immobilized microtubules at such a low rate that only a small number of processive events can be observed in this manner. However, we were able to reproducibly record processive movement of single NKin molecules on microtubules after first binding NKin to microtubules with AMP-PNP ($1-10 \mu\text{M}$) and then inducing movement by introducing an ATP-containing solution. Approximately 10% of the motors started to move. Most other fluorescent spots bleached before movement could be observed, and some spots remained stationary. Exemplary events of movement are shown in Figure II-4.

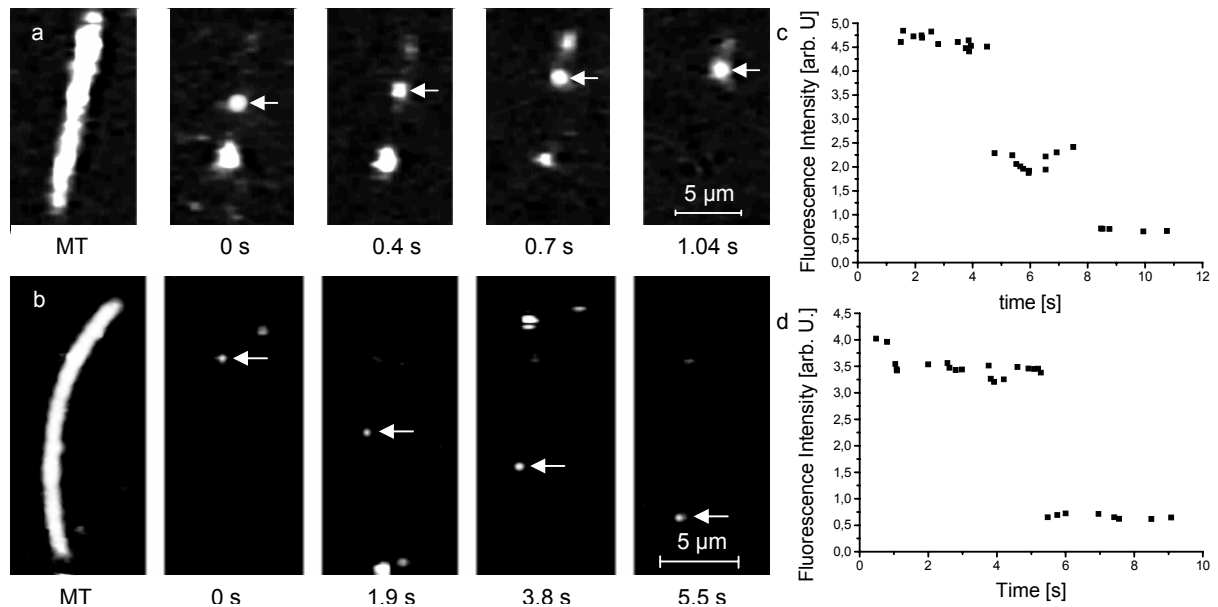


Fig. II-4: Single molecule fluorescence processivity assays for NKin

In contrast to HKin, fluorescently marked NKin molecules could only be observed to move along MT after immobilization on the MT by AMP-PNP and starting the assay by exchanging ATP containing buffer-solution into the assay chamber. The motor showed smooth unidirectional movement at wt-speed of about $1.7 \mu\text{m/s}$ (a, b). Surface adsorbed motors were detected to bleach in incremental steps (c, d).

The velocity of moving spots was $1.70 \pm 0.05 \mu\text{m}$ (N=182), which is in good agreement with the multiple and single molecule gliding assays under low salt conditions. We also performed single molecule fluorescence assays with NKin at 200mM KCl. The identified moving spots also moved long distances with a velocity of $2.19 \pm 0.13 \mu\text{m/s}$ (N=19) which again is in good agreement with the multiple and single molecule gliding assays in BRB80 supplemented with 200 mM KCl. To allow a direct comparison of the run lengths of HKin and NKin we decided to measure the run lengths in buffer without additional salt.

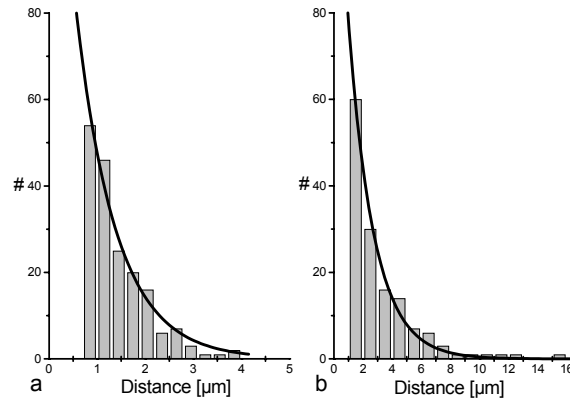


Fig. II-5: Histograms of the run-lengths of HKin and NKin

Run lengths of processive movement (see discussion) of HKin and NKin were combined in a histogram. The data were fit by a single exponential (red line). The decay constant of the exponential gives the mean run length of the motor molecule.

Histograms of the run lengths of our HKin ($N = 229$) and NKin ($N = 182$) processivity assays can be fit by single exponential distributions (Figure II-6). The mean distance calculated as the decay length of the fit is $0.83 \pm 0.06 \mu\text{m}$ for HKin and $1.75 \pm 0.09 \mu\text{m}$ for NKin. The run length for HKin obtained here is in very good agreement with data presented by Vale *et al.* (1996), although they reported a much lower average velocity ($0.3 \mu\text{m/s}$) on axonemes (Thorn *et al.*, 2000; Vale *et al.*, 1996). To determine the number of steps a kinesin takes before dissociating from the microtubule, the travel distance was divided by 8nm . Thus, HKin takes on average 104 steps while NKin takes 219 steps before dissociation from the microtubule. The motile behavior of HKin and NKin motors is summarized in Table II-1.

Table II-1 : Comparison of the motile properties of HKin560cys and NKin480cys.

Assay	HKin560cys			NKin480cys		
	MMGA	SMGA	PA	MMGA	SMGA	PA
Velocity	0.78 ± 0.09 μm/s, (N=101)	0.77 ± 0.20 μm/s (N=49)	0.83 ± 0.18 μm/s (N=229)	1.72 ± 0.18 μm/s (N=48, wt)	n.d.	1.70 ± 0.63 μm (N=182)
				2.20 ± 0.27 μm/s (N=103) (incl. 200mM KCl)	2.29 ± 0.81 μm/s (N=46) (incl. 200mM KCl)	2.19 ± 0.56 μm/s (N=19) (incl. 200mM KCl)
Density	high	~500/μm ²	-	High	~5000/μm ²	-
Run-length	-	0.77 ± 0.20 μm	0.83 ± 0.06 μm	-	2.14 ± 1.95 μm	1.75 ± 0.09 μm

DISCUSSION

In this report we quantitatively evaluated the processive behavior of a fast fungal, microtubule-based motor molecule, *Neurospora crassa* kinesin, NKin. We engineered a truncated, dimeric motor, NKin483, and introduced a reactive cysteine at the C-terminus for selective labeling with Cy3 dye. For comparison we also purified and labeled an analogous human kinesin construct, HKin560. Two independent methods, single molecule *in vitro* gliding assays and fluorescence-based single molecule assays, were exploited to quantify the processivity of both kinesins. Our observations, which are characterized by a robust quantitative agreement between the different processivity assays, demonstrate not only that NKin is processive, but also substantiate that NKin is at least twice as processive as HKin.

In vitro gliding assays

Initially, we attempted to quantify the processive properties of NKin by using single molecule *in vitro* gliding assays as first established by Howard *et al.* (1989). The single molecule gliding assays for NKin presented in this paper are characterized by similar motile

properties: (1) The average gliding speed of NKin single motor events ($\sim 1.7\mu\text{m/s}$ and $\sim 2.2\mu\text{m/s}$ with and without additional 200mM KCl in the buffer solution) was unchanged compared to that in multiple molecule gliding assays and (2) microtubules underwent substantial (ranging up to 45 degrees) angular diffusive rotations that were consistent with the measurements of (Hunt and Howard, 1993) for bovine kinesin. These results suggest, that NKin is also capable of processive movement along microtubules.

However, in contrast to HKin, other conventional animal kinesins or myosin V (Mehta *et al.*, 1999; Rief *et al.*, 2000), the density of motors in the NKin assays could not be varied systematically as the frequency of single motor events dropped abruptly with reduced motor density. Therefore, we were unable to confirm via dilution experiments that single motors were driving the observed microtubule gliding. Also, our single molecule NKin gliding events were recorded at motor densities much higher than expected on the basis of previous work with animal kinesins (Crevel *et al.*, 1999; Howard *et al.*, 1989; Romberg and Vale, 1993). The high densities required to observe the activity of single NKin molecules, which are in complete agreement with the bead and gliding assays of Crevel *et al.* (1999), challenge the interpretation that this kinesin is processive (Crevel *et al.*, 1999). On the other hand, the high NKin densities in single molecule assays could be explained if (1) the adsorption of our truncated Nkin483 construct to the glass surface is impaired, thus overestimating the number of functional kinesins, or (2) if the binding of NKin motors from solution to the microtubule is reduced dramatically. Experiments using constructs such as full-length NKin and NKin/HKin-tail-chimera, do not lead to significantly improved dilution behavior of NKin. Therefore we conclude, in agreement with our single molecule gliding assays (see discussion below) and a previous report (Crevel *et al.*, 1999), that adsorption of the motor to the surface is not impaired, rather binding of microtubules to the motor (or vice versa) near the glass surface is reduced by an unknown mechanism.

The average run length of about 1.09 μm for HKin in single molecule *in vitro* gliding assays agrees well with previous reports (Hancock and Howard, 1999; Howard *et al.*, 1989; Romberg *et al.*, 1998; Thorn *et al.*, 2000; Tomishige and Vale, 2000; Vale *et al.*, 1996) suggesting that the *in vitro* gliding approach used in this study yields reliable processivity measurements. The significantly longer average microtubule run length of NKin implies that this motor is more processive than HKin. However, this interpretation of our single molecule gliding assays is uncertain for two reasons: (1) The length of the microtubules in the NKin assays ranged from 2-5 μm and some of the observed events were terminated by the motor reaching the end of the microtubule rather than the microtubule dissociating from the pivoting

point. We excluded these events from the analysis. (2) The actual number of molecules per μm^2 could not be reliably reduced (see above), possibly allowing more than one motor to simultaneously interact with the microtubule and thus increasing the apparent processivity. In order to circumvent these difficulties, we used an adsorption-independent method, the single molecule fluorescence assay first performed by Vale *et al.* (1996).

TIRF microscopy-based processivity assays

For our assays truncated HKin and NKin motors were labeled at an artificially introduced, reactive cysteine residue with the fluorescent dye Cy3. As expected from the measured cysteine labeling ratio (about 0.8), single- and double-labeled fluorescent spots could be detected in the TIRF microscope. The characteristic bleaching behavior and the agreement of the average lifetime of a fluorophore with the globally observed rate of fluorescence photobleaching support the conclusion that the observed fluorescent spots are indeed single kinesin motor molecules. Using our TIRF system we were able to track the binding and subsequent movement of single, fluorescently-labeled kinesins along microtubules. Kinesins moved micrometer-long distances before dissociating from the microtubule or photobleaching. First we performed single molecule fluorescence processivity assays with HKin, because HKin is the best studied model system for processive movement and therefore is best suited for a comparison with Nkin. Gliding speed and distance agreed well with both multiple and single molecule *in vitro* gliding assays and single molecule fluorescence processivity assays. We determined the mean run length of HKin by fitting a single exponential function to a run-length histogram calculated from all events observed for HKin. The mean run-length of 0.8 μm corresponds well to the reported values for conventional kinesin (Rice *et al.*, 1999; Romberg *et al.*, 1998; (Thorn *et al.*, 2000); Tomishige and Vale, 2000; Vale *et al.*, 1996). Our single molecule fluorescence experiments with HKin and the closed agreement with the results of other groups suggest that the TIRF assay is very robust.

However, the analysis of NKin's processivity with this assay proved more difficult. While we were able to observe single, fluorescently-labeled NKin motors land, move along and dissociate from microtubules in a manner virtually indistinguishable from HKin, these events were extremely rare. This observation agrees with our previous conclusions from gliding experiments and confirms that the initial binding of NKin to microtubules is markedly

reduced as compared to HKin. To allow collection of data at a reasonable rate, we first bound labeled motors to the microtubule with 1-5 μ M AMP-PNP and then started the assay by introducing an ATP-containing solution (4mM) into the flow chamber. Approximately 10% of the fluorescently motors immobilized on the microtubules started to move upon the addition of ATP. This can be accounted for by two mechanisms: 1) AMP-PNP exchanges slowly for ATP, even at high ATP concentrations. Therefore, in our experiments many motors bleach before they start moving. 2.) The kinesin-AMP-PNP state locks (at least) one head onto the microtubule. During incubation a transition of one or both heads into a rigor-like conformation is possible. Kinesin is very sensitive to such rigor-like conditions and consequently motors are bound irreversibly to microtubules. This behavior can be reduced by the addition of salt. Irreversible binding of motors is also believed to be the reason for the loss of functional protein during microtubule-binding and release protocols, where addition of salt also increases the yield substantially. The gliding speeds (1.70 μ m/s and 2.19 μ m/s with and without additional 200 mM KCl in the buffer solution, respectively) of fluorescently marked NKin motors in these assays were in very good agreement with speeds observed in multiple and single molecule *in vitro* gliding assays and demonstrate that there is no problem in exchanging AMP-PNP with saturating concentration of ATP. The increase in speed upon addition of salt is not easily explained but could for example be due to a weakened electrostatic interaction that is involved in a rate limiting step in the turnover of the processive motor. These experiments also proved beyond any reasonable doubt that NKin is really a processive motor. But *how* processive is NKin compared to HKin?

We compare the processivity of HKin and NKin by generating histograms of the run length of all events and fitting the resulting density functions with a single exponential distribution. As the speed of movement for NKin is sensitive to the ionic strength of the assay buffer (Crevel *et al.*, 1999; Steinberg and Schliwa, 1995; Steinberg and Schliwa, 1996) and we wanted to exclude any possible effect of additional salt on the processivity of NKin, we chose standard buffer conditions (P12 without additional KCl) for the direct comparison of the processivity of HKin and NKin. The mean run length of NKin determined directly from the exponential time constant was 1.75 μ m. This value corresponds very well to the values obtained in single molecule *in vitro* gliding assays (see above). Furthermore, observations on the biochemical processivity (K_{bi} ratio, ((Gilbert *et al.*, 1998; Gilbert *et al.*, 1995; Hackney, 1994b; Hackney, 1995) of various NKin constructs (Kallipolitou *et al.*, 2001) strongly support our measurements. Kallipolitou *et al.* (2001) showed that monomeric constructs hydrolyze few ATP molecules per diffusional encounter, while dimeric constructs displayed

significantly larger biochemical processivity, in the range of 400. Based on the reported step size of 8 nm for NKin (Crevel *et al.*, 1999), our measured average run length of 1.75 μm is equivalent to NKin483 taking about 220 steps before dissociating from the microtubule. The difference of a factor of two between the mechanical and biochemical processivity is probably based on intrinsic differences of the bulk biochemical experiment and slight differences in the buffer conditions. As steady state and kinetic measurements with NKin constructs are very sensitive to such changes, the data are in remarkably good agreement. Our fluorescence processivity assays not only qualitatively demonstrate that single NKin motors are processive, but also quantitatively confirm our earlier, tentative conclusion based on gliding assays that NKin is at least twice as processive as conventional animal kinesin. Is this quantitative agreement perhaps fortuitous, because the observed average run lengths of the spots will need to be corrected for the bleaching of the Cy3 fluorophores?

Other groups have corrected the apparent run length of kinesins (Rice *et al.*, 1999; Romberg *et al.*, 1998; Thorn *et al.*, 2000; Tomishige and Vale, 2000; Vale *et al.*, 1996). By showing that both the run length of the motor and the bleaching rate of the fluorescent dye are single exponential distributions, a simple correction of the observed average run length is possible. Thus the average run lengths for NKin and HKin in our experiments should be increased by 6.8% and 5.7%, respectively. The corrections are small, because in our hands the average lifetime of the fluorophores is much longer than the run time on the microtubule. When we applied such a correction to our data sets and fitted the resulting raw and corrected run length histograms with single exponential functions it became apparent that the raw data, not the corrected data, were fit significantly better by the expected single exponential distribution. We verified this observation by using a Q-Q plot analysis (Venerables and Ripley, 1997), which showed that the corrected histograms contained notably more events at long run length than expected. Considering that we are using dimeric kinesins with a labeling ratio of 0.8 this result is not surprising. We expect that about 64 % of our labeled motors contain 2, and about 32% contain 1 fluorophore. Double-labeled kinesin molecules will require bleaching of both fluorophores to be mistaken for a dissociation event, and assuming that both fluorophores bleach independently the probability density function for such a bleaching event is no longer a simple exponential but a jointly distributed density function (Larson HJ, 1982). Also, this function predicts that the average lifetime of double-labeled kinesins will be 1.5 times longer than that of single-labeled motors. Given that we determined the processivity from a mixture of single- and double-labeled kinesins, all our calculations, including the most conservative estimates, indicate that the correction for the observed run

length is smaller than 5% for NKin and HKin, and our best estimate for the corrected run length of NKin is 1.8 μm .

In summary, both single molecule *in vitro* gliding assays and single molecule fluorescence processivity assays showed that NKin is a processive motor. In agreement with previous work on the processivity of animal kinesins (Crevel *et al.*, 1999; Hackney, 1995) and the role of the dimeric nature of kinesin for processive motion (Crevel *et al.*, 1999; Hackney, 1995; Hancock and Howard, 1998; Hancock and Howard, 1999; Jiang and Hackney, 1997) a view emerges in which the processivity of kinesin is linked to a 'head-over-head' interaction within the dimer. This widely accepted view (Schief and Howard, 2001) has recently been challenged (Hua *et al.*, 2002), and experiments with a natural, single-headed kinesin suggest that other mechanisms might contribute significantly to the processivity of kinesins (Kikkawa *et al.*, 2000; Kikkawa *et al.*, 2001) Okada and Hirokawa, 1999; Okada and Hirokawa, 2000). Our quantitative analysis of the processivity of HKin and NKin shows convincingly that NKin is at least twice as processive as HKin. An important question raised by this finding relates to understanding possible mechanisms and domains involved in controlling the processivity of kinesins.

Physiological basis of fast, processive movement

The high gliding speed of NKin in multiple molecule *in vitro* gliding assays raised the possibility that this motor might take double-sized steps. A step size of 16 nm would explain nicely the doubled processivity and increased gliding speed while maintaining most features of conventional animal kinesin. Interestingly, both HKin and NKin exhibit similar run times on the microtubule of about 1 s under saturating ATP conditions. But, as reported by Crevel *et al.* (1999), NKin has a step size of 8 nm. Thus, the observed increase in the rate of ATP-turnover, k_{cat} , must be responsible for the faster gliding speed; k_{cat} for HKin is about 40-50 ATP/head/s and for Nkin about 75-85 ATP/head/s.

Do we have any insights into why NKin is so fast and yet processive? From the studies of truncated *Drosophila melanogaster* conventional kinesin and NKin molecules (Gilbert *et al.*, 1998; Gilbert *et al.*, 1995; Hackney, 1994; Hackney, 1995; Kallipolitou *et al.*, 2001) we know that the isolated motor domain turns over ATP very fast (96 ATP/head/s and 250 ATP/heads, respectively). Addition of the neck domain to the isolated motor domain reduces

the ATPase of NKin monomers substantially (24-27 ATP/head/s) and only dimerization of the motor by formation of a stable coiled coil (starting at amino acid residue 373 for conventional kinesin and at residue 391 for NKin) yields a fully processive motor with high ATPase turnover. Biochemical studies of truncation and deletion mutants (Gilbert *et al.*, 1995; (Grummt *et al.*, 1998b; Jiang, M. Y. and Sheetz, 1995; Jiang, W. *et al.*, 1997); Hackney, 1995; Kallipolitou *et al.*, 2001) support the following hypothesis: The core motor's catalytic turnover, measured by the ATPase activity of the isolated (truncated) monomeric kinesin, provides an upper limit of the performance of the motor. In the dimeric motor processive movement is achieved by the tight coupling of the two heads, thus, by clocking each other's ATPase cycle, the heads will be slowed down. The reduced ATP-turnover of truncated, monomeric motor constructs with neck region suggests an inhibitory role of the neck domain (Kallipolitou *et al.*, 2001). This inhibition is overcome by binding of the dimeric motor molecule to the microtubule, resulting in the coordinated catalytic activity of the two heads and processive movement. Further evidence for an inhibitory effect of the neck domain comes from (1) the high turnover rate (150 ATP/head s) of a dimeric neck-deletion mutant of another fast fungal kinesin (*Syncephalastrum*) with large sequence homology to NKin (Grummt *et al.*, 1998a; Grummt *et al.*, 1998b), and (2) recent work on a point mutant in the neck region of NKin. Woehlke and Schäfer (2002) showed that the NKinY362K point mutation in the neck abolishes tight coupling between the two heads, leading to slow motility and an ATP-hydrolysis at the maximal rate of 260 ATP/head/s. An inhibitory interaction of the motor with its neck domain might serve as an important physiological adaptation, as a cargo-bound (versus an unbound motor) kinesin is no longer inhibited by the back-folding of the tail region (Hackney *et al.*, 1992; Hackney and Stock, 2000; (Coy *et al.*, 1999a; Kirchner *et al.*, 1999a); Seiler *et al.*, 2000; Seiler *et al.*, 1999). A cargo-bound motor that is not attached to (and moving along) a microtubule would, if no neck inhibition were to be present, rapidly hydrolyze ATP without doing any mechanical work.

The higher gliding speed of NKin, as compared to HKin, is therefore dependent on (1) the intrinsic properties of the motor domain (i.e. its catalytic activity) and (2) the rate of coupling between individual head domains. Based on the above discussion, we expect the neck domain to be of crucial importance. Crystallographic data by Song *et al.* (2001) point at a possible structural correlate for the high intrinsic ATPase activity of NKin's head. They speculate that the comparatively open ATP-binding pocket enables NKin to bind and exchange nucleotides more readily (Foster *et al.*, 2001; Gilbert, 2001).

What mechanisms might influence NKin's processivity? Several experimental pieces of evidence hint at a direct interaction between the neck of the motor molecule and the flexible C-terminal portion – the so-called E-hook - of both α - and β -tubulin in the microtubule. First evidence for this interaction came from crosslinking studies (Tucker and Goldstein, 1997). Subsequently, Wang and Sheetz (Tucker and Goldstein, 1997; Wang and Sheetz, 2000) characterized processive movement of kinesin- (and dynein) coated beads on subtilisin-digested microtubules and showed that removal of the flexible C-terminus of tubulin (E-hook, negatively charged), reduces the run length, but not the gliding speed of conventional kinesin. Therefore, they hypothesized that an electrostatic interaction of the positively charged neck-domain of the motor molecule with the flexible E-hook of tubulin might either keep the motor attached to or properly positioned on the microtubule such that complete dissociation of the motor from the microtubule is less likely. The influence of the length (Romberg *et al.*, 1998; Thorn *et al.*, 2000) and/or the charge of the neck domain of conventional kinesin (Thorn *et al.*, 2000) on processive movement supports this hypothesis. Furthermore, studies of a genetically modified (C351) naturally monomeric kinesin, KIF1A, showed that a tight electrostatic interaction of a lysine-rich region, the so-called K-loop, of the motor domain allowed the monomeric motor to move along microtubules in a quasi-processive fashion (Kikkawa *et al.*, 2000; Kikkawa *et al.*, 2001; Okada and Hirokawa, 1999; Okada and Hirokawa, 2000), better described as a unilaterally biased diffusion. It is still unknown how strong this interaction with the microtubule is, and how much force can be produced by a monomeric KIF1a motor during processive motion. Okada and Hirokawa proposed a biased Brownian motion-based mechanism for this quasi-processive motion of the motor. While such a mechanism predicts that single KIF1A-motors will not be able to produce movement against a substantial force (unlike conventional kinesins), the KIF1A data do suggest potential electrostatic contributions on the interaction of kinesin and microtubules (Okada and Hirokawa, 2000). The increased processivity of NKin could therefore be due to an increased electrostatic interaction of the neck portion of NKin with the E-hook of the microtubule. In contrast to this hypothesis, the neck domain does not show an increase of positive charges compared to other conventional kinesins, but a decrease (overall charge of the neck is +4, +4 and 0, for HKin, *Drosophila* kinesin and NKin, respectively). We suspect a more subtle mechanism to be at work in this case. Clearly, NKin has been shown to have unique properties in the neck domain (Kallipolitou *et al.*, 2001). One might actually argue that the reduced positive charge facilitates the dissociation of motor-microtubule-interaction, thus allowing the rate of turnover during processive movement to increase without rendering the

motor less processive. Because fungal kinesins have a conserved, but different residue organization in the neck domain, we suggest that the processivity of NKin might be substantially influenced by its neck domain. Further studies of the processivity of the fungal kinesins with subtilisin-digested microtubules should now be conducted to gain further insights into the potential role of electrostatic interactions in the motile mechanism of kinesins.

Chapter III: The E-hook of the microtubule strongly influences processivity and speed of kinesin motors

Introduction

Conventional kinesins are dimeric microtubule-based motors that use the energy of binding and hydrolysis of ATP to drive unidirectional, plus-end directed movement in the cell (Vale, R. D., 2003). Conventional kinesin show gliding speeds of about 0.6-0.8 $\mu\text{m/s}$ (Coy *et al.*, 1999a). The filamentous fungus *Neurospora crassa* and other fungi express motors that are characterized by unusually high gliding speeds in the range of 1.7-2.5 $\mu\text{m/s}$ (Steinberg and Schliwa, 1995; Steinberg and Schliwa, 1996). Based on their primary sequence they have been arranged in the sub-group of fungal conventional kinesins, as they show the same overall domain organization with their animal counterparts (Kirchner *et al.*, 1999b). The N-terminal ~330 AA form a globular domain, called “head”, that carries ATPase and MT binding activity. The following 10-12 amino acids form a flexible structure that has been shown to undergo nucleotide-dependent docking to the head domain (Rice *et al.*, 1999; Sindelar *et al.*, 2002). This so called neck-linker is believed to confer the critical conformational changes leading to movement (Mogilner *et al.*, 2001), also because the entity of head and neck-linker is the minimal truncated kinesin to drive motility in *in vitro* gliding assays (Huang and Hackney, 1994; Kallipolitou *et al.*, 2001). Further C-terminal to the neck-linker the neck domain follows which is able to form coiled-coils, leading to the dimerization of the motor molecule (de Cuevas *et al.*, 1992; Song and Mandelkow, 1994). Dimerization of conventional kinesin is a necessary requirement to drive processive movement (Hancock and Howard, 1998; Hancock and Howard, 1999), which describes the motors ability to take hundreds of 8 nm steps before dissociating from the (Coy *et al.*, 1999b). This allows long-range transport of vesicles or small particles in the cell with the help of single or only very few motors (Vale, R. D., 2003). Vesicles or particles, generally referred to as cargoes, are attached to the motor through interactions in the C-terminal tail or light chain binding domain, that is connected to the neck by the coiled coil-forming stalk (Seiler *et al.*, 2000; Verhey *et al.*, 1998; Verhey *et al.*, 2001). Two flexible regions between neck, stalk and tail domain, the so-called hinge and kink allow back-folding of the motors tail to inhibit futile ATP consumption when no cargo is bound (Coy *et al.*, 1999a; Hackney and Stock, 2000; Seiler *et al.*, 2000).

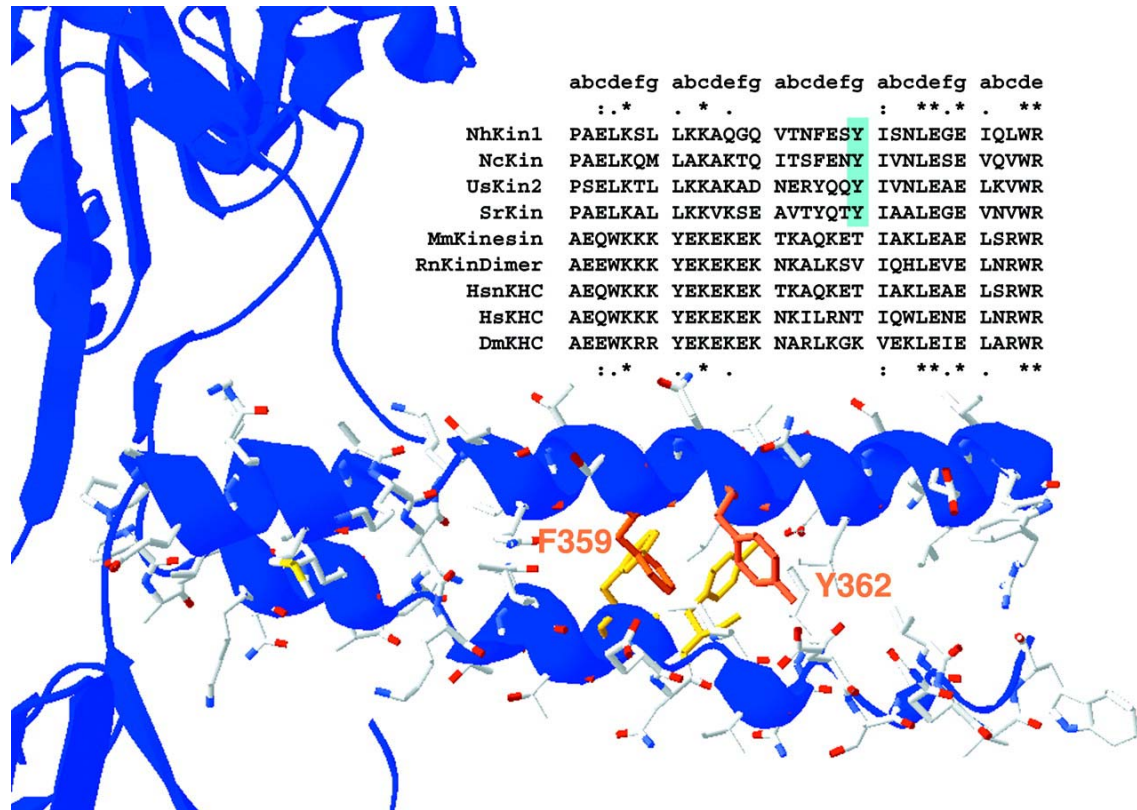


Figure III-1 : Sequence Alignment and structural details of the neck of NKin (from Schäfer *et al.*, 2003)

NKin has been shown to be an unusually fast (Steinberg and Schliwa, 1995; Steinberg and Schliwa, 1996) and highly processive motor, taking approximately double the amount of steps (220) before dissociating from the microtubule as compared to human kinesins (HKin, 100 steps, (Lakamper *et al.*, 2003). How is that achieved? While the fast ATPase and gliding speed was hypothesized to be due to a comparatively open ATP-binding pocket as determined from the NKin crystal structure, the crystal structure did not reveal insight on structural elements leading to the unusually high processivity (Song *et al.*, 2001). The close superposition of the rat kinesin and Nkin structures also suggests, that crucial conformational changes, which are required for communicating strain signals from one head to another and thus allowing processive movement, are basically the same. Recent studies by Crevel *et al.*, Kallipolitou *et al.*, and Schäfer *et al.* show that, while NKin shows the same overall domain organization as animal kinesins, details of the neck domain organization and function differ dramatically from its animal counterparts (Figure III-1). The first third of the Neck domain shows a fungal specific sequence pattern that has a significantly lower coiled-coil forming propensity. This is reflected by the inability of some truncated NKin motors (NK378, NK383) to form dimers, while shortened animal kinesins truncated at homologous residues form

stable dimers (Young *et al.*, 1998). Furthermore, a conserved tyrosine residue in the neck of fungal kinesins regulates not only dimerization, but also influences ATPase activity of the catalytic motor core (Schafer *et al.*, 2003). Are these unusual properties of the NKin neck domain maybe responsible for the high processivity of NKin? How could this effect be conferred?

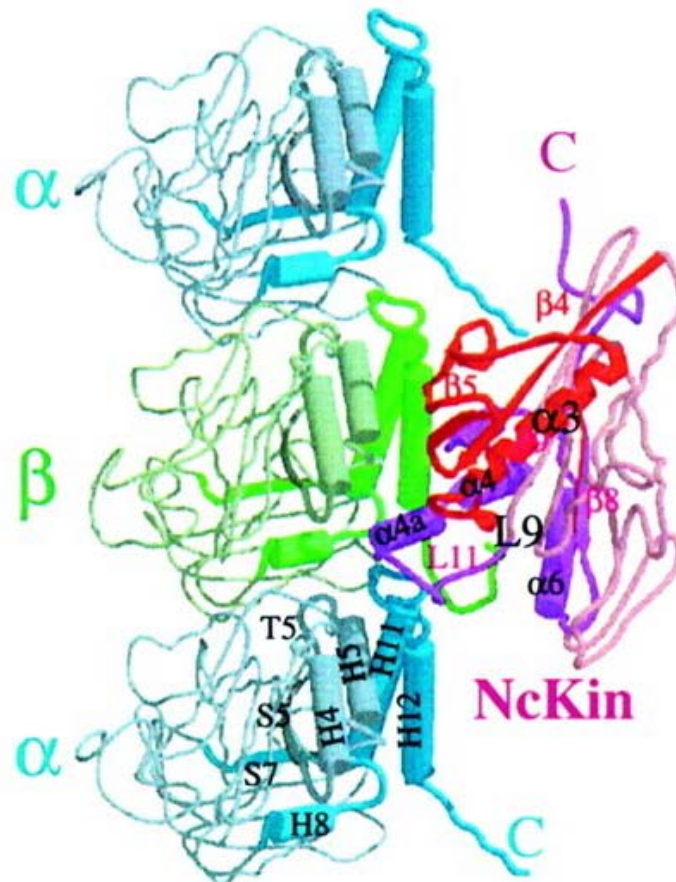


Fig. III-2: Interaction of the Nkin motor head with the microtubule

The crystal structure of the monomeric NKin head domain was modeled onto a $\alpha\beta$ -trimer of tubulin. The picture was adapted from Song *et al.*, 2001.

Three lines of evidence from studies with animal conventional kinesin and the minus end-directed kinesin motor *ncd* support the idea that the neck domain is a structure that determines the degree of processivity.

1.) Multiplication of the positively charged first or fifth heptade repeat of the neck of human kinesin leads to dramatic increases in processive run lengths observed in single molecule assays. On the other hand the introduction of negatively charged residues reduced processivity by a factor of 3. The effect was significantly salt-dependent, suggesting an electrostatic interaction (Romberg et al. ,1998, Thorn et a.,, 2000). 2.) It could be shown that the removal of the highly flexible C-Terminus of both α - and β -tubulin - termed E-hook because of the high number of glutamic acid residues in this structure - by limited digestion with subtilisin leads to a significant reduction of processivity of kinesin and dynein motors (Wang and Sheetz, 1999). This finding supports the proposed electrostatic interaction between the motors neck and the tubulin's E-hook. Although the study by Thorn clearly shows a strong influence of the E-hook on the processivity of HKin with a quadruplicated first heptade repeat (HIQ), no direct evidence for an interaction between the two structures has been reported. 3.) A similar, highly positively charged structure, however, the tail of the minus end-directed motor NCD, could be shown to interact directly with the E-hook, by cross-linking the two structures with EDC/NHS (Karabay and Walker, 2003; Wendt *et al.*, 2003). Despite apparent differences between the positions of the neck of kinesin and the tail of NCD this study shows the possibility of strong electrostatic interactions between the E-hook and structures of motor molecules. Could such an interaction between the unusual neck of NKin and the E-hook be the reason of the high processivity of NKin?

Judging from the charge distribution on the neck of NKin, the degree of an electrostatic interaction with the E-hook influencing Nkins processivity would be relatively small, as the neck has no or even a negative net charge, as compared to a net charge of +8 in wt-HKin. Nevertheless, the first two heptade repeats of the neck that, according to Thorn et al. (2000) play a more important role in determining the processivity, show a slighty positive net charge of +2. These considerations and the unusual properties of the neck, going along with the features of the amino acid sequence make predictions of the role of the neck in the processive behavior of NKin motors impossible. Therefore, it needed to be experimentally tested if the removal of the E-hook by partial digestion with subtilisin has a similar effect on processive movement of NKin as it has on HKin, and if such an effect could at least qualitatively be explained by the structural peculiarities of NKins neck domain.

The following questions were addressed:

- 1.) Does the removal of the E-hook have an influence on processivity of NKin?
- 2.) Does the removal of the E-hook have an influence on the speed of NKin?

To answer these questions multiple molecule gliding assays, single molecule fluorescence gliding assays as well as ATPase and ADP-release measurements were performed with monomeric and dimeric NKin motor constructs. Plasmids for the NKin constructs NK433cys and NK343cys were provided by Dr. Athina Kallipolitou and Kathrin Hahlen from the Institute of Cell Biology of the Ludwig-Maximilians-Universität in Munich, Germany.

Results

Partial Digestion of Microtubules with subtilisin removes the E-hook of tubulin

Microtubules, polymerized from either bovine or porcine tubulin, were digested using a ratio of tubulin to subtilisin of 1/0.06 (w/w) at 37°C for 20 min. Ratios of 1/0.6, as reported earlier by Wang and Sheetz (2001), resulted in complete digestion and loss of tubulin. The reaction was stopped by addition of 2 mM PMSF for 5 min. The microtubules were separated from subtilisin and PMSF by sedimentation through a 40% (w/v) sucrose cushion. This procedure resulted in a loss of about 50% tubulin as measured spectro-photometrically after denaturation of the microtubules with GndHCl. No difference between undigested and digested microtubules could be observed microscopically. A reduction in microtubule length was attributed to mechanically breaking microtubules during the repeated sedimentation- and resuspension-steps. Apparent differences disappeared when undigested microtubules were subjected to the same additional separation steps. All microtubule digestions were run on SDS gels with undigested tubulin as control.

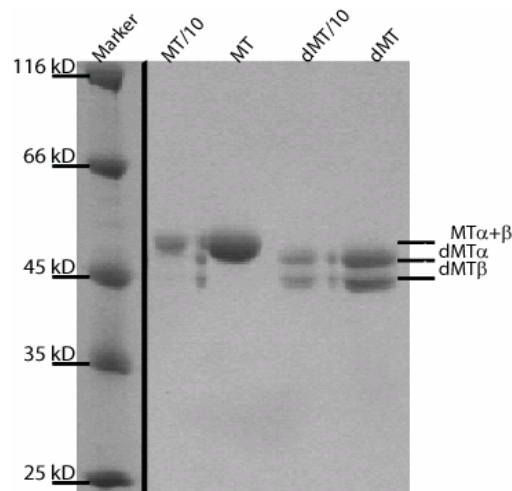


Fig. III-3: Partial Digestion of Tubulin controlled by SDS-PAGE

The panel shows a typical digestion pattern of tubulin with subtilisin. After digestion, the α - and β - subunit clearly resolve and the reduction of size for about 4-10 kD in both subunits is visible.

Very reliable digestion patterns were observed: the undigested α - and β -tubulin do not separate on a standard 10% SDS-PAGE under our standard conditions, whereas the digested tubulin shows two distinct bands. These were earlier reported to be α - and β -tubulin (Tucker and Goldstein, 1997), the latter being the lower band resolved on the gel (Fig. III-3). As kinesin motors bind the β -subunit of tubulin, we wanted to ensure, that the digestion yields complete digestions of the β -subunit, resulting in a reduction of size of about 4-5 kD. Therefore, western blot analysis of digested and undigested microtubules with monoclonal antibodies directed against the β -subunit of tubulin was performed. The resulting blots show a single, clear band for both digested and undigested microtubules, suggesting complete digestion, without other digestion products present as judged from the available length of the gels (Fig. III-4).

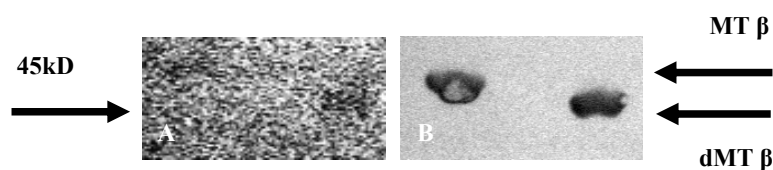


Fig. III-4: Western-blot analysis of a tubulin digestion

Partial digestion of β -Tubulin assayed in a Western-blot with monoclonal antibodies against β -Tubulin. (A) shows the PonceauS-stained blot before incubation with antibodies. (B) shows developed blot after incubating for 10 min in NCB/BCIP-solution.

In order to answer the question if processivity of NKin is reduced upon removal of the E-hook, we performed single molecule fluorescence assays of NKin motors as described in chapter II on digested microtubules (dMT).

Removal of the E-hook leads to reduced processivity and speed of NK433cys

TIRF based low background fluorescence assays with fluorescently labeled motors allow the direct determination of the processive run length and speed of single kinesin motors (Lakamper *et al.*, 2003; Vale, R. D. *et al.*, 1996). As described earlier, in order to observe statistically meaningful numbers of events, NKin motors had to be immobilized to the microtubule using μ M concentrations of AMP-PNP, before introducing antibleach-solutions containing saturating amounts of ATP. Only then Cy3-labeled NKin motors (NK433 and

NKHK560cys) were observed to move processively along microtubules. This behavior was also observed for NKin motors on digested microtubules. Motors moved unidirectionally and uniformly along the microtubule, until they either reached the end, detached or photo-bleached. All events were combined in a histogram. The data could be fit by a single exponential (Howard, 1997; Vale, R. D. *et al.*, 1996). The average run length was determined from the time constant of this single exponential (Fig. III-5).

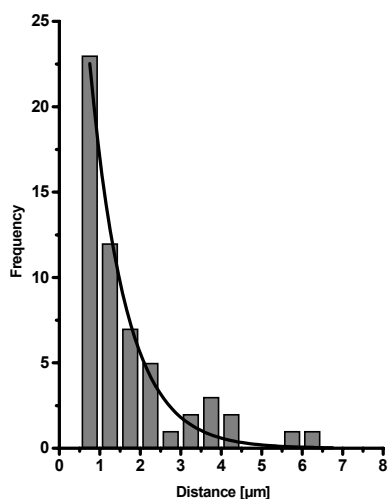


Fig. III-5: Histogram of run-lengths of NKin motors on digested microtubules

Data from 61 individual processive runs were combined in a histogram and the data were fit with a single exponential. The resulting average run length is $0.89 \pm 0.09 \mu\text{m}$.

In complete agreement with reports on conventional kinesins, the average run length of NKin dropped from $1.75 \pm 0.08 \mu\text{m}$ on MT (N=183, see chapter II) to $0.89 \pm 0.09 \mu\text{m}$ on dMT (N= 61) upon digestion. Surprisingly, and in contrast to HKin, the gliding speed of NKin along dMT dramatically decreased from $1.75 \pm 0.60 \mu\text{m/s}$ to $0.97 \pm 0.45 \mu\text{m/s}$. As this reduced speed could be the result of interrupted stretches of fast movement, uniformity of movement is confirmed by constructing kymographs (Fig. III-6). Kymographs plot the intensity profile of a given line in a single frame - in this case the microtubule - versus time. Uniform movement of single fluorescently labeled motors is seen as a straight inclined line. Pauses in movement can be seen as horizontal lines. The inclination of the lines indicates the speed of the motors movement.

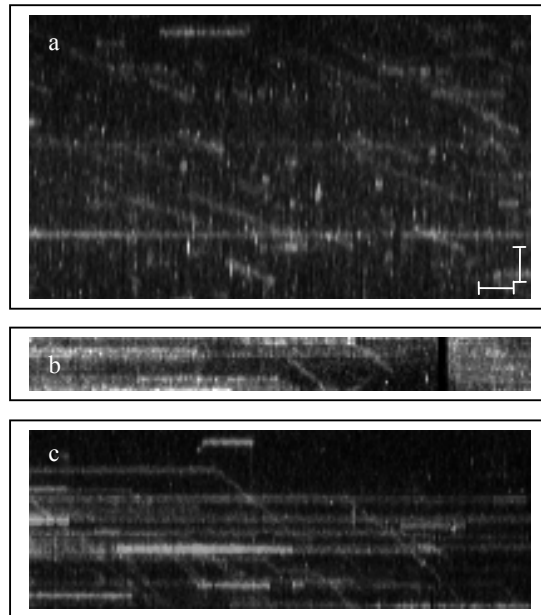


Fig. III-6: Kymographs for HKin and NKin single molecule fluorescence assays

Panels show several single molecule fluorescence gliding assays for (a) HKin and (b and c) NKin motors. (b) shows single NKin motors moving uniformly along digested microtubules at a speed ($\sim 1 \mu\text{m/s}$), intermediate between (a) HKin and (c) NKin on undigested microtubules ($\sim 0.8 \mu\text{m/s}$ and $\sim 1.7 \mu\text{m/s}$, respectively). Horizontal and Vertical scale bars represent 1s and $1 \mu\text{m}$, respectively.

Figure III-6 shows kymographs of single Nkin motors moving on MT (c) and dMT (b). As a comparison a kymograph of fluorescently labeled Hkin motors moving on MT is given in (a). All events are seen as straight, uninterrupted, inclined lines, indicating that movement of NKin motors on both MT and dMT occurred in a uniform, uninterrupted fashion. To exclude possible artifacts due to the AMP-PNP present in the assay or artifacts leading to such reduced speeds, the reduction of speed was confirmed in independent measurements using multiple molecule gliding assays and the determination of k_{cat} -values in bulk biochemical ATPase measurements.

Digested microtubules are transported at lower speeds in multiple motor gliding assays

Fluorescently labeled microtubules were subjected to the digestion procedure as described earlier. Digestion was checked on an SDS-gel and gliding assays of digested and

undigested were performed on surfaces covered with motor at high densities. The gliding velocity of digested microtubules was significantly reduced compared to MT for both NKin433cys and NKHKtail motors ($1.25 \pm 0.14 \mu\text{m/s}$ (N=39) and $1.30 \pm 0.11 \mu\text{m/s}$ (N=40), respectively, see also Table II-1). NKin 433cys does not bind unspecifically to glass surfaces. Therefore, the motor was biotinylated using a biotin-maleimide and a subsequent microtubule affinity purification was performed. Gliding assays were then performed in assays chambers pre-incubated with streptavidin. Both motors showed uniform gliding of MT and dMT. The gliding speed of digested microtubules on both constructs was reduced by 25- 30%. The reduction in speed was unaffected by increased salt conditions: at 200 mM additional KCl in the assays buffer (BRB80) the reduction of gliding speed was still about 30%: undigested microtubules were transported at $2.14 \pm 0.13 \mu\text{m/s}$ $2.48 \pm 0.18 \mu\text{m/s}$ for NK433 and NKHKtail, while digested microtubules moved at $1.30 \pm 0.11 \mu\text{m/s}$ and $1.58 \pm 0.07 \mu\text{m/s}$, respectively. Histograms of the gliding speeds recorded for digested and undigested microtubules were fitted to a Gaussian distribution and the data were subjected to a t-test to statistically verify that the distributions use sample from two different populations. The t-test indicates that the two mean velocities are significantly different at a level of confidence of 99.9%.

ATPase measurements of dimeric NKin motors on dMT show decreased k_{cat} -values

The determination of k_{cat} -values in an enzyme coupled steady state ATPase assays as described in Woehlke *et al.*, 1997, allowed an independent approach to verify the effect of the digestion on the NKin activity. In brief, the consumption of ATP is enzymatically linked to the oxidation of NADH, the rate of which can be observed photometrically at 340 nm. The rate of change of absorption is determined at varying tubulin concentrations. The increase in ATP consumption with increasing microtubule concentrations can be fitted by a hyperbolic curve, describing the motor as an ATPase that follows basic Michelis-Menten-kinetics (Gilbert and Taylor). The maximal ATP turnover rate of a motor, the k_{cat} , is then back-calculated from the saturation values of the hyperbolic fit. From the same data the $K_{0.5, \text{MT}}$ value, which describes the concentration of microtubuli at which half-maximal activation of the motor occurs, can be determined. This value is interpreted as an apparent affinity to the microtubule (Hackney, 1995)). More accurately, the ratio of $V_{\text{max}} / K_{0.5, \text{MT}}$ is an “apparent” second order rate constant, $k_{\text{bi,ATPase}}$, and therefore, a indirect measure of the motors affinity to the microtubule. Here, the

steady state ATPase of this motor was assayed on both digested and undigested microtubules (Fig. III-7).

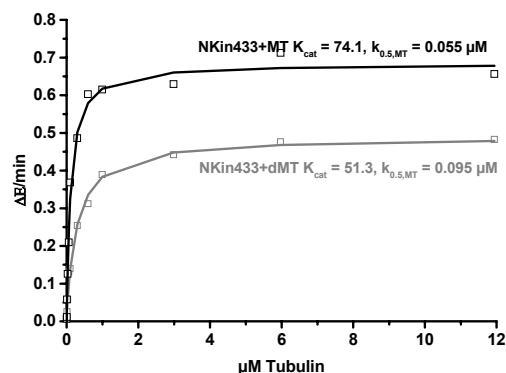


Fig. III-7: Comparison of the ATPase-activity of NKin433 on digested and undigested microtubules

The k_{cat} values for NK433cys on undigested microtubules could be determined very robustly to be 74.1 ± 1.3 ATP/(head*s), which is in very good agreement with previously published values. Also, the $K_{0.5,MT}$ -values obtained from these measurements are in very good agreement, yielding $K_{0.5,MT} = 0.055 \pm 0.008$ μ M.

ATPase measurements with digested microtubules show reduced k_{cat} (54.3 ± 0.8 ATP/(head*s) and increased $K_{0.5,MT}$ values (0.095 ± 0.015 μ M), verifying the effect observed in single molecule fluorescence and multiple molecule gliding assays. The decrease in $K_{0.5,MT}$ values indicates a decrease in affinity of the motor to the microtubule as calculated from the ratio $k_{cat}/K_{0.5,MT}$. This indicates that the processivity of Nkin is measurably reduced in these assays as well. In order to accurately calculate a reduce biochemical processivity (Hackney, 1995) for Nkin on digested microtubules, the true rate of initial binding of the motor to the microtubule had to be determined by mant-ADP release experiments.

Dimeric NK433cys binds at a reduced rate to digested microtubules

To also be able to account in bulk-biochemical assays for the loss of processivity upon digestion, mant ADP-release experiments as first described by Hackney were performed with NK433cys on MT and dMT. In brief, dimeric motors are loaded with mant-ATP, which is quickly hydrolyzed to form a comparatively stable complex of mant-ADP with the NKin

motor. Upon binding of such labeled motors to comparatively high concentrations of microtubules, the motor loses the ADP in the head binding first, resulting in a decrease in fluorescence as the mant-ADP is released from the hydrophobic binding pocket and enters solution where fluorescence is largely quenched. Provided no ATP is present in the solution, the second head, which at this point is still unbound, only very slowly loses its bound mant-ADP. Upon addition of ATP, this step is accelerated several thousand fold and the motor start walking along the microtubule, such that mant ADP releases from the second head and fluorescence reaches a baseline niveau. A titration of such stepwise binding of dimeric Nk433cys on both digested and undigested microtubule is shown in Fig. III-8 A. .

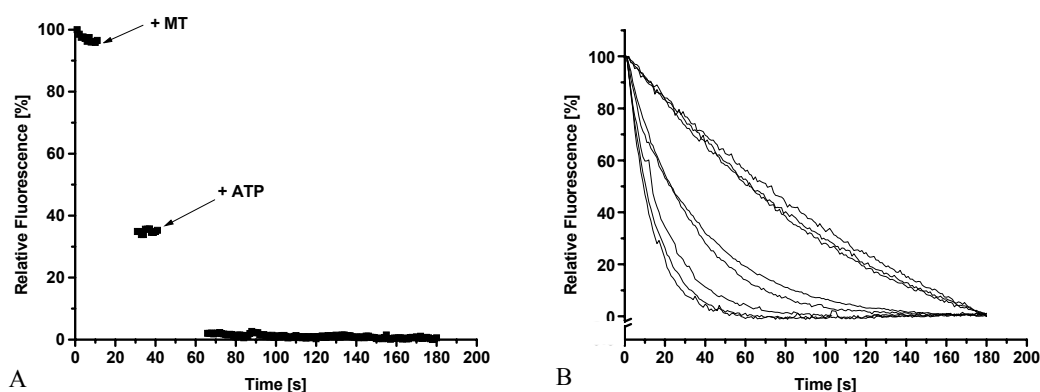


Fig. III-8: Mant-ADP-Titration of dimeric NKin on digested and undigested microtubules

- (A) Mant-ADP-Titration of dimeric NKin on undigested microtubules.
- (B) Exponential fluorescence decay of mant-ADP loaded NK433 at various sub-stoichiometric tubulin concentrations (normalized). Details in the text.

In offering mant-ADP-loaded motors sub-stoichiometric amounts of microtubules in the presence of ATP, however, the rate limiting step is not the hydrolysis of ATP and the subsequent binding of the second head, but rather the initial binding event between the motor and the microtubule. Under such conditions, mixing motor with substoichiometric amounts of microtubules the fluorescence decay can be observed and fitted to a mono-exponential function (Figure III-8). Within sub-stoichiometric microtubule concentrations the rate of exponential fluorescence decay is linearly dependent on the microtubule concentration. A linear fit of these data yields a “true” bi-molecular rate constant, $k_{bi,ADP}$, for the initial binding of the kinesin motor to the microtubule under steady state conditions, in other words the number of encounters of the motors per time per given concentration of microtubules (Figure

III-9). Division of the apparent second order rate constant obtained from steady state ATPase measurements and the true bimolecular reaction constant from mantADP-release measurements allows a biochemical measurement of how many ATP molecules are consumed per diffusional encounter with the microtubule, i.e. a so-called “biochemical processivity”.

$$\frac{(k_{cat} / k_{0.5,MT})}{k_{bi,ADP}} = k_{bi, ratio}$$

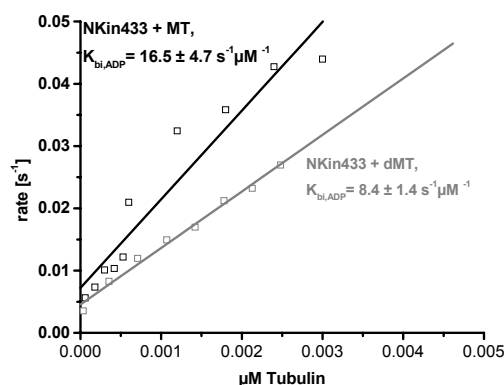


Fig. III-9: Comparison of the rate of ADPrelease, $k_{bi,ADP}$, of NKin 433 on digested and undigested microtubules

Measurements of $k_{bi,ADP}$ for NKin 433cys were performed both on digested and undigested microtubules. As seen in Fig. the second order rate constant for the binding of NKin433cys to dMT is significantly reduced by about 50% from $16.5 \pm 4.7 \mu\text{M}^{-1}\text{s}^{-1}$ to $8.4 \pm 1.4 \mu\text{M}^{-1}\text{s}^{-1}$. Together with the apparent bi-molecular rate constant from ATPase measurements, $k_{bi,ATPase}$, the number of ATPase cycles NKin performs per productive encounter with a digested or undigested microtubule can be calculated. According to this measurement Nkin performs on average 82 ATPase cycles on undigested microtubules and 66 ATPase cycles on digested microtubules. As conventional kinesins tightly couple hydrolysis of ATP to a single step, this corresponds 82 and 66 steps, respectively, in a mechanical experiment. This reduction of the biochemical processivity for 20 % is in close agreement with the values obtained from single molecule fluorescence assays.

Therefore the reduction of processivity and speed of the dimeric motor Nkin433cys upon removal of the E-hook as initially observed in single molecule fluorescence assays could be confirmed in both multiple molecule gliding assays and bulk biochemical assays.

But how can these effects be explained? Docking the crystal structure of Nkin on the binding site on β .tubulin reveals at least two possible interaction sites of the E-hook of tubulin with the motor molecule: 1.) The E-hook could be interacting with the motor in a fashion that leads to faster binding of the leading head, either because the leading head is held in close proximity of the microtubule by an interaction with the dimeric neck domain or by electrostatically “guiding” the leading head to its binding site. Both scenarios suggest an indirect effect of the E-hook on the ATPase activity/gliding speed. This kind of interaction implicates that monomeric NKin constructs do not display reduced ATPase activity upon removal of the E-hook. 2.) The E-hook might directly interact with structures at the ATPase site and thus directly accelerates the ATPase activity of the motor. In this scenario the ATPase activity of monomeric NKin constructs would significantly differ between digested and undigested microtubules.

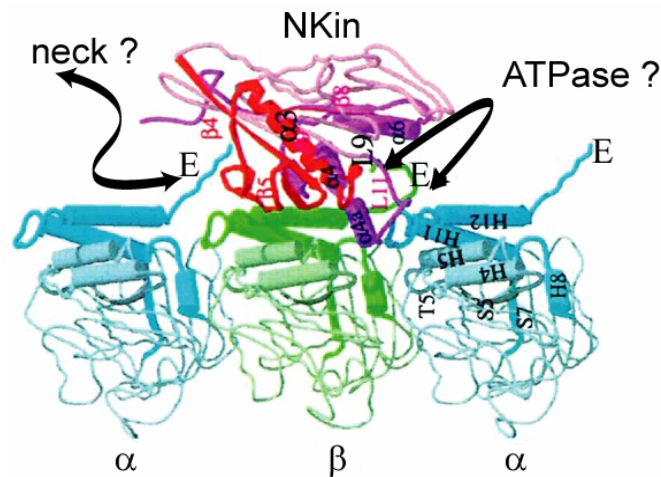


Fig. III-10: Possible interactions of the E-hook with NKin-head

In order to challenge the latter hypothesis we measured the ATPase activity of monomeric Nkin construct NK343cys on digested and undigested microtubules. NKin 343cys comprises only the head domain and the neck.linker structure and is the minimal motor unit of Nkin. It shows very high ATPase values ($k_{cat} = 260 \pm 74$ ATP/(head*s), Kallipolitou, et al. 2001) and therefore should be able to act as a sensitive sensor for direct effects on the ATPase

site. Furthermore, measurement of the $k_{bi,ADP}$ for NK343cys with digested microtubules should indicate, if there is an influence of the E-hook on the rate of productive encounters.

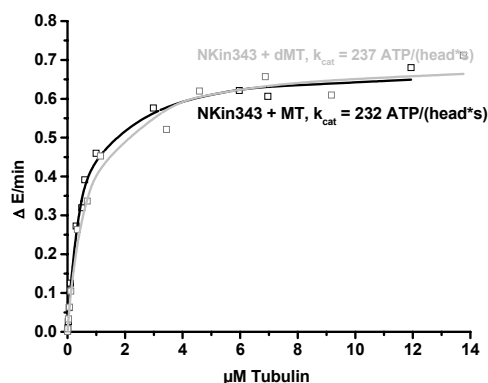


Fig. III-11: Comparison of the ATPase-activity of NKin343 on digested and undigested microtubules

The E-hook does neither affect ATPase nor $k_{bi,ADP}$ of monomeric construct NK343cys.

We determined the k_{cat} -values for the monomeric NK343cys on digested and undigested microtubules in steady state ATPase measurements. Figure III-11 shows representative ATPase-measurements. The k_{cat} for NKin 343cys was determined to be 206 ± 35.8 ATP/(head*s) and 208 ± 25.9 ATP/(head*s) for digested and undigested microtubules, respectively (Fig. III-11). Thus, the ATPase activity of the monomeric construct does not differ between digested and undigested microtubules, indicating that there is no direct effect of the E-hook on the ATPase site.

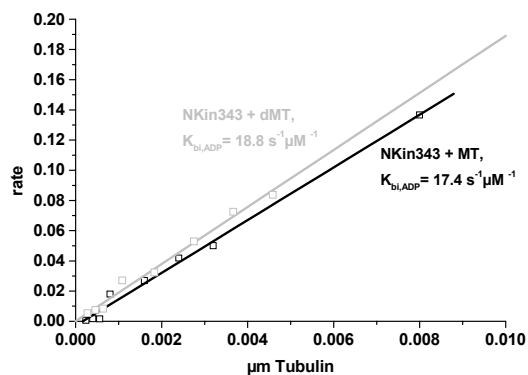


Fig. III-12: Comparison of the rate of ADPrelease of NKin343 on digested and undigested microtubules

To evaluate an effect of the E-hook on the initial binding rate of monomeric constructs, the $k_{bi,ADP}$ for mant-ADP labeled NK343cys was determined in the same manner as for the dimeric construct. The $k_{bi,ADP}$ is determined to be $19.9 \pm 3.4 \mu^{-1}s^{-1}$ for MT $21.7 \pm 4.1 \mu^{-1}s^{-1}$ for dMT. Thus the bi-molecular rate constant for NK343 binding to he MT does not differ between digested and undigested microtubules (Fig. III-12)

Table III-1: Summary of the motile behavior of NKin motors on digested microtubules.

Motor	Single molecule fluorescence assays				Gliding assay		ATP ase				ADP-release	
	Gliding speed		Run lenght		Gliding speed		K_{cat}		$K_{0.5,MT}$		$K_{bi,ADP}$	
	MT	dMT	MT	dMT	MT	dMT	MT	dMT	MT	dMT	MT	dMT
NK433	1.75 ± 0.08 (183)	0.89 ± 0.09 (61)	1.75 ± 0.60 (183)	0.97 ± 0.45 (0.45)	1.72 ± 0.18 (38)	1.25 ± 0.14 (39)	74.1 ± 1.3 (5)	51.3 ± 0.8 (5)	0.055 ± 0.008 (5)	0.095 ± 0.0015 (5)	16.5 ± 4.7 (5)	8.4 ± 1.4 (5)
NK343	n.d.	n.d.	n.d.	n.d.	n.d.	n.d.	206.1 ± 35.8 (2)	208.2 ± 25.9 (2)	0.61 ± 0.15 (2)	0.57 ± 0.12 (2)	19.9 ± 3.4 (2)	21.7 ± 4.1 (2)
NK383	n.d.	n.d.	n.d.	n.d.	n.d.	n.d.	38 (1)	40 (1)	0.5 (1)	1.1 (1)	n.d.	n.d.

Discussion

This study addressed the question whether the highly negatively charged, flexible C-terminus of tubulin, called E-hook, influenced processivity of the fast and highly processive fungal kinesin NKin from *Neurospora crassa*. Several lines of evidence from studies with animal conventional kinesins suggested that an interaction of the E-hook with the positively charged neck enables highly processive movement of these motors. NKin displays a fungal specific sequence pattern in the neck domain, which is reflected in a reduced coiled-coil forming propensity of the first 40 % of the heptade-repeats and a reduced overall positive charge of the neck compared to animal conventional kinesins. These features suggest a reduced electrostatic effect of the E-hook on the processivity of NKin, a motor that shows double the run lengths as compared to conventional kinesins. To test this hypothesis, we wanted to determine if the removal of the E-hook by partial proteolysis with subtilisin reduced processive run lengths, as has been shown for conventional kinesins.

Single molecule fluorescence processivity assays of Cy3-labeled NKin motors (NK433cys) on Cy5-labeled digested microtubules were observed in a prism-based TIRF-microscope. Unidirectional and uniform movement of singly labeled motor molecules was confirmed by kymograph analysis. In these assays the processive run-length of NKin was significantly reduced by about 50%. This reduction in processivity is in agreement with the reduction processive run-length of animal conventional kinesins. However, the reduction for animal conventional kinesins was explained by an strong electrostatic interaction between the positively charged neck-coiled coil and the negatively charged E-hook of the motor. NKin, however, shows only an overall charge of +2 in the neck-domain, compared to +8 in the animal kinesins. Thus, although the reduction in processive run lengths is in agreement with such an interaction, the degree of reduction is surprisingly high. This might be due to additional or alternate effects of the E-hook on NKin, which are unknown for animal conventional kinesins. Indications for additional effects of the E-hook on the performance of NKin-motors also come from the very same experiment: in contrast to animal conventional kinesins, the speed of single NKin motors on digested microtubules is significantly reduced for about 50 %. We confirmed the effects of the digestion on speed on single molecule experiments in multiple molecule gliding assays and bulk-biochemical measurements of both the maximal ATPase turnover, k_{cat} , and the biochemical processivity, $k_{bi, ratio}$, calculated from $b_{i, ADP}$ -values measured with the help of mant-ADP release experiments. Effects of the removal of the E-hook on both ATP-turnover and biochemical processivity are well discernable, although less pronounced than in single molecule fluorescence observations.

Interestingly, the $b_{i, ADP}$ -values measured in this study are significantly higher than values reported earlier (Gilbert *et al.*, 1998; Hackney, 1995; Kallipolitou *et al.*, 2001). Furthermore the titration of the mant-ADP bound to dimeric NKin shows decreases of ~60-70% upon binding to the microtubule, which is in slight disagreement to conventional kinesin (Hackney *et al.*, 2003), but in full agreement with other reports on NKin mant-ADP-release experiments (Schafer *et al.*, 2003). Recent reports suggest that increasing the length of the neck-linker increases the amount of ADP released from the tethered head, as the increased length and flexibility of the connecting structures now allows binding of the second head (Hackney *et al.*, 2003). Therefore, the relatively weak coiled-coil forming propensities of the neck of NKin, which suggest increased flexibility in this region, might explain the

consistently higher amount of mant-ADP released from the second head, as compared to animal conventional kinesins.

Earlier reports on the effect of the E-hook on processive run lengths of single molecule experiments stated only a very small effect of digestion on speed (Wang and Sheetz, 2000; Thorn et al., 2001). This significantly smaller effect on the speed of the motor on digested microtubules might be due to three reasons:

1.) The reduction in speed might have been masked by the large range of speeds reported for the animal conventional kinesin motors, above all Hkin, of $\sim 0.3\text{-}0.8 \mu\text{m/s}$, making it difficult to interpret isolated experiments.

2.) In the processive movement of NKin the E-hook performs functions that act in addition to the mechanism that accounts for the observed small reductions in speed in conventional kinesins. One such additional effect could be a direct interaction of the E-hook with structures of the motor domain, that directly influence ATPase activity.

3.) The E-hook of tubulin influences NKin using mechanisms completely different from an electrostatic interaction with the neck, which is rather weakly, if at all, charged.

The k_{cat} and $K_{0.5, \text{MT}}$ of the monomeric NKin motor, NK343cys, on digested microtubules was not reduced of ATPase turnover as compared to undigested microtubules. Therefore, a direct influence of the E-hook on ATPase activity by interaction with structural elements of this region seemed unlikely. Furthermore, initial binding rates for the monomers as measured by mant-ADP-release do not depend on the E-hook. Rates are, however, on a comparatively high niveau compared to earlier reports, but agree very well with rates for dimeric motors on undigested microtubules. Therefore, the effects of the removal of the E-hook of tubulin on the ATPase and speed of NKin is due to other, more indirect mechanism by which the E-hook accelerates ATPase in the dimeric NKin.

One hypothesis that might possibly explain the effects of the E-hook on processivity and speed of NKin could be a “guiding” effect of the E-hook: The charged E-hook acts as an electrostatic short range “guide” or “threading tool”, that leads to increased binding rates of the second head. Such an effect could be masked by extremely high futile ATP-turnover, but would be mirrored in a reduction of the rate of productive encounters with the microtubule, as measured in ADP-release experiments. Dimeric motors bind only with half the rate to digested microtubules compared to undigested microtubules, supporting such a model.

However, measurement of $k_{bi,ADP}$ for the monomeric NK343cys do not support this view: $k_{bi,ADP}$ values for NK343cys to digested and undigested microtubules are comparable to rates for NKin 433cys to undigested microtubules. The hypothesis of a short-range electrostatic “guidance” by the E-hook would postulate $k_{bi,ADP}$ -values of monomeric NK343cys comparable to the values for Nk433 on digested microtubules. If the E-hook acts as a kind of “guidance” towards the binding site, this would probably have been visible in the ADP-release. As the monomeric NK343 shows extremely high ATPase turnovers, it has been argued, that this motor is only very loosely attached to the microtubule and therefore might not represent a fully comparable model for motor function. Thus additional mant-ADP-release experiments with longer monomers, for example NK383cys and NK391 are necessary to either confirm the measurements performed with NK343cys or further dissect a possible effect of the E-hook in the context of this “guiding” hypothesis. Preliminary ATPase measurements of NKin 383cys motors, however, show no influence of the E-hook on the ATPase activity (Table III-1).

Another hypothesis that might unify the somewhat contradictory results of this work involves an fungal-specific inhibition of the motors head domain by a conserved tyrosine in the neck domain. This hypothesis suggests that the inhibition of ATPase as reported by Schäfer *et al.*, 2003, is mediated not by directly inhibiting the ATPase but rather by inhibiting the binding of the head to the microtubule. The interaction of the E-hook with the neck releases the Y362-inhibition and allows fast binding of the head, resulting in the accelerated ATPases and highly processive movement. This hypothesis, however, postulates that longer monomeric constructs comprising the inhibition-carrying sequences will show reduced $k_{bi,ADP}$ -values, and - depending on their dimerization status – also reduced k_{cat} values on digested microtubules. Further studies with constructs of intermediate length already under way to dissect less complex hypothesis will allow to test this rather complex proposed interaction. Finally, such an interaction of the E-hook with any of the suggested regions of the motor head or neck should to be shown directly by either cross-linking or single molecule FRET.

One explanation for the bimolecular rate constant for NK433cys being significantly reduced ~50 % upon removal of the E-hook has not been mentioned so far involves the affinity of the motor head to the microtubule binding site. If the E-hook is essential part of the motors strong binding state, acting as sealing or lining for the strong binding state of kinesin that is necessary to be established before the motor can communicate strain to the lagging

head, the removal of the E-hook would not only lead to reduced speeds and reduced processivity, it would also result in significantly reduced stall-forces as measured in single molecule trapping experiment. This hypothesis is further explained and challenged in chapter IV.

Chapter IV: NKin generates 5 pN force on both digested and undigested microtubules

Introduction

Kinesin is a microtubule-based, dimeric motor molecule that takes hundreds of steps along a microtubule before dissociating (Howard *et al.*, 1989). Processive movement of conventional kinesin requires the two heads - globular N-terminal domains carrying the microtubule binding and ATPase site - joined in a stable dimer (Hancock and Howard, 1998). Processivity is explained largely by the hand-over hand-model: during a processive run, one of the motor's two heads remains attached to the microtubule until the other head has firmly attached to the subsequent binding site. Only then is the first head released. The binding and release of heads is largely governed by the nucleotide bound (Schief and Howard, 2001). Therefore the alternate stepping of the two heads in processive movement is achieved by carefully keeping the events in the process of microtubule binding, ATP-hydrolysis and detachment of each head out of phase (Gilbert *et al.*, 1998; Hackney, 1995). To achieve this the heads need to communicate their respective nucleotide binding state to each other. The mechanisms of this communication have not yet been completely understood, but an emerging body of evidence suggests that at least one strain-dependent conformational change in the ATPase-cycle (Rosenfeld *et al.*, 2003; Visscher *et al.*, 1999). Thus, in a dimeric motor, the lagging head is able to sense the state of the leading head. While these features can explain the fundamental ability of the motor to move processively, the mechanisms that determine the degree of processivity, i.e. the number of steps taken by a motor on average during a processive run, supposedly also involve structures outside the motor domain: It has been suggested that the positively charged neck of dimeric animal conventional kinesin interacts electro-statically with the highly negatively charged C-terminus of tubulin, the so-called E-hook. Motors with increased overall positive charge in the neck domain shown increased run lengths (Romberg *et al.*, 1998; Thorn *et al.*, 2000). Conversely, the removal of the E-hook by limited proteolysis leads to reduced run lengths (Wang and Sheetz, 2000). Contrary to this model, the fungal conventional kinesin NKin from *Neurospora crassa* shows double the processive run length of animal conventional kinesins while displaying unique properties in the neck coiled coil, including an overall reduced charge of +2 compared to +8 in Hkin (Kallipolitou *et al.*, 2001; Lakamper *et al.*, 2003). Single molecule fluorescence

assays and bulk biochemical experiments, however, show that the removal of the E-hook of tubulin has dramatic effects on both processivity and speed of the motor (see Chapter III). While the proposed electrostatic interaction between the neck and the E-hook can explain part of the observed effects, the reduced charge of the neck domain and the pronounced loss of speed and processivity on digested microtubules suggest that additional mechanisms influencing speed of single NKin motors. A trivial explanation might be that the lattice of binding sites on the microtubule is destroyed and therefore the motor has to search the microtubule for binding sites. This searching-process might slow down the fast-paced NKin considerably more than animal conventional kinesins, which move about half the speed. Electron microscopy studies have not revealed such defects. Also, motors show clearly uniform movement in single molecule fluorescence gliding assays.

Assuming the microtubules structural integrity is not changed by the proteolysis of the E-hook, decreased processivity and velocity of single motor molecules on digested microtubules might be explained by a reduced strength of binding (affinity) of the motor domain to the microtubule in the strongly bound state of the kinesins ATPase cycle. In other words, the E-hook might contribute significantly to the interactions that in total form the strong-binding state of the kinesin motor. Although both processivity and ATP-turnover (speed) are mutually dependent of each other and therefore difficult to view in an isolated model, the proposed hypothesis might explain both decreased run lengths and lowered speeds on digested microtubules independently. A reduced strong binding state can be viewed as a lower affinity-constant of the motors head to the microtubule, defined as the ratio of the rate of attachment and the rate of detachment. Thus, if the dissociation rate of one head is increased upon removal of the E-hook, also the overall dissociation rate of the dimer would be reduced. In other words, the motor dissociates prematurely from the digested microtubule as compared to undigested microtubules, measured as a reduced run-length in single molecule fluorescence assays. If the removal of the E-hook affects the strong binding state of the kinesin motor, reduced speeds during processive movement might be due to a hampered ability of the leading head to communicate strain to the lagging head, necessary to allow hydrolysis and detachment to occur in the lagging head. The communication between the two heads might be slowed down, because the motor might not be able to attach in a conformation stable enough to allow the strain-communicating conformational changes to take place.

Thus a reduced affinity of the motor to the strong binding state on digested microtubules might account for the changes in both speed and processivity. This hypothesis can be challenged by measuring the stall forces of single NKin motor molecules on digested and undigested microtubules in a single bead laser trapping experiments (Block *et al.*, 1990). As a reference, the force generated by single biotinylated HKin motors was measured. To challenge the given hypothesis, the following questions had to be answered

- 1.) How much force do single HKin-motors produce in a single bead laser trapping experiments?
- 2.) How much force do single NKin motors produce in these assays?
- 3.) Does NKin produce comparable forces on digested microtubules?

Results

Cloning and Purification of motors

To be able to specifically attach even shortened motor constructs, motor constructs were designed to carry a reactive cysteine residue in a 10 AA C-terminal sequence. The plasmid pHK560c, intended to carry this tag, actually carried a Stop codon at the position 546. In addition the sequence of the cys-tag was incorrect. As HK560cys and the construct NKHKtail560cys were reference points in this study and the basis for further investigations, the mutations were corrected using site directed mutagenesis according a slightly modified Quick-Change protocol (Stratagene).

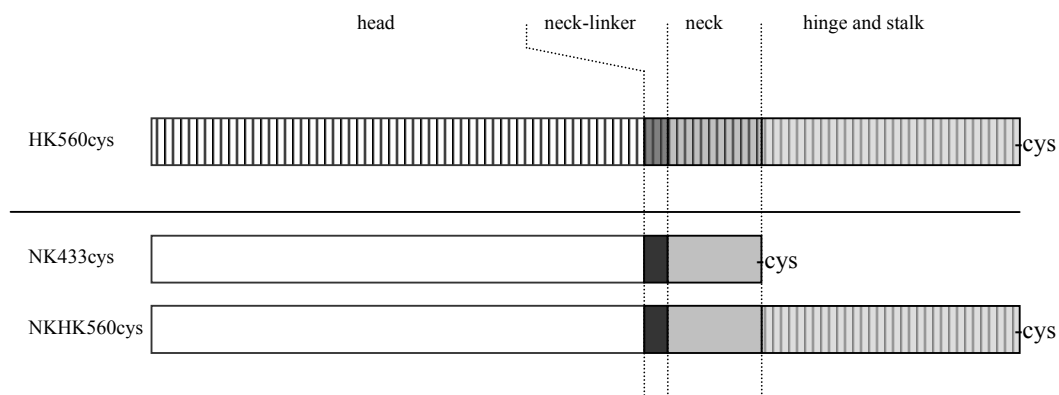


Fig. IV-1: Motors used in this study

Corrected genes were then sub-cloned in a fresh pET17b+- or pT7.7- vector backbone for HKin or NKHK560cys, respectively, using NdeI/XhoI or NdeI/PstI to re-establish a correct original vector backbone. All cloning steps were verified by sequencing. Especially

for HKin the levels of expression were very poor and the yield of corrected protein using the two-step column chromatography of P11 and MonoQ was critical (0.05-0.2 mg/ml, total protein yield ~ 300 µg). Expression levels and purification of NKin was uncritical and yielded comparatively large amounts and high concentrations of motor (1-3 mg total yield).

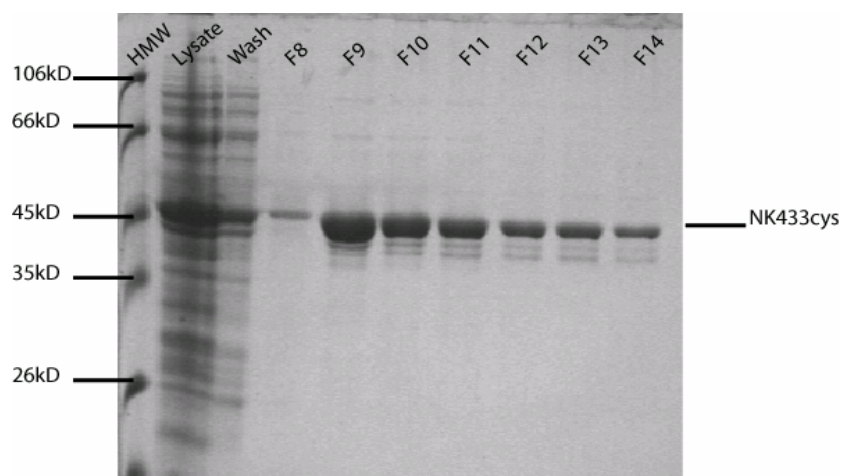


Fig. IV-2: Purification of NK433cys. Fractions 8-10 of the 20% elution contain highest amounts of motor at 90% purity.

Laser trapping nanometry

1 µm latex beads were trapped in the focus of a Yd-YAG-Laser (Schäfter and Kirchhoff, Germany, Ashkin). The signal generated by the interference pattern of the bead on a quadrant photo-detector allowed to observe the thermal fluctuations of the bead in the trap. The trap stiffness of the trap and the sensitivity of detection (nm/V) were calculated by correlating the power-spectrum, fit by a Lorentzian, and the Stokes-behavior of the bead in the trap when moving the stage at defined speeds. Each bead was calibrated before measurements. The calibration of the trap determined stiffnesses in the range of 0.040-0.042 pN/nm, when calibrating far (~10 µm) from the specimen plane. Calibration closer to the surface led to lower trap stiffnesses, most probable due to increasing perturbations by drag effects of the coverslip. Position data were acquired and plotted in a custom program for 128 s (Labview). Data were filtered at 50-150 Hz bandwidth and analyzed by linearly fitting

variable segments of individual single molecule events. Data of many such events were averaged and plotted in a commercial software package (Origin) Representative data traces are shown in Fig III-5.

Biotinylation of HKin and Nkin motors.

Cys-tag containing motors were biotinylated using a biotin-maleimide. A subsequent microtubule affinity purification was performed to select for motors that are both able to bind and detach from the microtubule, suggesting that they are uncompromised by the biotinylation procedure. Usually, about 60% of the protein is lost during such a procedure.

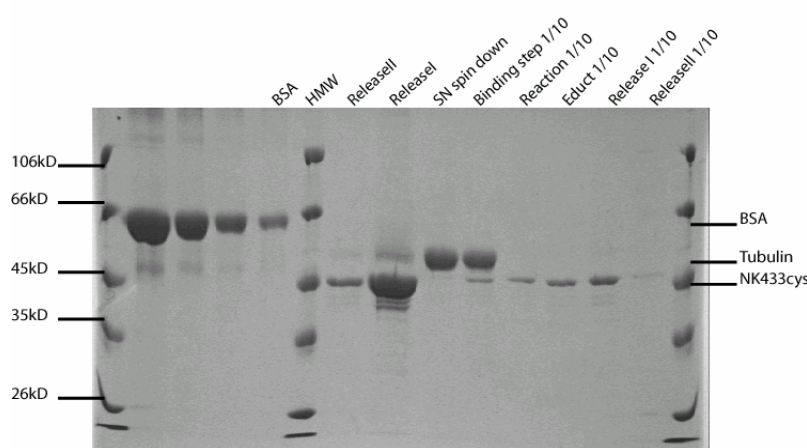


Fig. IV-3: Biotinylation procedure for NK433cys

Gliding speeds of the affinity purified motors show wild type gliding speeds, as summarized in Table IV-1.

Bead assays

Streptavidin coated beads were incubated for 15-30 minutes on ice with decreasing motor concentrations. For further quantifications it was assumed that all motors obtained from microtubule affinity procedures are biotinlyated at the cys-tag and assuming quantitative attachment of all motors present in the incubation mixture to the beads. At motor densities higher than 2000 motors/bead, beads presented to a microtubule in the laser trap started to move immediately and evaded from the trap (Fig. IV-5a). Most of the beads ran to the end of

the microtubule, where they either detached and diffused back into the solution to be re-trapped or they attached to the glass surface. At motor densities of <1000 motors/bead the beads engaged in motile events but were unable to evade from the trap (Fig. IV-5b). Events partially overlapped and sometimes forces produced by the motor molecules were higher than the limiting force of the trap, resulting in beads that evaded the trap regimen. Most of these beads then started to move along the microtubule, but detached before the reached the end, suggesting motor intermediate motor concentrations on the beads. To be able to analyze clearly isolated events of single motors, the motor density was usually further decrease to densities of about 300 -500 motors/bead. Given the geometry of the bead and a statistical distribution of motors on the beads surface, this leads to a the assumption that only individual motor molecules can interact with the microtubule (Fig. IV-5 c). Transient and isolated engagements of the beads were observed and recorded for 123 s intervals.

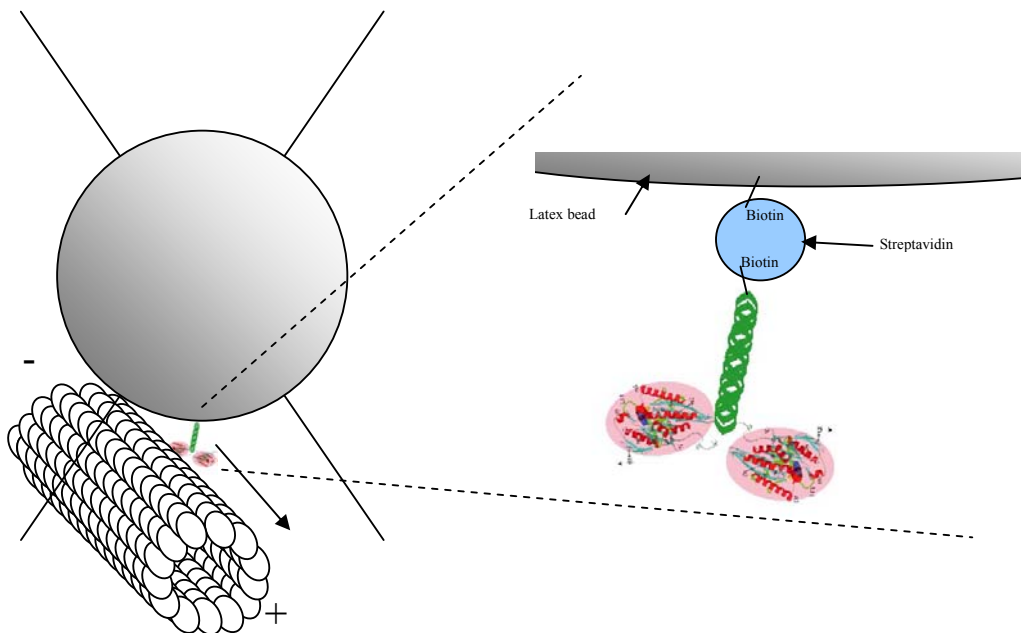


Fig. IV-4: Schematic view of the attachment of the motor to the bead

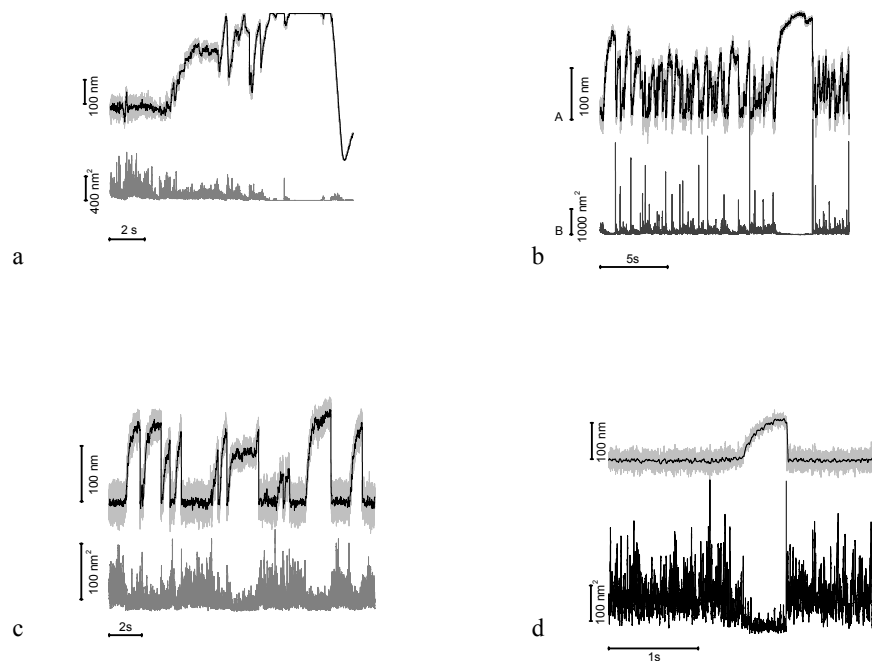


Figure IV-5: Data traces from single molecule recordings at (a) high, (b) intermediate, and (c) low motor density. (d) shows a single isolated event on an expanded time scale. In each panel, upper traces represent acquisition signal (grey) and filtered data (black). Lower traces show the variance of the bead movement.

HKin generates ~5 pN force on undigested microtubules

Multiple isolated events of biotinylated Hkin560cys-motors sparsely coated on Streptavidin-beads were recorded at saturating ATP concentrations (2mM MgATP) and later analyzed using a custom designed program. To determine the velocity of bead movement, segments of varying length (40-300 ms) were fit to linearly to the data. Force and velocity were determined for multiple engagements of many traces. The velocities for intervals of 0.5 pN was averaged for all these events. The force produced was plotted against velocities and the data were fit to a linear regression. Figure IV-3 shows a representative Force-Velocity diagram for HKin560cys .

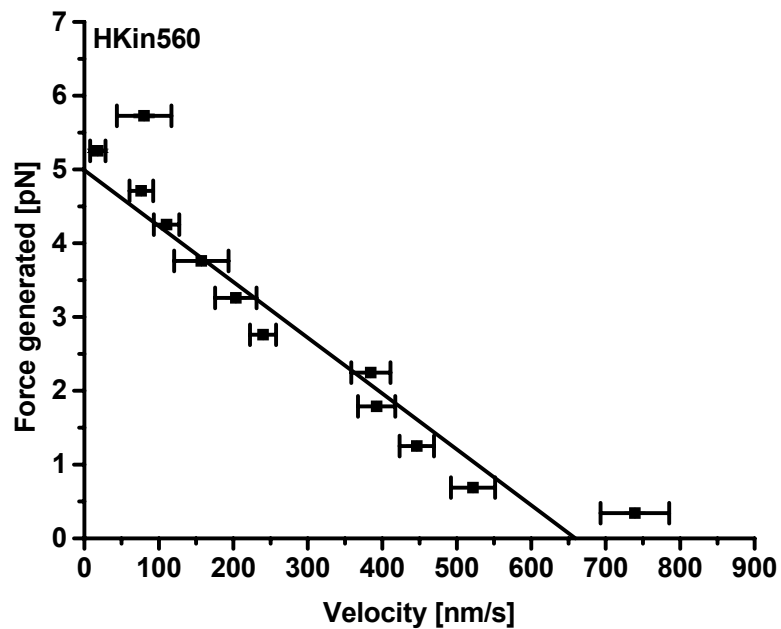


Fig: IV-6: Force velocity diagram for HKin560cys

Data-points represent averages of force and speed of 50-160 individual segments, averaged in 0.5 pN increments. Error bars show square errors of the mean.

The average initial velocity of beads is $0.59 \mu\text{m/s} \pm 0.08 \mu\text{m/s}$. The velocity decreases nearly linearly with increasing force. The average stall force for single biotinlyated HKin-motors is 5.22 ± 0.25 (sd) pN.

NKin generates ~5 pN force on undigested microtubules.

At calculated densities of about 500 motors/bead clearly separated individual engagements of biotinylated NKin433cys and NKHK560cys motors with undigested microtubules could be observed. Events at high ATP (2mM MgATP) displayed the same stereotyped behavior as HKin molecules (Fig IV-5). Force-velocity diagrams were constructed either from individual, later from many traces, comprising multiple, isolated events (Fig. IV-7).

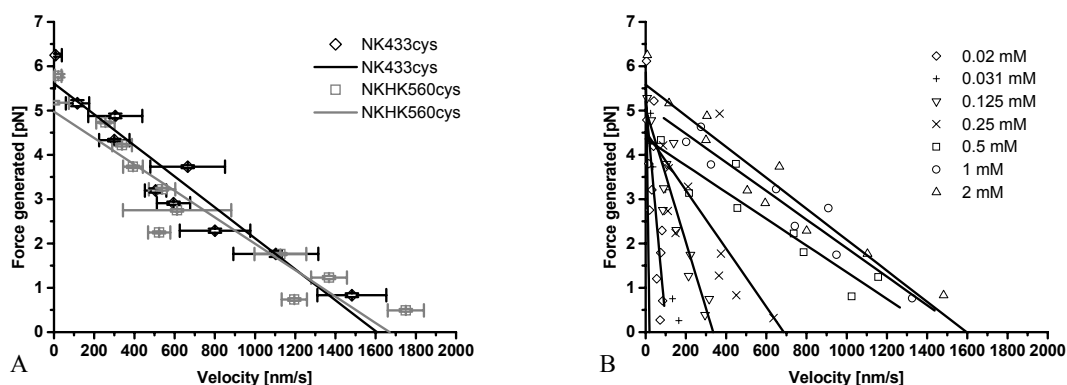


Fig. IV-7: Force-velocity diagrams for NKin motors

(A) Representative force-velocity diagram for NKin-Motors NK433cys (grey) and NKHK560cys (black) at saturating ATP-concentrations. The motors differ very little in initial velocity and force generated. Errors are given as SE of 15-150 individual values.

(B) Force-velocity diagram for NK433cys at different ATP concentrations. Error bars are omitted for easier survey. Linear fits converge at ~5 pN force. Initial speeds are further analyzed in Fig.IV-8

The initial gliding velocity of both biotinylated NK433cys and NKHK560cys is 1.71 ± 0.19 (sd) $\mu\text{m/s}$ and 1.79 ± 0.33 (sd) $\mu\text{m/s}$, respectively. Similar to HKin560cys the velocity decreased with increasing force in a linear fashion. The extrapolated average stall forces for NKin433 and NKHK560cys were determined to be 5.1 ± 0.5 pN and 4.9 ± 0.39 pN, respectively.

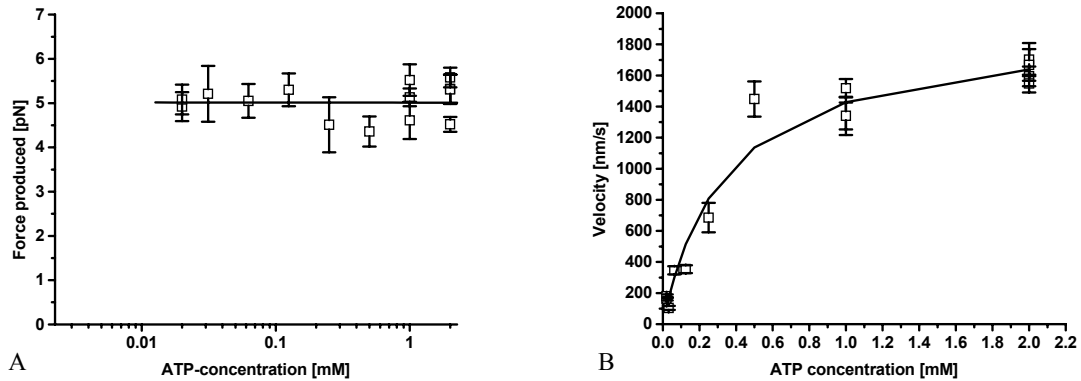


Fig. IV-8:

(A) Dependence of Stall forces of NKin433cys on ATP concentration: The data can be fit with a linear regression of the formula $Y = 5.01 \pm 0.12 - 0.00235 \pm 0.17 * X$ indicating that the stall force is independent of the ATP concentration. All errors are given as standard deviations.

(B) Dependence of Force and initial speed on ATP concentration in NK433. The data are fit to a hyperbolic function following Michaelis-Menten Kinetics. The calculated $K_{M,ATP}$ for NK433cys from this measurement is 0.35 ± 0.12 mM. All errors are given as standard deviations.

The gradual reduction of the ATP-concentration to clearly sub-saturating levels in standardized bead assays, here performed only for biotinylated NK433cys, resulted in gradually decreased motor speeds. The initial speed of these events was plotted against the ATP-concentration (Fig. IV-8B) The data were fit to a hyperbolic function, resulting in a $K_{M,ATP}$ for NK433cys in these bead assays of 0.35 ± 0.12 (sd) mM ATP. The ATP-concentration had no effect on the stall force (Fig. IV-8A).

NKin motors generate ~5 pN on digested microtubules.

After establishing the force-velocity-curves for HKin and NKin single molecule bead assays were performed for NKin motors on digested microtubules. At a given motor concentration NKin motors engaged to the microtubules at comparable rates and the appearance of isolated individual events indicated single molecule interactions.

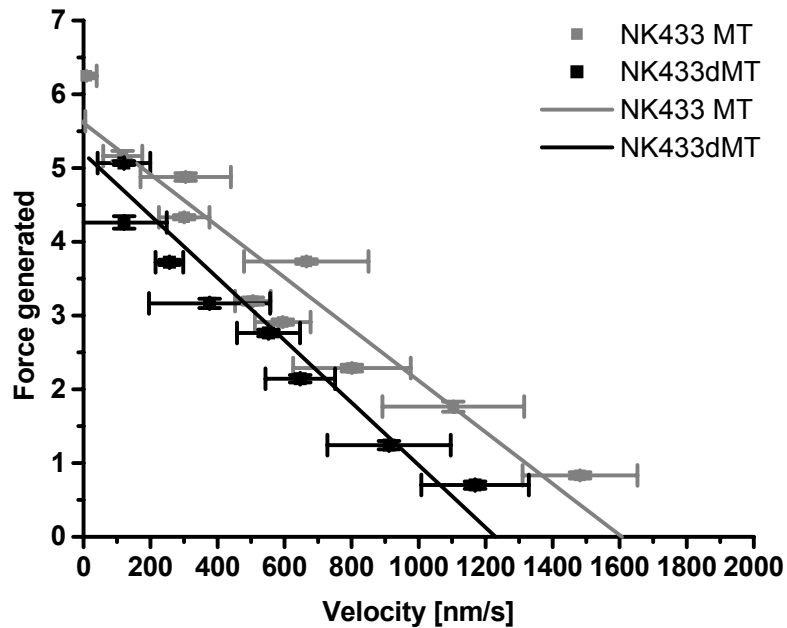


Fig. IV-9: Representative force-velocity diagram for Nk433 on digested microtubules

The force generated by NKin motors on digested microtubules (dMT, black) does not differ from undigested microtubules (MT, grey), whereas the initial gliding speed is reduced by about 30 %. This particular force velocity diagrams were established from relatively few traces with comparatively few segments. Thus, the errors - given as SEM of only 5-50 data points - are comparatively large.

Initial rising phases showed smooth movement. Force-velocity diagrams constructed from individual or multiple traces reveal slightly reduced initial gliding speeds of 1.3 $\mu\text{m/s}$ for both NK433cys and NKHK560cys on digested microtubules. Similarly to movement of NKin on undigested microtubules the velocity of beads movement decreased linearly with increasing forces (Fig IV-9). Stall forces displayed robust values of ~ 5 pN. Initial velocities at decreasing ATP-concentrations were used to extract a $K_{M,ATP}$ of NK433 on digested microtubules. Similar to undigested microtubules the stall forces did not depend significantly on the ATP concentration and remained unchanged at ~ 5 pN.

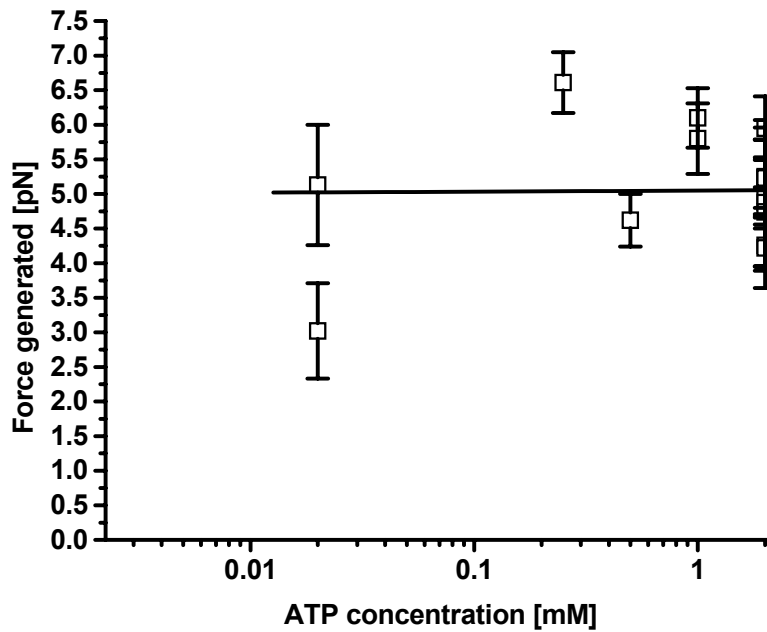


Fig. IV-10: The force generated by NKin-motors on digested microtubules does not depend on ATP-concentrations.

The data can be fit with a linear regression of the formula $Y = 5.05 \pm 0.21 - 0.015 \pm 0.45 * X$ indicating that the stall force is independent of the ATP concentration. All errors are given as standard deviations.

Table IV-1. Summary of trapping results

	MULTIPLE MOLECULE GLIDING ASSAYS			SINGLE MOLECULE TRAPPING EXPERIMENTS			
	$\mu\text{m/s} \pm \text{se (N)}$			$\mu\text{m/s} \pm \text{se (N)}$		$\text{pN} \pm \text{se (N)}$	
	MT		dMT	Initial speeds		Stall forces	
	0 mM KCL	200 mM KCL	0 mM KCL	MT	dMT	MT	dMT
b-Hk560cys	0.65 ± 0.03 (47)	n.d.	n.d.	0.59 ± 0.04 (3)	n.d.	5.2 ± 0.14 (3)	n.d.
b-NK433cys	1.66 ± 0.40 (18)	2.14 ± 0.13 (22)	1.25 ± 0.14 (39)	1.70 ± 0.08 (6)	1.36 ± 0.04 (10)	5.07 ± 0.21 (6)	4.97 ± 0.18 (10)
b-NKHK560cys	1.58 ± 0.18 (20)	2.49 ± 0.18 (19)	1.30 ± 0.11 (30)	1.79 ± 0.15 (3)	1.16 ± 0.17 (2)	4.91 ± 0.17 (3)	5.43 ± 0.28 (2)

Discussion

The goal of this study was to determine, whether the E-hook of tubulin contributes significantly to contacts forming the strong binding state of the motor domain of NKin, by measuring the maximal forces single NKin motors can produce while moving along digested and undigested microtubules. Therefore, it was necessary to first establish a single bead laser trapping experiment using HKin as a reference motor. At saturating ATP-concentrations, streptavidin covered beads sparsely coated with biotinylated HKin motors showed transient engagements with a microtubule, resulting in maximal displacements of the beads from the center of the laser trap that correspond to about 5 pN force. These displacements were believed to be caused by single molecules for three reasons. 1.) Taken together the conservative estimates that all motors in the preparation are biotinylated and all biotinylated motors are quantitatively adsorbed to the streptavidin coated beads, the motor density per bead was calculated to be ~300-500 motors/bead. Under such conditions the geometry of the bead allows only the interaction of single motors with the microtubules. Furthermore, only about every third bead produced movement under such conditions. Most recordings were performed at slightly higher motor densities to allow appreciable rate of data collection. 2.) The displacements were observed not to differ in appearance from one assay to the next or one bead to the next, suggesting that they are produced by a uniformly behaving, uniformly distributed entity, believed to represent a single motor molecule. Assuming irregular aggregates of motors would produce displacements, the signature would also differ in displacements as force generated most probably increases with the number of motors interacting simultaneously. 3.) The forces generated agree to a high degree with several reported values for stall forces of single molecule bead assays for animal kinesins, as well as the initial speed of displacement is in very good agreement with speeds measured in multiple molecule gliding assays performed with biotinylated HKin560cys. The results indicated that in fact force-generation of single molecules was observed. Thus, the experimental setup and procedure is suitable for the determination of stall forces of NKin on digested and undigested microtubules.

The stall forces of the short NKin motor NK433cys and the chimeric motor NKHK560cys using the same experimental conditions as for HKin. The average stall force

does not differ between NKin and NKHK560cys and is determined to be 5 pN on undigested microtubules. The assays were performed at saturating ATP-concentrations in BRB80 buffer without additional salt to ensure comparable conditions to the single molecule assays described in chapter III. Initial gliding speeds of bead displacement agree very well with the speed determined in multiple molecule gliding assays (see Chapter III) for biotinylated NKin433cys and NKHKtail560cys. Stall forces are in agreement with reported values from laser trapping experiments reported by Crevel et al. 1999. In contrast to these measurements, the motor density could be quantitatively reduced to single molecule level. This can be attributed to the highly specific and largely irreversible attachment of the motors to the beads with the Streptavidin-biotin linkage, as compared to the Ni-NTA-His interaction, which was not quantitative (Crevel). Regardless of the difference in attachment, the stall forces and overall behavior of the beads are in very good agreement. As has been reported for animal kinesins the stall forces do not change when reducing the ATP concentration gradually. Although it has been expected to be able to resolve individual steps at very low ATP-concentrations, filtering the data with various time windows did not reveal clearly definable step sizes. The determination of step-sizes is critically dependent on the reduction of thermal noise of the bead upon engagement with the microtubule. This reduction of noise, determined here as a reduced variance, can be interpreted as the addition of another set of springs (the series of linkages from bead to glass surface) to an existing one (the bead in the trap), to yield a series of elastic elements. The stiffness of each element adds to the total stiffness. Therefore, a very high stiffness of each element is desirable. While the covalent attachment of biotin to both bead and motor is rather indefinitely stiff, and the interaction of Streptavidin and biotin has been reported to be extremely stiff, the attachment of the microtubule to the glass surface is rather poorly characterized and controlled. Other methods of unspecific attachment or specific attachments using antibodies or modified kinesins will be used to improve noise reduction and allow step-size measurements. However, there is little doubt about the step size of NKin being 8 nm as has been reported by Crevel et al.

Having established the stall force of single Nkin motors on undigested microtubules, the same set of experiments was performed on digested microtubules. All digestions were checked by SDS-Gel-electrophoresis. At saturating ATP-concentrations the initial gliding speed shows the decreased values, as measured in both single molecule fluorescence and multiple molecule gliding assays. The reduction in speed, however, is about 30 %, corresponding to the reduction in multiple molecule gliding assays of NKin motors, but in

contrast to 50 % as measured in the initial single molecule fluorescence assays. Apart from this value the agreement of speeds measured in multiple motor gliding assays, single molecule fluorescence assays and single molecule trapping experiments for both HKin and NKin is remarkably good. Finally the determination of the stall force of NKin motors on digested microtubules yields values of 5 pN for saturating and sub-saturating ATP-concentrations.

Therefore the results strongly suggest that the removal of the E-hook does not impair the strong binding of the motor domain to the microtubule. The effects on motors speed must therefore be due to another mechanism as proposed in chapter III.

Chapter V: Do conserved Lysine residues in the Neck-linker region of NKin confer fast motility to HKin? – a short analysis of point mutants

Introduction

The dimeric microtubule based motor molecule kinesin is able to take hundreds of successive 8 nm steps along the microtubule. During such processive movements the motor is able to generate forces of about 5 pN (Hunt *et al.*, 1994; Meyhofer and Howard, 1995; Visscher *et al.*, 1999). The energy required for movement and work generated in movement is derived from binding and subsequent hydrolysis of ATP. ATPase-activity and microtubule binding sites are located in the globular N-terminal head domain. Processivity requires a stable dimer which is formed by coiled coil interactions of the so-called neck domain (Hancock and Howard, 1998). The neck is connected to the motor domain by the so-called neck-linker, a short ~10 AA long sequence, that dynamically interacts with the head in a nucleotide dependent fashion. Binding of ATP to the head leads to immobilization of the neck-linker that is highly mobile in both ADP and rigor states of motors bound to the microtubule (Rice *et al.*, 1999). Additional studies reveal that reversible immobilization of the neck-linker by bivalent cross-linkers abolished processive movement (Tomishige and Vale, 2000). Consequently, the neck-linker plays important roles in the generation of movement (Mogilner *et al.*, 2001). Recent crystallographic and EPR studies reveal that the neck-linker is docked in an ADP-state, provided high amounts of sulfate or phosphate ions are present (Sindelar *et al.*, 2002). This is explained by a possible phosphate binding site that allows the stabilization of the docked state of the neck-linker by the phosphate released from the ATPase site after hydrolysis. Furthermore this study reveals a significant movement of the Switch-II cluster as compared to the previously determined monomeric crystal structures with disordered neck-linkers. The movement of this structure suggests an obstructive and unobstructive position of the Switch-II Cluster, a movement that in the stepping cycle might be communicated from the nucleotide sensing Switch-II through Loop11, which links the two structure, but is unresolved in crystal structures (Sindelar *et al.*, 2002). Nevertheless, contacts to the microtubule upon binding of the motor might lock the Loop11 in a stable conformation that could then act as a relay structure. What are the actual contacts that allow the neck-linker

to interact with the microtubule? Do conserved residues in the Neck-linker influence the speed of motor molecules?

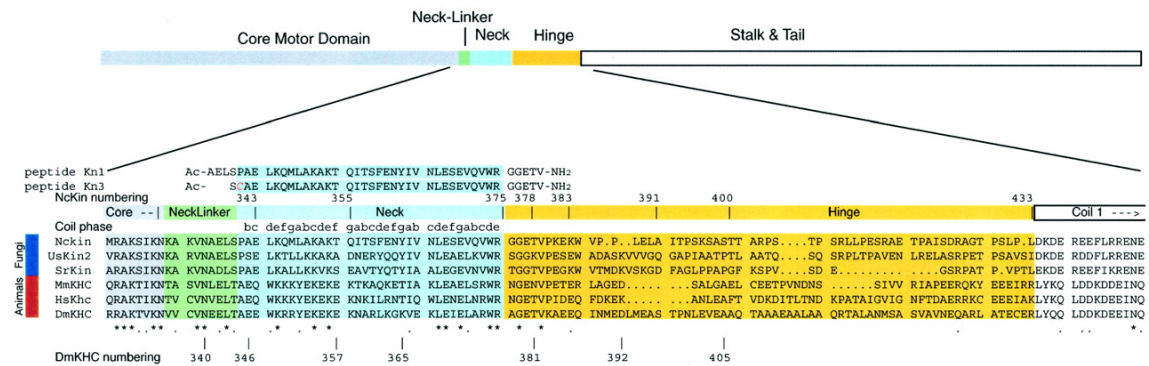


Fig. V-1: Sequence comparison of animal and fungal conventional kinesins (from (Kallipolitou *et al.*, 2001))

The family of fast fungal kinesins shows a high degree of sequence similarity in the motor domain and the neck-linker to animal conventional kinesins. However, two residues that differ considerably are strongly conserved, the positively charged Lysine 332 and Lysine 334 as numbered in NKin, are strongly conserved in all fast fungal kinesins. In UsKin the Lysine 334 is exchanged for an even more strongly charged arginine. All fungal kinesins move at considerably higher speeds than animal conventional kinesins as summarized in Table I. Interestingly, the characteristics of these residues are opposite to those of the corresponding residues in HKin and other conventional kinesins: The homologous residues in mouse and rat kinesin are threonine and serine, carrying hydroxyl groups. In Human kinesin the serine is exchanged for less charged but structurally comparative cysteine. Fig 1 show a sequence comparison of the above mentioned kinesin for the neck-linker and adjacent regions.

While there is no obvious mechanism with which these residues might influence the speed of kinesin motors their strong conservation and the opposite charge of the residues compared to the slower animal kinesins suggest an important function in fast motility of fungal kinesins. To determine a possible effect of the positively charged Lysines, single and double point-mutants of corresponding residues in the comparatively slow motor HKin were mutated to lysine using site directed mutagenesis (HKT28K, HKC330K, HKT328KC330K or short HKTCKK). Their activity was assayed in multiple molecule gliding assays, and in part by ATPase assays.

Results

Point mutants were generated in the context of HK560cys to possibly allow biotinylation and fluorescent labeling for single molecule fluorescence. All correct point-mutants were sub-cloned in the original pET17b+ expression vector and checked by DNA-sequencing. The expression levels of HKin and the mutants were extremely low limiting the yield and therefore the possible applications. Multiple molecule gliding assays were performed for motor preparations directly without freezing to avoid loss of activity and protein. We observe consistently low motor concentrations for all motors in a total three rounds of purifications for each HK560cys, HKT328, HKC330K and HKTCKK. Nevertheless, final motor containing fractions showed stable gliding activity in standard multiple motor gliding assays. Gliding assays were repeated for motors after storing one night at 4°C to check for possible time effects. Motor concentration was sufficient for initial ATPase measurements of HKin560cys and the double mutant HKTCKK but not for the single mutants. Gliding speeds of all assays of column purified motors are summarized in Figure 3 and Table 3.

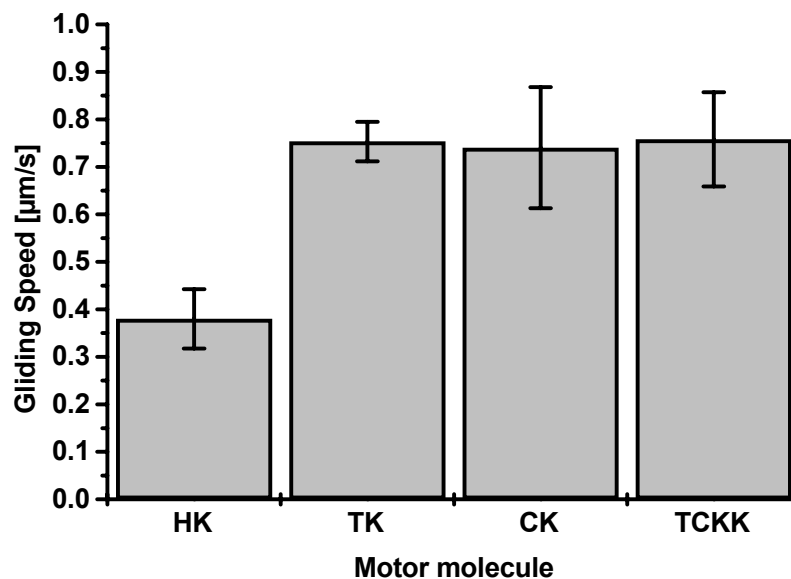


Fig. V-2: Comparison of multiple motor gliding speeds

Gliding Speeds of HK560cys (HK) and the point mutants HKT328K560cys (TK), HKC330K560cys (CK), and HKT328KC330K560cys (TCKK) in multiple molecule gliding assays from freshly purified motors. The average gliding speeds together with ranges of speeds of the motors are summarize in Table V-1.

We observe consistently higher gliding speeds for all the single or double mutants, regardless of the concentration of the motor. The average increase in speed compared to HKin560cys was significant as judged from the standard deviation.

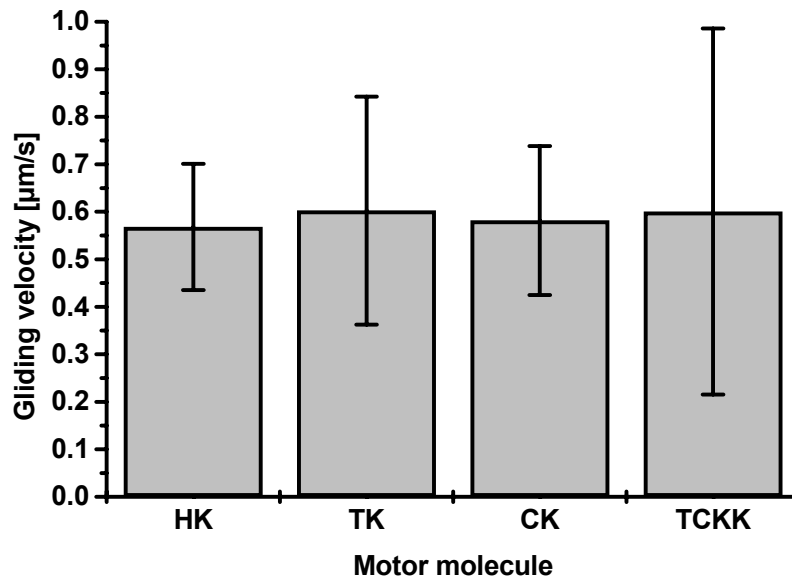


Fig. V-3: Comparison of microtubule affinity purified motors.

Gliding Speeds of HK560cys (HK) and the point mutants HKT328K560cys (TK), HKC330K560cys (CK) , and HKT328KC330K560cys (TCKK) in multiple molecule gliding assays for motors that have been further purified by Microtubule affinity purification after freezing column purified motor. The average gliding speeds together with ranges of speeds of the motors are summarize in Table V-1.

It was tried to purify motors by a MT-affinity purification to test for both the gliding activity of more specifically purified and concentrated motor and to evaluate if motors are concentrated for possible single molecule fluorescence assays. Surprisingly, gliding speeds observed for these microtubule affinity purified mutants were statistically indistinguishable from HKin560cys. ATPase measurements were severely compromised by the extremely low motor concentrations and the errors associated with the determination of motor concentration at these concentrations.

Table V-1: Comparison of gliding speeds of the Neck-linker mutants measured in multiple motor gliding assays

Motor	Assays from column-purified motor	Assays from affinity-purified motor
	Average \pm sd (N)	Average \pm sd (N)
HK560cys	0.36 \pm 0.06 (32)	0.57 \pm 0.13 (39)
HK560cys	0.45 \pm 0.13 (29)	-
HK560cys	0.33 \pm 0.09 (26)	-
HK560cys all	0.38 \pm 0.06 (3)	-
HK T328K	0.80 \pm 0.43 (20)	0.60 \pm 0.24 (39)
HK T328K	0.72 \pm 0.21 (37)	-
HK T328K	0.75 \pm 0.13 (32)	-
HK T328K all	0.75 \pm 0.04 (3)	-
HK C330K	0.89 \pm 0.14 (55)	0.58 \pm 0.16 (60)
HK C330K	0.71 \pm 0.05 (18)	-
HK C330K	0.63 \pm 0.08 (22)	-
HK C330K all	0.74 \pm 0.12 (3)	-
HK T328KC330K	0.90 \pm 0.09 (38)	0.60 \pm 0.39 (41)
HK T328KC330K	0.67 \pm 0.11 (36)	-
HK T328KC330K	0.73 \pm 0.06 (44)	-
HK T328KC330K all	0.75 \pm 0.10 (3)	-

Discussion

The goal of this short study was, to determine whether the substitution of conserved OH/SH-carrying-amino acid-residues T328 and C330 in the neck-linker of HKin with the positively charged lysine, which is strongly conserved in fast fungal kinesins, increases the speed of the HKin motor molecule as measured in multiple motor gliding assays.

The expression of HKin and the mutants HKT328, HKC330K and HKTCKK was extremely low and purification resulted in extremely low yields. These very low expression values seem to represent a flawed expression protocol rather than a errors in the regulating sequences of the plasmid or the actual gene, as the genes were sub-clone in a freshly purchased pET17b+ vector background and the sequence was checked for errors by sequencing. The Expression of HKin motors in this context has been reported previously although no specific reference was made about yields or un-surmountable problems in the expression. However, it has been reported that the levels of protein expression were very low and that a three step column Chromatography was necessary for sufficient protein yields. Microtubule affinity purifications from bacterial lysates did not yield detectable amounts of motor, which might be either due to the low expression level or systematic errors in the purification procedure.

The amount of proteins purified from a two step procedure was sufficient to perform multiple molecule gliding assays. To avoid loss of protein activity due to freezing gliding assays were performed the day of the preparation and after storing the protein on ice in the 4°C fridge to check for loss of activity. HK560cys showed gliding values that were significantly below gliding speeds observed for biotinylated and Cy3-labeled HKin motors purified by microtubule affinity used in the laser trapping experiments and single molecule fluorescence assays described in the previous chapters. However, three independent preparations of Hkin 560cys under identical conditions showed gliding speeds of 0.38 ± 0.06 $\mu\text{m/s}$. These values are inconsistent with values measured earlier in our hands but are within the range reported in several studies using exactly this motor construct.

The three mutant HKin560cys motors were purified under the same conditions. Surprisingly, multiple motor gliding assays of freshly purified mutant motors displayed significantly increased average gliding speeds compared to HKin560cys preparation. In contrast to fresh preparations, a single set of motors further purified by microtubule binding and release protocols display indistinguishable speeds of about 0.6 $\mu\text{m/s}$. However gliding speeds of microtubule affinity purified motors HkT328K and HKTCKK show increased standard deviations.

Ultimately, single molecule studies of these mutant motors are necessary to determine their speed and the processivity. Unfortunately, Cy3-labeling mutant motors was again impaired by the low amount of motors purified. While the amount was enough to perform MT-affinity purifications in principle, the additional chemical reaction with Cy3-maleimide caused the motor concentration to drop even lower, impairing single molecule fluorescence gliding assays as described for HKin in chapter II. Expression studies to overcome these limitations are currently under way.

Summary and outlook

Conventional kinesins are two-headed molecular motors that move as single molecules micrometer-long distances on microtubules by using energy derived from ATP-hydrolysis. The presence of two heads is a prerequisite for this processive motility, but other domains, like the neck, influence the processivity and are implicated in allowing some single-headed kinesins to move processively. NKin is a phylogenetically distant, dimeric kinesin from *Neurospora crassa* with high gliding speed and an unusual neck domain. We quantified the processivity of NKin and compared it to human kinesin, HKin, using single molecule gliding and fluorescence-based processivity assays. Our data show that NKin is a processive motor. Single NKin molecules translocated microtubules in gliding assays on average 2.14 μm (N=46). When we tracked single, fluorescently labeled NKin motors they moved on average 1.75 μm (N=182) before detaching from the microtubule, while HKin motors moved shorter distances (0.83 μm , N = 229) under identical conditions. NKin is therefore at least twice as processive as HKin. These studies, together with biochemical work, provide a basis for experiments to dissect the molecular mechanisms of processive movement.

Kinesin's processive movement requires coordination of the ATPase cycles of both heads. Recent work suggests that electrostatic interactions of tubulin's C-terminus (E-hook) with the neck of human kinesin (HKin) increase the processivity: removal of the E-hook by partial digestion of microtubules with subtilisin (dMT) reduces run lengths, and HKin constructs with multiple neck domains have increased run lengths on MT.

To investigate the role of the neck in processive movement, the run length of fast fungal kinesin NKin (NKin433) on dMT was determined using single molecule fluorescence assays. The average run length of NKin drops from $1.75 \pm 0.08 \mu\text{m}$ to $0.89 \pm 0.09 \mu\text{m}$ on dMT. Surprisingly, and in contrast to HKin, the gliding speed of NKin along dMT also decreases from $1.75 \pm 0.60 \mu\text{m/s}$ to $0.97 \pm 0.45 \mu\text{m/s}$. The reduced gliding speed is consistent with the reduced steady state rate of ATP-hydrolysis (k_{cat}). However, the k_{cat} of the monomeric NKin-construct NKin343 does not differ between MT and dMT. This result strongly suggests, that the E-hook does not influence the ATPase directly, but rather increases the speed of NKin via an interaction that allows either accelerated binding of leading head or accelerated communication of the two heads in processive movement.

These findings may be explained by at least two hypotheses: 1.) The motor directly interacts with the E-hook, accelerating binding of the leading head but leaving the kinesin binding site unaltered. 2.) In the strong binding state, the E-hook is integral part of the motor's binding site on the microtubule, suggesting that during processive events stall forces are significantly reduced if the E-hook is removed. In order to test the latter hypothesis we measured force-velocity response and stall forces of NKin motors on MT and dMT. The displacement of streptavidin-beads, sparsely coated with biotinylated NKin motors, was recorded in a single bead laser-trapping assay. We observe stall forces of ~ 5 pN for both MT and dMT. We conclude that interactions of the dimer with the E-hook of tubulin accelerate stepping kinetics. Cross-linking experiments are in progress to determine whether the neck is fact the interaction partner of the E-hook.

Processive movement is explained by the alternating head catalysis model and the hand-over hand-model. Speed of kinesin movement is most probably determined by the inherent maximal ATPase activity of the motor domain and limited by connecting structures to allow coordinated movement. The so-called neck-linker, a short β -strand that links the motors head domain to the coiled-coil-forming neck, has been shown to undergo nucleotide-dependent movement. Cross-linking studies revealed that mobility of this domain is critical for the generation of movement and processivity. But does it also influence the speed of kinesin motors? Here, two Threonine- and Cysteine-residues in Hkin, which are weakly conserved in animal conventional kinesins, were substituted with Lysine-residues, strongly conserved in the neck linker of fast fungal kinesins. In direct comparison to HKin in multiple motor gliding assays, however, the mutants displayed significantly increased gliding speeds. Further more detailed investigations using single molecule and bulk biochemical approaches will be performed to determine, if these findings can be confirmed with independent methods.

Appendices

Methods

Unless stated all chemicals were purchased from (Sigma-Aldrich, St.-Louis, MO, USA). Restriction enzymes and DNA-modifying enzymes were obtained from New England Biolabs (NEB, Beverly, MA, USA.)

Molecular biology methods

Vectors

The following vectors were used for cloning and expression.

pET17b+ (Novagen, Madison, USA)

pT7.7 (Tabor, 1990)

Bacterial strains

The following E.coli strains were used for cloning and expression

DH5 α (Invitrogen)

BL21 RIL

BL21 (Studier et al., 1990)

BL21 star (Invitrogen)

Media

LB medium

1 % (w/v) Trypton (Bacto trypton, Gibco)

0.5 % (w/v) Yeast Extract (Gibco)

0.5 % (w/v) NaCl

or LB broth Sigma L 3022

TPM medium

2 % (w/v) Trypton (Bacto trypton, Gibco)

1.5 % (w/v) Yeast Extract (Gibco)

0.8 % (w/v) NaCl

0.2 % (w/v) Na₂HPO₄

0.1 % (w/v) KH₂PO₄

after autoclaving add 1% (v/v) 1M Glucose (sterile,), resulting in a final 0.2% (w/v) Glucose.

SOB Medium
 2 % (w/v) Trypton
 0.5 % (w/v) Yeast Extract
 10 mM NaCl
 2.55 mM KCl

SOC-Medium

SOC medium is SOB-Medium supplemented with 20 mM Glucose (sterile, add after autoclaving the SOB medium)

TB-medium

10 mM PIPES
 55 mM MnCl₂
 15 mM CaCl₂
 250 mM KCl

Antibiotics

Ampicilin 50 mg/ml is 1000x stock
 Kanamycin 50 mg/ml is a 1000x stock

Primers/Oligonucleotides

Primers were either purchased from Novagen (Madison, WI, USA), Invitrogen (Carlsbad, CA, USA) or Thermo Hybaid (Ulm, Germany).

Name	Sequence (5'-3')	Purpose
T7 Promotor	TAATACGACTCACTATAGGG	Sequencing
T7 Terminator	CCGCTGAGCAATAACTAGC	Sequencing
HK1 upstream	GCACAGTCATTATACACTTGC	Seuquencing
N-Term I	CGACAGGAGCACGATCATGCGC	Sequencing
N-Term II	CCAGAAGGCATGGGAATTATTCC	Sequencing
N-Term III	GCTCTTGAAATGTTATTTCTGC	Sequencing
N-Term IV	GCAACCGCAATTGGAGTTATAGG	Sequencing
C-Term I	CCGGATATAGTTCCTCCTTTTCAGC	Sequencing
pNK433_103-123 down	rc CTCTGCCTGAAAGCCGTGCC	Sequencing
pNK433_103-124 up	GGCACGGCTTTCAGGCAGGAGC	Sequencing
pNK433_14-37 up	GACAGCTTATCATCGATGATAAGC	Sequencing
HK560cysrepairFWD1	GGAAATGACCAACCACCAGAAAAACGAGCAGCTGAGAT GATGGC	Repair stop
HK560cysrepairREV1	GCCATCATCTCAGCTGCTCGTTTTTCTGGTGGTTGGTCAT TTCC	Repair stop
HK560cysrepairFWD2	GGAAATGACCAACCACCAGAAAAACGAGC	Repair stop
HK560cysrepairREV2	GCTCGTTTTTCTGGTGGTTGGTCATTTC	Repair stop
Hkeys repair fwd	CCGCTATTGTGCATCGTAAATGCTTTTAATCTAGACTCGA GCAGATCC	Repair cys- tag

Hkys repair rev	GGATCTGCTCGAGTCTAGATTTAAAAGCATTTACGATGCAC AATAGACGG	Repari cys- tag
NK433cys G238Aforward	GATCTGGCTGCTTCCGAAAAAGTC	Introduces G238Amuta tion in Nkin
NKG238Areverse	GACTTTTTTCGGAAGCAGCCAGATC	Introduces G238Amuta tion in Nkin
HK560cysC330K- 1forward	GCCAAAACAATTAAGAACACAGTTAAAGTCAATGTGGAG	Introduces C330K
HK560cysC330K- 1reverse	CTCCACATTGACTTTAACTGTGTTCTTAATTGTTTTGGC	Introduces C330K
HK560cysT328K- 1forward	GCCAAAACAATTAAGAACAAAGTTTGTGTCAATGTGGAG	Introduces T328K
HK560cysT328K- 1reverse	CTCCACATTGACACAAACTTTGTTCTTAATTGTTTTGGC	Introduces T328K
HK560cysT328KC330K -1forward	GCCAAAACAATTAAGAACAAAGTTAAAGTCAATGTGGAG	Introduces T328KC330 K
HK560cysT328KC330K -1reverse	CTCCACATTGACTttAACTtTGTTCTTAATTGTTTTGGC	Introduces T328KC330 K

Agarose Gel-Electrophoresis

Analytical or preparative separation of DNA Fragments was performed by electrophoresis in 1%-1.5% Agarose Gels in TAE. For preparative Gels, special low melting agarose (Invitrogen) was used to avoid contamination with substances that inhibit ligation. The Agarose was stirred into TAE and then heated to boiling temperatures in a household microwave til the agarose was completely dissolved. The DNA was mixed with 6x loading buffer before loading on the gel. Electrophoresis was performed at voltages between 60 V and 200 V depending on size of the gel and concentration of agarose. DNA was labeled by incubating the gel in TAE supplemented with low amounts Ethidium-Bromide (0.05 µg/ml). Ethidium-bromide fluoresces at 590 nm under illumination with UV light (absorption maxima at 254 nm , 366 nm and 302 nm). The fluorescence increases 25-fold if incorporated in DNA, which allowed detection and documentation of the separation of DNA Fragments in agarose gels with a commercial photo documentation system (Eagle Eye, Biorad, or GelDoc, Biorad). For preparative gels the gels were illuminated at 302 nm to reduce the possibility of UV induced mutations.

TAE 50x stock solution

2 M Tris-Acetate
50 mM EDTA

TAE 1x

40 mM Tris-Acetate
1 mM EDTA

Agarose Gel

1-1.5% (w/v) Agarose in TAE 1x

DNA Isolation from Agarose Gels

DNA bands corresponding to the desired molecular weight were cut out of the stained 1.5% Low melting agarose gel with a stainless steel cutting device. The pieces were weighed in a sterile Eppendorf cup. The extraction of DNA was performed with the “QuiaQuick GEL-Extraction kit” from Quiagen, Inc..

Determination of DNA concentration

The determination of the DNA concentration was determined spectrophotometrically at a wavelength of 260 nm.

Usually a 1/100 dilution of DNA in distilled water was measured and the concentration of the initial solution calculated simply by multiplying the Photometer reading by 5. This corresponds to 50 µg/µl DNA = 1OD, as referred by Sambrook et al 1989.

Purification of Plasmid-DNA

The Preparation of Plasmid DNA relies on short alkaline lysis of bacteria followed by either a iso-propanol precipitation for Mini-Preps or an selective anion-exchange process for large scale Midi/Maxi-Preparations. We used both buffers and cartridges from the Quiagen Plasmid Purification kits.

Mini-Preps

Bacteria of a single colony on Media plates were inoculated in 3-4 ml LB medium with the appropriate antibiotic. The cultures were shaken at 37°C and 200 rpm over night. The bacteria were harvested by centrifugation for 30 min at ~3000 x g for 20-30 min at 4°C. Pellets were resuspended in 250 µl of P1 and incubated for ~20 min. Then 250µl of P2 is added and the mixture is inverted 5-6 times. Then 250 µl of P3 are added and the mixture is again inverted 5-6 times. The cell debris are removed by centrifugation at 13000 rpm for 20 min in a tabletop centrifuge. The 750 µl supernatant are transferred in a fresh sterile Eppendorf cup and the same volume of fresh iso-propanol is added. Precipitated DNA is sedimented by centrifugation at 13000 rpm for 60 min at RT. The supernatant is carefully removed. To reduce the amount of salt present in the DNA, the pellet is again washed by adding 250 µl of 70% cold Ethanol and a subsequent centrifugation at 13000 rpm for 15 at RT. The Supernatant is carefully removed and the DNA dried. For subsequent use the DNA is resuspended in 30-50 µl distilled sterile water.

Midi/Maxipreps

Bacteria of a single colony on Media plates were inoculated in 50-250 ml LB medium with the appropriate antibiotic. The cultures were shaken at 37°C and 200 rpm over night. The

bacteria were harvested by centrifugation for 30 min at $\sim 3000 \times g$ for 20-30 min at 4°C. depending on the culture volume and the size of the pellet it was determined if a midi (4 ml steps) or maxi-prep (10 ml steps) was performed. Pellets were resuspended in 4 or 10 of P1 and incubated for ~ 20 min. Then 4 or 10 ml of P2 is added and the mixture is inverted 5-6 times. Then 4 or 10 ml of P3 are added and the mixture is again inverted 5-6 times. The cell debris are removed by centrifugation at 20000 g for 20 min at 4°C. The supernatant is transferred on a pre-equilibrated Midi or Maxi column. To prevent cell debris from clogging the column material, the supernatant is poured through gauze. The loaded column is washed twice with either 10 or 30 ml of wash buffer. Bound DNA is eluted with 5 or 10 ml Elution buffer. The eluted DNA is precipitated by addition of 0.7 x Vol Iso-Propanol. The DNA is sedimented at 20000xg for 60 min at 4°C and the supernatant is carefully decanted. The DNA pellet is washed with 3-5 ml Ethanol and a last Centrifugation at 20000xg for 10 min at 4°C. The supernatant is removed and the DNA pellet is dried. Dried DNA is resuspended in 50-200 μ l of sterile distilled water.

P1

50 mM Tris-CL
10 mM EDTA
100 μ g/ml RNaseA
pH 8.0
store at 4°C

P2

200 mM NaOH
1% (w/v) SDS
store at RT

P3

3.0 M Potassium-Acetate
pH 5.5
store at 4°C

QBT - Equilibration buffer

750 mM NaCl
50 mM MOPS
15% (v/v) iso-Propanol
pH 7.0
store at RT

QC - Wash buffer

1.0 M NaCl
50 mM MOPS
15% (v/v) iso-Propanol
pH 7.0
store at RT

QF – Elution buffer

1.25 M NaCl
50 mM MOPS
15% (v/v) iso-Propanol
pH 7.0
store at RT

Restriction of DNA

For analytical restrictions, varying amounts of DNA were incubated with max. 1 μ l of Enzyme (or 0.5 μ l of two enzymes) in a 10 μ l reaction mix for 1h at 37°C. A typical digestion would include 2-5 μ l of mini-prep-DNA (0.1-0.5 μ g/ μ l). This corresponds to about 1-5 U Enzyme per 1 μ g DNA.

For preparative restrictions of plasmid DNA about 10 μ g of DNA are cut with 5 U/ μ g DNA of each enzyme for 1 h at 37°C. The Restriction enzymes were heat inactivated by incubation at either 65°C or 85°C for 20 min depending on the used enzyme. For preparative restrictions of PCR-products close to the ends, the isolated PCR-DNA was rather cut at 37°C over night.

Dephosphorylation of 5'-ends of DNA

To reduce the probability of relegation of restricted vectors in ligations, the cut vector-DNA is dephosphorylated by incubation of 100 μ l of 0.1 μ g/ μ l restricted DNA with 1 μ l of Calf Intestinal Phosphatase (CIP) for 1 h at 37°C. The Enzyme is subsequently heat inactivated at 65 °C for 20 min.

Ligation of DNA Fragments

Ligation of cohesive (sticky) restricted DNA fragments is mediated by T4-DNA ligase in an ATP containing buffer. Reaction volumes varied from 10 -25 μ l, mainly depending on the concentration of isolated insert DNA. Usually, the reaction contained equal or three fold amounts of insert DNA over the vector DNA. A relegation control of the cut vector without insert was included. The ligation was performed at 16°C over night. The enzyme was heat inactivated for 20 min at 65°C. Ligation products were usually checked on a agarose gel and 1-2 μ l of the ligation was transformed in SEM-competent or Electrocompetent E.coli.

Preparation of competent bacteria

Electro-competent bacteria

The transformation of DNA by electroporation works by transiently disrupting the cell walls of bacteria in very low salt solutions, usually water, by applying a short pulse of high voltage. The transformation efficiencies are considerably higher than heat shock transformations.

A single colony of E.coli was inoculated in 50 ml of LB medium. The culture was shaken over night at 37°C and 190 rpm. Each 25 ml of the over night culture were inoculated in 500 ml prewarmed LB medium in a 2 l flask. At an OD600 of 0.4 the flasks were rapidly transferred to a water/ice bath to cool down the culture for about 15-30 min. The cells are centrifuged in sterile, ice cold centrifuge bottles for 15 min at 1000xg and 4°C. The pellet is carefully re-suspended in 500 ml ice-cold sterile distilled water. The cells are again sedimented for 15 min at 1000xg for 20 min at 4°C. The pellet is carefully resuspended in 250 ml sterile ice-cold 10%Glycerol, before sedimenting again for 20 min at 1000xg at 4°C. After resuspending the pellet in 10 ml sterile ice-cold 10%Glycerol the suspension is centrifuged in a sterile conical tube for 20 min at 4°C and 1000xg. The cells are resuspended in 1 ml of GYT medium and the concentration of cells is determined photometrically (1.0 OD₆₀₀= ~2.5 10⁸ cells/ml). The concentration os adjusted to 2-3 x 10⁸ cells/ml. Aliquots of 50 µl are frozen in liquid nitrogen and stored at -70 °C. (Sambrook)

Solutions

Sterile distilled Water

Sterile 10% (v/v) Glycerol (molecular biology grade)

GYT medium

10% (v/v) Glycerol

0.125 (w/v) yeast extract

0.25 (w/v) tryptone

Heat-shock competent bacteria

A single colony of E.coli was inoculated in 100 ml of LB or SOB medium in a 1 l flask. At an OD600 of 0.4 the suspension was rapidly transferred into sterile ice-cold conical tubes which are subsequently cooled for 10 min on ice. The cells are recovered by centrifugation at 2700xg for 10 min at 4°C. after decanting the medium, the cells are resuspended in 30 ml in MgCl₂-CaCl₂ solution and centrifuged again for 10 min at 4°C and 2700xg. The resulting pellet os resuspended in 2ml CaCl₂ solution/ 50 ml initial culture medium. Aliquots of 50 µl are frozen in liquid nitrogen and stored at -80 °C.

CaCl₂-solution

1M CaCl₂ x 2H₂O in distilled water

MgCl₂-CaCl₂-solution

80 mM MgCl₂

20 mM CaCl₂

SEM competent cells

A single colony was inoculated in 3 ml LB and incubated over night. The initial culture was transferred to 250 ml of SOB medium and incubated at 37°C and 190 rpm until the OD reached 0.6. The flask was rapidly transferred to a water/ice bath and cooled down for 15 min. Cells were harvested at 2500xg for 10 min at 4°C and the pellet was re-suspended in 100 ml ice cold TB medium. After sedimenting the cells again at 2500xg and 4°C for 10 min the bacteria were re-suspended in 20 ml TB medium and, after adding 7% DMSO, 50 µl aliquots were rapidly frozen in liquid nitrogen. The cells were stored at -80°C til used.

Transformation of DNA in E.coli

Electroporation

A 50 µl aliquot of electrocompetent cells was slowly thawed on ice. 1-2µl of a DNA solution (usually 0.1µg/µl or ligation mixture) was pipetted in a fresh sterile eppendorf cup. The competent cells were carefully pipetted on the DNA and slowly aspirated to mix and subsequently transfer the mixture to a fresh or recycled electroporation cuvette (0.1 cm gap, biorad). To avoid arcs bubbles were removed from the cuvette by slightly tapping the cuvette. The cuvette was placed in the electroporation device. Bacteria were transformed with a short pulse of 2.5 kV, at a field strength of 25 mF and a resistance of 2000Ohm. Usually time constants of successful transformations were in the the range of 1.9-2.8 ms. After successful pulses the cells were rapidly resuspended in 1 ml of warm SOC medium and transferred to a sterile Eppendorf cup. The resuspended cells were shaken for 30 min at 37 °C in an incubator shaker to allow the cells to express the antibiotic resistance genes. Usually the cells were subsequently sedimented at 3000 rpm for 15 min and the supernatant was removed except about 50 µl. The remaining medium was used to resuspend the cells and plated out to a pre-warmed LB-Agar-plate with the appropriate antibiotic (LB-AMP-Agar) and incubated over night at 37°C in an incubator.

Heat-schock transformation

A aliquot of PEG- or SEM competent cells is slowly thawed on ice. 1 µl of plamid-DNA (usually 0.1µg/µl) is added and the reaction is incubated on ice for 30 min. The eppendorf cup is then placed in a 42°C water bath for exactly 30 seconds and then again placed on ice for about 3-5 min. The cells were either directly plated out or first shaken with LB or SOC medium as described for electrocompetent cells.

PCR reaction

PCR reactions use thermostable DNA polymerases and an excess short defined oligonucleotides (short oligo's or primers) to amplify specific DNA-Sequences from a template-DNA by repeated denaturing, annealing and elongation cycles.

Usually, a reaction consisted of 1 µl template DNA (0.1 µg/µl), 2.5 µl of each primer (10 pmol/µl) and 0.75 µl of Thermostable DNA-Polymerase (Expand polymerase, Roche), and 200 µM dNTP in a 100 µl reaction including the PCR-buffer containing 25 mM MgCl₂. The standard cycling program consisted of an initial denaturation step at 95 °C for 2 min, followed by 30 cycles of denaturing for 30 seconds at 95°C, annealing for 30 s at 50 °C, and elongation for 2 min at 72°C. We did not increase the elongation phase as compensation for loss of possible polymerase activity. New primers were run as single primers with an intended template to control for possible PCR products.

PCR-products were isolated by gel-electrophoresis and subsequent gel-extraction.

DNA-Sequencing

DNA-Sequencing is based on the termination of DNA-Polymerization by addition of fluorescently labeled dideoxy-nucleotides in a single primer-PCR reaction. Repeated initiation and termination of DNA-polymerization yields a mixture of DNA fragments that are terminated at each possible base by adding a fluorescently labeled dideoxy-nucleotide. The DNA fragments in the resulting mixture is separated by size in a capillary electrophoresis and the fluorescent signal allows direct reading of the DNA sequence.

DNA-Sequencing was mainly performed at the University of Michigan Sequencing Core. 10 µl/reaction of DNA to be sequenced was prepared to a concentration of 0.2 µg/µl as well as 10 µl/reaction of appropriate sequencing primer at a concentration of 3.2 pMol/µl.

Sequencing results were analysed using the software Jellyfish (Labvelocity) and Chromas, (Chromas Inc.)

Site directed mutagenesis

Site-directed mutagenesis strategies rely mostly on PCR based approaches. Either PCR primers of standard PCRs contained single or multiple mismatches that were introduced in the original gene by subsequent subcloning procedures, or a pair of complementary primers containing the desired mismatch was used to amplify a complete plasmid (based on the Quick-change Protocol, Stratagene), followed by specific digestion of the hemi-methylated template DNA. In the context of this work only the latter strategy was used:

Quick change protocol

In a reaction volume of 50 µl varying very low amounts of template-vector (1-10 ng) were combined with constant amounts of the two complementary mutagenesis primers. We used 200 µM dNTP and 0.75 µl Expand polymerase, which yielded good results, although Polymerases with low proofreading activity are recommended. Initial denaturation for 2 min at 95°C was followed by 15 cycles of denaturation at 95°C for 30 s, annealing at 50°C for 30 s and elongation at 72 for 2 min /1000bp of Vector-Template. To destroy the hemi-methylated template-DNA, the reaction mixture was incubated with 1 µl of DpnI for 1 hour at 37°C. The enzyme was heat inactivated for 20 min at 65°C. 1-2 µl of the mixture was transformed in

E.coli and grown clone were screened by sequencing and/or restriction for the desired mutation. Usually the gene containing the desired mutation was subcloned in a fresh vector backbone, to avoid uncontrolled mutations in the vector backbone introduced by the long elongation stretches.

Bacterial expression of Nkin and Hkin motors

A freshly transformed culture of BL21 cells was inoculated on 50 ml LB over night at 37°C and 200 rpm. The culture was transferred into 2 l TPM medium and incubated at 22°C and 190 rpm. The expression of motors was induced by addition of 0.1 - 0.5 mM IPTG. Cells were harvested after about 14-20 hours and frozen at -80°C until used.

Biochemical Methods

SDS – Polyacrylamid – Gelelectrophoresis (PAGE)

This method separates a mixture of proteins a polymeric network (gel) of poly-acrylamid in an electric field. Provided disulfide bonds are reduced, the proteins are completely denatured and uniformly charged by the detergent SDS the relative distance the protein is transported in the gel is strictly linked to its molecular weight (Laemmli, 1970).

For the separation-gel, 16.6 ml of bis/acryl-amid solution, 12.5 ml 1.5 M Tris-HCl , and 20.6 ml distilled water are mixed and the polymerization is started by addition of 275 µl of APS and 30 µl TEMED. After introducing the mixture (for about 8-10 gels) in the gel-casting stand, about 600 µl of iso-propanol was layerd carefully on the polymerization mixture, to ensure smooth upper surfaces. After complete polymerization (30-60 min), the isopropanol was decanted and the surface briefly washed with distilled water. For the stacking gel, the polymerization of a mixture of 2.5 ml bis/acryl-amid, 4.9 ml 0.5 M Tris-HCl and 11.4 ml was started by addition of 55 µl APS and 22 µl TEMED. About 2.5 ml of this mixture per gel was introduced into the casting stand and the desired combs (10-15 wells) were placed in the slots. Completely polymerized gels were stored at 4°C in a plastic bag.

Solutions

Bis/Acrylamide-solution 30% (1/29)

1.5 M Tris-HCl – pH 8.8

0.5 M tris HCl – pH 6.8

10 % (w/v) Ammonium-persulfate (APS) in distilled water

Coomassie-staining of PAGES

Coomassie allows convenient and permanent staining of proteins separated previously on a PAGE (see). The reaction is based on non-specific binding of the dye to proteins fixed in the gel matrix (Fazekas de St Groth et al., 1963, Meyer and Lamberts 1965).

After the separation of proteins in a standard PAGE, the gel is stained in a filtered solution of coomassie for at least 30 min to 2 h depending on the age of the solution. De-staining the gel for at least 30 min reveals the stained proteins. For quantifications of protein concentrations the gel needs to be de-stained to a very low level of background staining.

Staining

7.5 % (v/v) Acetic acid
50% (v/v) Methanol
0.25% (w/v) Coomassie brilliant blue R-250

De-Staining

10% (v/v) Acetic acid
30% (v/v) Methanol

Loading dye 6x

300 mM Tris-HCl pH 6.8
15 mM EDTA
12% SDS
30% (v/v) Glycerol
15% (v/v) β -mercapto-Ethanol
0.06 % (w/v) Bromophenolblue

Detection of Proteins via Western Blot

The detection of proteins in a western blot is based on the specific interaction of protein of interest – immobilized on a nitrocellulose membrane - with a (monoclonal) antibody that itself is then detected by another antibody conjugated to an enzyme (Towbin et al, 1979). The reaction of the enzyme and an appropriate substrate is either a chromogenic or a chemiluminescent reaction; we used the NBT/BCIP based chromogenic reaction of alkaline phosphatase-conjugated secondary antibodies.

Proteins are separated by size on a standard SDS-Gel. Meanwhile, a Nitrocellulose membrane (Schleicher and Schuell, Germany, 45 μ m) is floated in distilled water and then stored in blot buffer until used. The transfer of proteins to the nitrocellulose membrane is achieved in a wet-blot chamber (Termo-Forma): the gel is placed on a blot paper pre-wetted with blot buffer, then the nitrocellulose membrane is placed on the gel. A second layer of blot pre-wetted blot paper covers the membrane. With the help of porous pads the sandwich is firmly placed in the wetblot chamber that subsequently is filled with blot buffer. Proteins are transferred on to the nitrocellulose membrane in the direction of the anode for 1-2 hours at ~400 mA. Make sure the level of blot buffer is always above the membrane. After blotting the proteins are transiently stained with ponceau S solution (2 min), de-stained with distilled water and the position of the standards is marked. The blot is washed 3x5 min in TBST and then blocked in 5% milk powder in TBST with 0.1% Na-Azide for at least 1 hour at RT or

over night at 4 °C. After washing 3x5 min with TBST, the blot is incubated for 1 h in the solution of the primary antibody (TBST, 1 mg/ml BSA, 0.1% azide, primary antibody as recommended), washed again 3x5 min in TBST and incubated in the secondary antibody solution for 1 h at RT. After washing the blot twice 5 min in TBST and once in TBS, the blot is submerged in fresh NBT/BCIP solution until sufficient staining is reached.

A blot can be used for a second detection protocol if washed in TBST and then incubated in Strip buffer for 45-60 min at 60°C. The blot has to be blocked again with blocking solution.

Blot buffer

30 mM Tris
240 mM Glycin
0.05% (w/v) SDS
25% (v/v) Methanol

Ponceau S-Solution

0.25 % (w/v) Ponceau S
40% (v/v) Methanol
15% (v/v) Acetic acid

TBS

20 mM Tris HCl , pH 7.2
150 mM NaCl

TBST

TBS + 0.05 % (v/v) Tween 20

Strip buffer

20 mM Tris-HCl, pH 7.2
2 % (w/v) SDS
100 mM β -Mercapto-Ethanol

Protein purifications

Tubulin purification

Two fresh cow brains or 16-20 half pig brains were obtained from a slaughterhouse total of about 700 g tissue). Blood vessels and meninges were removed. MES buffer was supplemented with 1 mM ATP, 0.25 mM GTP, 0.1% BME, 4 mM DTT, 0.7 ml of each of the inhibitors. 300 ml MES buffer and ~300 g brain tissue is mixed in a household blender. Homogenize tissue by mixing 4 times for 15 s, pausing for 1 min between strokes. The slurry was transferred into ice cold 250 ml centrifuge tubes. Cell debris were sedimented for 60 min

at 4°C at 23000xg. Combine supernatants and add 50% (v/v) Glycerol. To the mixture add 5 mM MgCl₂, 0.2 mM GTP, and 2 mM ATP and incubate for 45 min at 37°C, to polymerize microtubules. The microtubules are transferred in pre-warmed 45Ti centrifuge bottles and placed in a pre-warmed 45Ti rotor. Microtubules are sedimented for 30 min at 45 000 rpm at 37°C. repeat with second half of the polymerization mixture. After the spin discard supernatant and re-suspend the pellet in 100 ml ice-cold PIPE-buffer, supplemented with 0.1 mM GTP, 0.1 mM ATP, 1mM DTT and 0.1 ml of each inhibitor. To de-polymerize the microtubules, the re-suspended pellet is placed on ice for 40 min. Aggregates and microtubules, which are not de-polymerized were removed by centrifugation at 38 000 rpm and 4°C for 30 min in the 70Ti rotor. The supernatants were combined and Glycerol was added to a final concentration of 33 % (v/v). After adding 1 mM GTP, 2mM ATP, 5 mM MgCl₂, and 1 mM DTT, the mixture was incubated for 45 min at 37°C to again polymerize microtubules. Subsequently, the polymerized microtubules were carefully layered on a pre-warmed low-pH-cushion (60% (v/v) Glycerol in 1x BRB80) and the microtubules were sedimented again at 37°C and 45 000 rpm for 45 min in the pre-warmed 70Ti-rotor. The resulting pellet is carefully re-suspended in about 40 ml column buffer supplemented with 0.1 mM GTP and 1.0 mM DTT. The re-suspended Microtubules are de-polymerized for 40 min on ice and aggregates are removed by centrifugation for 15 min at 38 000 rpm an 4°C in the cold 70Ti rotor. The supernatant is combined and loaded on activated P11 Phosphocellulosed, pre-equilibrated with column buffer. Microtubule associated proteins (MAPs) bind to the column material, tubulin does not. The flow-through is collected at fractions of 5 ml. Fractions of >25% of the maximal absorption are pooled. The solution is converted to BRB80, by addition of 1/20 vol. of Conversion buffer. The resulting solution is supplemented with 33% (v/v) Glycerol, 1.0 mM GTP, 5 mM MgCl₂, and 1 mM DTT and incubated for 40 min at 37°C to allow polymerization of Microtubules. Polymerized microtubules are again layered on a pre-warmed low-pH-cushion and sedimented by centrifugation at 38 000 rpm and 37°C for 90 min in a pre-warmed 70Ti rotor. The resulting pellet is carefully washed and re-suspended in ice cold BRB80. Microtubules are de-polymerized for 15-30 min on ice and aggregates are removed by centrifugation for 15 min at 38 000 rpm and 4°C in a cold 70Ti rotor. The supernatant is shock-frozen in aliquots in liquid nitrogen and stored at -80°C until use.

MES: 100mM MES
 0.5 mM MgCl₂
 2.0 mM EGTA
 0.1 mM EDTA pH 6.5 700ml

Collumn buffer
 50 mM K-PIPES
 0.2 mM MgCl₂
 1.0 mM EGTA
 0.01 mM GTP (added only the day of the prep) pH 6,8 500ml

PIPES buffer
 100mM K-PIPES
 0.5 mM MgCl₂
 2.0 mM EGTA
 0.1 mM EDTA pH 6.8 1000 ml

BRB80

80 mM K-PIPES
1.0 mM MgCl₂
1.0 mM EGTA pH 6.8 700ml

BRB80 conversion Buffer

650mM K-PIPES
18.2 mM MgCl₂
1.0 mM EGTA pH 6.8 10 ml

low pH cushion

60% Glycerol (v/v) in BRB80
ph 6.8
50 ml (better make 200 ml of this, pH at cold 6.8, is needed at 37°C though)

other solutions (prepare the day before and freeze in -20°C)

2 ml 1M DTT (D0623)
5ml 0.1M GTP (only weighing out, dissolve on prep day!) (G8877)
20 ml 0.1M ATP pH8.0 carefully!!!! (A2647)
1M MgCl₂ (Fluka 63068)
BME (M6250)

Inhibitors (weigh out the day before the prep. Store at -20°C. Addeach in 1 ml solvent the day of the preparation)

- 1.) water
 - a. 5mg Leupeptin (L0649)
 - b. 10 mg Soybean Trypsin Inhibitor (T9003)
- 2.) DMSO
 - a. 1mg Pepstatin (P5318)
 - b. 1mg Aprotinin (A1153)
 - c. 1mg TAME (T4627)
 - d. 1mg TPCK (T4376)
- 3.) Ethanol
 - a. PMSF (P7626)

Tubulin labeling

The labeling of tubulin relies on the mild and fast reaction of monofunctional succinimidylesters of fluorescent dyes like TMR (Molecular probes, Eugene, OR, USA), Cy3 or Cy5 (Amersham Biosciences, Piscataway, NJ, USA), with surface exposed amine residues of tubulin under slightly basic conditions. As this unspecific labeling could also occur at essential contact sites between tubulin subunits in the microtubule, and therefore destroying tubulins polymerization-activity, labeling is performed in the polymerized state followed by on complete cycle of depolymerization polymerization and depolymerization, thus selecting only for active tubulin, much like in the tubulin purification itself. High tubulin concentrations of 1-15 mg/ml in the educt are desirable to scale down volumes in order to use table top centrifuges which speed up the labeling procedure considerably.

50 mg of tubulin were thawed and the solution is supplemented with 50 & (v/v) Glycerol to improve the yield of polymerization. After adding 1 mM GTP and 4 mM MgCl₂, the mixture

was incubated for 40 min at 37°C to polymerize microtubules. Meanwhile the low pH cushion on the TLA100.3 rotor was warmed to 37°C. The polymerized MT were layered on the low pH-cushion and were centrifuged for 15 min at 80.000 rpm at 37 °C. Half the supernatant was carefully removed and the cushion was washed carefully with warm labeling buffer. Then the rest of the cushion was removed. It was made sure that all processes are performed at 37°C as microtubules de-polymerized at this pH will not be able to polymerize. The microtubules are resuspended in warm labeling buffer and the concentration is determined spectrophotometrically in order to calculate the correct label amount. Usually a 10-20x excess of dye was used. The dye was dissolved in dry DMSO, warmed for 5 min at 37°C and shortly centrifuged to remove remaining aggregates. The reagent was carefully mixed to the resuspended microtubules and the mixture was incubated for 30 min at 37°C. After adding the same volume of prewarmed Quench buffer, the mixture was layered on a pre-warmed low pH-cushion and the microtubules were sedimented for 15 min at 80.000 rpm and 37°C in the TLA 100.3 rotor. The cushion was aspirated and the pellet resuspended in ice cold BRB80 using the Ultraturray device. The microtubules were depolymerized for 15 min on ice, followed by a centrifugation for 5 min at 80K and 4°C to remove microtubules that were unable to depolymerize. The supernatant was supplemented with 50% (v/v) Glycerol, 2 mM GTP and 8 mM MgCl₂, and the mixture was incubated at 37°C for 45 min to allow polymerization of microtubules. After layering on a prewarmed low pH cushion, the polymerized MT were sedimented by centrifugation for 15 min at 37°C and 80.000 rpm in TLA100.3. The cushion was washed and then removed completely. The pellet was resuspended carefully in ice-cold BR80 and depolymerized on ice for 30 min. The MT that were unable to depolymerize were again separated by centrifugation for 5 min at 80 k in the TLA120.1 Rotor. The supernatant was frozen in very small aliquots and co-polymerization of the labeled tubulin with unlabeled tubulin into microtubules was tested. Amount of labeled tubulin used had to be determined empirically, depending on the use and the final concentration.

Protein determination

Bradford

For each measurement a standard row or BSA was prepared with various dilutions of a 1 mg/ml stock of BSA in a total of 500 µl distilled water. The sample was also diluted in 500 µl distilled water. The reaction was started by addition of 500 µl of Bradford reagent. After mixing the reaction was allowed to proceed for about 30 min in the dark. Then absorption at 595 nm was read in a spectrophotometer. The concentration of samples was calculated from the standard curve.

Photometric

The concentration of desalted proteins was determined spectrophotometrically from their molar extinction coefficient at 280 nm. The molar extinction coefficients were obtained from web based protein programs (Expasy server) or the GCG suite.

Densitometry

A defined volume of the sample was loaded on a standard gel together with standard dilution of BSA. The gel was stained and destained completely. Digital pictures of the destained gels

were analysed with the Gel-Doc documentation system or Image J to establish a BSA. Standard curve and then calculate the concentration of the unknown sample.

Polymerization of microtubules

Polymerization of Tubulin to microtubules occurs above a critical concentration of about 0.22 mg/ml above a and critical temperature of 34 °C under consumption of MgGTP. Depending on the application, the microtubules were polymerized from varying ratios of unlabeled tubulin to Cy5- or TMR-labeled tubulin and in varying amounts. For ATPases and MT-affinity protocols, only unlabeled tubulin was polymerized.

BRB80

80 mM –K-PIPES
1 mM MgCl₂
1 mM EDTA
pH 6.8

Taxol

1 mM in DMSO store at -80 °C!

Microtubule for gliding and single molecule fluorescence

A 6.25 to 25 µl batch of 2.2 mg/ml total tubulin, at least 1 mM GTP and 2 mM MgCl₂, and 5% (v/v) DMSO was prepared and polymerized for at least 20 min at 37°C. Labeling ratios highly depended on the following application and varied from 1/100 to ½. After polymerizing the MT were stabilized by adding 100 µl 10µM Taxol in BRB80/25 µl batch. For use in gliding assays the MT are usually diluted 1/100 in the appropriate buffer system.

Microtubules for ATPases or MT-affinity purification procedures.

P11 Tubulin or ultra-competent tubulin of a concentration higher than 5 mg/ml was thawed on ice and aggregates were removed by centrifugation for 5 min at 4°C at 80000 rpm in the TLA100.3 rotor. The solution was supplemented with 1 mM GTP and 2 mM MgCl₂ and then incubated for 10 min at 37 °C. Then Taxol was added to a concentration of 10-20 µM and the mixture was mixed thoroughly, before incubating another 20 min. The mixture was layered on a 40 % (w/v) Sucrose cushion in either AcesATPase-buffer or BRB80 buffer, depending on further use. After centrifugation for 10 min at 37°C at 80000 rpm for 10 min in TLA100.3, the pellet was washed and the MT resuspended in AcesATPase or BRB80 supplemented with 10 µM Taxol.

Concentration determination of microtubules

20 µl of a 1/10 and a 1/5 dilution of MT in the used buffer system are mixed with 180 µl of 6.6M GndHCl. After thoroughly mixing the Absorption at 280 nm is read against a blank of just 20 µl buffer + 180 µl GndHCl solution. The apparent Extinction coefficient for tubulin 1.04. Assuming a molecular weight of 100 000 g/mol for a tubulin dimer, the tubulin concentration was calculated as follows

$$(\text{OD } 280 / 1.04) * \text{dilution} * 100 = x \text{ } \mu\text{M Tubulin}$$

Partial digestion of microtubules

Microtubules are polymerized according to the desired application and the concentration was determined as described above. The microtubules were incubated for 20 min at 37°C with 6% relative to the amount of tubulin. The reaction was stopped by addition of 2 mM PMSF. The microtubules were then again separated from tubulin, PMSF and Subtilisin by centrifugation over a 40% sucrose cushion and re-suspended in about half the original volume of the appropriate buffer supplemented with 10 µM Taxol. All digests were controlled on an SDS-gel

Purification of NKin motors

Motors were expressed as described above. 3 g of frozen cells are resuspended in 9 ml Buffer A, supplemented with 10 µM ATP, 50 mM NaCl, 90 µl Pi, 36 µl Pe, 9 ml 1 M DTT, 9 µl 0.5 M EDTA, and traces of DNase I and Lysozyme. The cells were slowly re-suspended to homogeneity and then lysed by sonification (Branson Sonifier 250, 4 x 30 s, output 4, duty cycle 50%, timer on hold) Between the 30 s pulses the sonifier tip was cooled down and the solution put on ice to avoid excessively heating the solution. The lysate was centrifuged for 47 min at 42.000 rpm and 4°C in 70Ti rotor. The following chromatography steps were performed in the Äkta-FPLC system (Amersham Biosciences). The supernatant was quickly separated from the pellet and diluted 3.5 fold with distilled water and the concentration of ATP, EDTA and MgCl₂ adjusted. The diluted lysate is loaded directly on a 5 ml SP FF HiTrap column, pre-equilibrated with 0% Buffer B, at 2 ml /min. The column is washed with 0 % Buffer A until the Absorption has reached basal levels again. Elution was performed in steps of 5%, 10%, 20%, 30 %, 50 % and 100% buffer B in 1.5 ml fractions at 2 ml/min. After washing the column with 0% Buffer B, water and 20% Ethanol. The column can be reused several times. Motor concentration is determined on SDS-gels and activity assayed in an ATPase assay. Motor containing fractions are supplemented with ~5-10% sucrose, shock-frozen in liquid nitrogen and stored at -80°C for further use.

Buffer A

25 mM Na-Phosphate buffer pH 7.4
1 mM MgCl₂
0.5 mM EGTA
10 µM ATP freshly added the day of the preparation

Buffer B

Buffer A with 1M NaCl

Pe
Pefabloc

Pi 100x
1 mg/ml soybean trypsin inhibitor
1 mg/ml TAME
250 µg/ ml Leupeptin
100 µg/ml Pepstatin A
100 µg/ml Aprotinin

Purification of HKin motors

Motors were expressed as described above . 3 g of frozen cells are resuspended in 9 ml 7.5% Buffer B, supplemented with 10 µM ATP, 90 µl Pi, 36 µl Pe, 9 ml 1 M DTT, 9 µl 0.5 M EDTA, and traces of DNase I and Lysozyme. The cells were slowly re-suspended to homogeneity and then lysed by sonification (Branson Sonifier 250, 4 x 30 s, output 4, duty cycle 50%, timer on hold) Between the 30 s pulses the sonifier tip was cooled down and the solution put on ice to avoid excessively heating the solution. The lysate was centrifuged for 47 min at 42.000 rpm and 4°C in 70Ti rotor. The following chromatography steps were performed in the Äkta-FPLC system (Amersham Biosciences). The supernatant was quickly separated from the pellet and diluted 3.5 fold with buffer A and the concentration of ATP adjusted to 10 µM. The diluted lysate is loaded directly on ~50ml regenerated P11 material in a XK26 column, pre-equilibrated with 7.5% Buffer B, at 1.5 ml/min. The column is washed with 7.5 % Buffer B until the absorption has reached basal levels again. Elution was performed in a gradient from 7.5 to 100 % buffer B in about 70 ml at 1.5 ml fractions at 1.5 ml/min. Motor concentration is determined on SDS-gels and activity assayed in an ATPase assay. Activity containing fractions are pooled and diluted ~5 fold with buffer A. Using a 50 ml superloop the diluted pool is loaded on a MonoQ column, pre-equilibrated with 7.5 % buffer B at 1 ml/min. After washing the column with 7.5 % buffer B until absorption has reached basal levels, motors are eluted in a gradient from 7.5 % - 100 % B in 60 min at 0.5 ml fractions. Fractions are assayed for activity and analysed on a SDS gel for proteins of correct size. Motor containing fractions are pooled and either used for experiments directly or supplemented with 5-10% sucrose before shock-freezing them in liquid nitrogen. Aliquots are stored at -80°C until further use. The MonoQ column was then washed first with water and then 20% Ethanol. P11 material was not reused.

Buffer A

25 mM K-PIPES
1 mM EGTA
10 µM ATP freshly added the day of the preparation
pH 6.8

Buffer B

Buffer A with 1 M KCl
Microtubule affinity purification of kinesin motors.

The microtubule affinity uses the non-hydrolyzable nucleotide analogon AMP-PNP to transiently immobilize kinesin on the microtubule. Microtubules are then separated by centrifugation and re-suspended in a solution containing high concentrations of ATP and KCl, which allows the motor to detach from the microtubule. The microtubules are again separated by centrifugation and active motor is enriched in the supernatant. This procedure allows to select for motors able to bind to and release from the microtubule.

Microtubules are polymerized according to the procedure described in . The amount of tubulin is chosen to result in a 4-fold molar excess over the amount of motor to be purified. Then the motor aliquot is thawed on ice and thoroughly mixed. 10 μ M Taxol were added in order to allow addition of a 4-fold molar excess of microtubules supplemented with 2 mM AMP-PNP, to immobilized the motor on the microtubule. The mixture was incubated for 10-15 min at RT. Then the mixture was layered on 1 ml of 40% (w/v) sucrose in BRB80 supplemented with 10 μ M taxol. Microtubules with bound motor were sedimented by centrifugation for 10 min at 37°C and 80000 rpm in a TLA 100.3 rotor. The cushion was carefully washed to remove AMP-PNP from the interface. Then the cushion was removed and the pellet was carefully washed with a small volume release II. Then the pellet was very carefully re-suspended in Release II solution. The mixture was incubated for 10-20 min at RT, to allow motors to dissociate from the microtubule. The microtubules were then sedimented again for 10 min at 80000 rpm and 37 °C in the TLA 100.3 and the motor-containing supernatant was transferred to a new eppendorf-cup. Aliquots of the purified motor were either used directly for experiments or shock-frozen in liquid nitrogen and stored at -80°C until use.

Labelling kinesin motors at reactive cysteines

The labeling of motors is based on the reaction of a maleimide tagged compound (either biotin or Cy3) with a highly reactive cystein residue at the C-terminus of the motor. A subsequent Microtubule affinity purification selects for active motors. As a general rule the motor is reacted with a 6-fold molar excess of maleimide and subsequently bound to a 4-fold molar excess microtubules.

Microtubules are polymerized according to the procedure described above. The amount of tubulin is chosen to result in a 4-fold molar excess over the amount of motor to be labeled in the subsequent reaction. Then the motor aliquot is thawed on ice and thoroughly mixed. The maleimide is dissolved in dry-DMSO by vortexing for about 2 min, heating to 37°C for 5 min and a short centrifugation in the tabletop centrifuge to remove aggregates. A 6-fold molar excess of maleimide reactive reagent is added to the motor aliquot and the solution is mixed thoroughly. The reaction was allowed to proceed for 1 hour on ice. Then the reaction was stopped by addition of 10 mM DTT . The motor aliquot was allowed to heat up to RT. 10 μ M Taxol were added in order to allow addition of a 4-fold molar excess of microtubules supplemented with 2 mM AMP-PNP, to immobilized the motor on the microtubule. The mixture was incubated for 10-15 min at RT. Then the mixture was layered on 1 ml of 40% (w/v) sucrose in BRB80 supplemented with 10 μ M taxol. Microtubules with bound motor were sedimented by centrifugation for 10 min at 37°C and 80000 rpm in a TLA 100.3 rotor. The cushion was carefully washed to remove AMP-PNP from the interface. Then the cushion was removed and the pellet was carefully washed with a small volume release II. Then the pellet was very carefully re-suspended in Release II solution. The mixture was incubated for 10-20 min at RT, to allow motors to dissociate from the microtubule. The microtubules were

then sedimented again for 10 min at 80000 rpm and 37 °C in the TLA 100.3 and the motor-containing supernatant was transferred to a new eppendorf-cup. Aliquots of the labeled motor were either used directly for experiments or shock-frozen in liquid nitrogen and stored at -80°C until use.

In-gel tryptic digestion and subsequent mass spectrometric analysis.

To control, if labels were attached to the reactive cysteine, motors were digested by trypsin and fragments submitted to mass-spectroscopical analysis (MALDI-TOF). To be able to submit sufficient amounts of motor in sufficient purity, in-gel tryptic digestions were performed.

A sample of both labeled and unlabeled motor was run on a standard SDS-PAGE. The gel was stained in low acetic acid staining solution (0.25% (w/v) Coomassie, 0.5% acetic acid, 10% (v/v) Methanol) and de-stained in 30% Methanol. The band of the protein of interest and a piece of SDS gel of similar size was cut out with a clean razor blade, cut into small pieces (1 mm x 1 mm) and transferred to a sterile eppendorf cup. The pieces were further destained by addition of wash buffer for 30 min at 37°C. Of necessary the wash buffer was exchanged until the gel pieces were completely destained. The gel pieces were incubated for 10 min in acetonile before drying the pieces for 30 min at 45°C in a speed vac. Gel pieces were rehydrated with a Trypsin containing buffer until completely swollen to original size. Additional buffer A was added so that the gel pieces were partially submerged in the solution. Tryptic digestion was allowed to proceed for 24-48 hours at 37°C. The proteins were extracted by addition of 150 µl extraction buffer for 60 min at RT. The supernatant is removed to a fresh eppi and the extraction is repeated. The supernatants are combined. The samples are submitted for analysis on the same day.

Intrumentation

TIRF microscopy

We modified a Zeiss Axiovert 135 TV inverted microscope to observe single, fluorescently-labeled kinesin motor molecules via total internal reflection fluorescence microscopy. The basic setup is shown in Figure 1. For illumination we used the 514 nm line of an argon ion laser (Omnichrome 532 AP A01, Melles Griot, Bensheim, Germany) whose beam was coupled into a single mode, polarization maintaining optical fiber. On one side of the microscope stage we mounted a three-axis manipulator with a tilting stage that accepted the beam shaping output optics of the single mode fiber and a focusing lens. This arrangement allowed precise steering and focusing of the laser beam in the object plane, i.e., the quartz-solution interface. A second manipulator, mounted on the other side of the microscope stage, was used to position a small suprasil prism (Melles Griot, Bensheim, Germany) over a quartz microscope slide in the region of interest. The prism was optically coupled to a quartz slide with glycerol. The angle and position of the laser beam and position of the prism were adjusted such that the laser beam was coupled via the prism into the quartz slide at such an angle that total internal reflection took place at the quartz slide-solution interface (see Figure 1a). The laser beam was focused to a spot size of approximately 10 by 20 µm and the total power in the focal plane was adjusted to about 1.5 mW, resulting in an average power density of 0.01 mW/µm². The intensity difference of the evanescent wave over the illuminated spot

was about two-fold. To ensure approximately constant fluorescence excitation conditions we always used the same central area for all assays.

Fluorescent signals were recorded with a 1.4 NA, 100x Plan-Apochromat objective (Zeiss, Göttingen, Germany). The Cy5-fluorescence from labeled microtubules was recorded with a standard filter set consisting of a FT 580 dichroic mirror and a LP 590 long pass filter (both from Zeiss, Göttingen, Germany), which resulted in sub-maximal signal levels that were nonetheless sufficient to localize microtubules. Cy3-fluorescence signals were filtered with a HQ 580/75M band pass filter (Chroma, Battleboro, Vermont, USA), which blocks Cy-5 fluorescence completely. In addition, scattered excitation light (514 nm, Figure 1b) was blocked with a HQ 545 LP filter (Chroma, Battleboro, Vermont, USA). Signals were intensified with two image intensifiers connected in series, a Videoscope VS4-1845 (Videoscope International, Dulles, Virginia, USA) and a Hamamatsu Image Intensifier (C2400-87, Hamamatsu Photonics, Hamamatsu, Japan). Intensified output signals were visualized with a CCD-Camera (C3077, Hamamatsu Photonics, Hamamatsu, Japan) and enhanced by an Argus II image processor (Hamamatsu Photonics, Hamamatsu, Japan). All raw data were stored on S-VHS videotape and analyzed afterwards. Alternatively, the intensified images were acquired with the ORCA-ER camera (Hamamatsu, Hamamatsu, Japan). Sequences for 200-300 frames were stored and analysed using the open source code Image J (provided by the NIH, Bethesda, US).

Biophysical Methods

ATPase measurement

Kinesin is a microtubule activated ATPase. The measurement of the steady-state ATPase-activity at various microtubule concentration allows to extract k_{cat} and K_m , the basic key numbers in enzymes like kinesin following Michaelis-Menten kinetics (Gilbert and Johnson). In this assay, ATP-hydrolysis is enzymatically linked to the oxidation of NADH, which results in a decrease in Absorbance at 340 nm as measured photometrically (Huang and Hackney, 1994 a). The ATP hydrolysed by kinesin at saturating ATP concentration but varying microtubule concentration, is regenerated by the glycolytic enzyme pyruvate-kinase. It uses the substrate phospho-enol-pyruvate, as substrate and generates pyruvate. Lactate dehydrogenase then catalyses the reduction of pyruvate to lactate, oxidizing the NADH present in the solution to NAD, which results in a reduced absorbance at 340 nm that can be followed over time.

80 μ l reaction volumes of ATPase buffer containing 2 mM MgATP, 0.2 mg/ml K-PEP, 0.2 mM NADH, 25 U/ml Lactate-Dehydrogenase and 10 U/ml Pyruvate-Kinase, were mixed with microtubules yielding final concentrations between 0.005 μ M and 15 μ M Tubulin. The reaction was mixed with 1 μ l Kinesin-containing solution mixed rapidly and transferred to a 50 μ l Quartz-cuvette in the Spectrophotometer. Change of Absorbance over time was observed for 1-3 min. The initial fast rate of absorbance-decay was plotted against the Microtubule concentration and the data were fitted to a hyperbolic function, describing Michaelis-Menten kinetics.

$$\Delta E_{340nm} = V_{max} + (\text{Grummt } et al., 1998a) / ((\text{Grummt } et al., 1998a) + K_{0.5} \text{ MT})$$

The rate of maximal ATP-turnover (V_{max}) was calculated using the extinction coefficient of NADH (6.22/mM/cm) and using the reasonable assumption that oxidation of NADH is strictly coupled to ATP hydrolysis in a 1:1 fashion. Therefore the maximal rate of ATP turnover in the assay is equivalent to $\Delta c \text{ (ATP)} / \Delta t = V_{max} / 6.22 * 60 \mu\text{M s}^{-1}$. To calculate the specific maximal ATP-turnover for the enzyme, the k_{cat} , $\Delta c \text{ (ATP)} / \Delta t$ is divided by the kinesin concentration present in the assay

$$k_{cat} = (\Delta c \text{ (ATP)} / \Delta t) / (\text{Block } et \text{ al.}, 1990)$$

ATPase buffer:

12 mM ACE*KOH
25 mM K-Acetate
2 mM MG-Acetate
5 mM MgCL2
0.5 mM EGTA
pH 6.8

ADP release measurement

Loading of Kinesin Motors with Mant –ADP

Kinesin motors in free solution have ADP bound to the ATPase-site. To measure initial binding of kinesin motors to the microtubule, this ADP is exchanged for the fluorescent nucleotide analogon mant-ADP, which displays strong fluorescence while present in the hydrophobic environment of the ATP binding pocket, while fluorescence of the free analogon in solution is largely quenched. The motor is loaded by offering the motor mant-ATP, which is bound and turned over to bound mant-ADP due to the basal ATPase-activity of the motor.

The concentration of motor is calculated from the extinction coefficient. A 4-fold excess of mant-ATP was added and incubated for 15 to 30 min at RT. To remove free ATP and mant-ATP the motor was desalted using Sephadex G25 material. 300 μl of the material was applied to Mini-Spin column (reused Quia-quick gel-extraction columns) and shortly centrifuged. The material was washed with 300 μl ATPase buffer and then incubated for at least 30 min in 1 mg/ml in ATPase buffer. To remove unbound BSA, the columns were washed 6 times with 300 μl ATPase buffer containing 200 mM KCl. 50 μl of the solution of motor to be labeled are applied carefully to the column, which is then placed in a fresh eppendorf-cup and centrifuged for 1 min. The desalted protein-solutions were combined and protein concentration and labeling ratios were determined using a wavelength scan.

ADP-release measurements.

The release of bound mant-ADP upon binding of kinesin motors to the microtubule was observed in a Aminco Bowman AB2 Fluorimeter. The mant-ADP was excited at 365 nm with a slit width of 4 nm. Fluorescence was measured perpendicular to the direction of excitation at 445 nm at a slit width of 2 nm.

In a standard plastic cuvette about 100 nmol loaded motor supplied with 10 mM MgATP was mixed with increasing substoichiometric (0-20 nmol) amounts of microtubules. The resulting decay of fluorescence was observed for 180 s. The data were fit by a mono-exponential function and the resulting time constants of the decay were plotted against the tubulin concentration. The slope of a linear regression through these data is the bimolecular binding rate $k_{\text{bi,ADP}}$ in $\mu\text{m}^{-1}\text{s}^{-1}$.

Gliding assay

Motility assays at high and low motor densities were performed following standard procedures (Howard *et al.*, 1989). Briefly, flow chambers were pre-coated with BRB80 (80 mM PIPES/KOH, 1 mM EGTA, 2 mM MgCl₂, pH 6.9) containing 0.1 mg/ml casein for 3 min, then motor dilutions in BRB80 containing 0.05 mg/ml casein were introduced and allowed to incubate for 3 min. TMR-labelled microtubules were diluted in an MgATP containing oxygen-scavenger solution (0.1 mg/ml glucose-oxidase, 0.08 mg/ml catalase, 1 mM DTT, 10 mM glucose) with additional 10 μM taxol and introduced into the flow-chamber. Microtubules were observed using an epifluorescence microscope (Axiovert 135 TV, Zeiss, Göttingen, Germany). For gliding assays at very low motor densities (single molecule *in vitro* gliding assays) microtubules were triturated to lengths of 1-5 μm by passing the solution through a 30-gauge needle before introduction into the flow-chamber. Images were stored on S-VHS and analyzed afterwards.

Single molecule fluorescence processivity assay

Single molecule processivity assays in Prism-based TIRFM

Single molecule processivity assays were performed following the procedure given in Vale *et al.* (1996). Briefly, fluorescently-labeled motor molecules were diluted to approximately 5 nM in a P12 buffer (12mM PIPES/KOH, 1mM EGTA, 2mM MgCl₂, pH 6.8) containing 30mg/ml BSA (11930, Serva, Heidelberg, Germany). Diluted motor protein was combined with equal parts (1.1 μl each) of the following three solutions: (1.) Glucose-oxidase (0.4 mg/ml) and catalase (0.32 mg/ml) in P12, (2.) MgCl₂ (4 mM), ATP (16 mM), DTT (4 mM) and glucose (40 mM) in P12, and (3.) Cy5-labeled microtubules (diluted about 100-fold depending on the individual preparation) in BRB80 stabilized with 40 μM taxol, resulting in a final concentration of 29 nM PIPES. Directly after mixing the solution was applied to a clean fused silica slide and covered with a coverglass. Processivity assays with single NKin molecules required a slight modification: instead of 4mM ATP the buffer contained a final concentration of 1-10 μM AMP-PNP and the solutions were incubated for approximately 5-15 minutes to allow the motor to bind to the microtubules before applying a 4 μl volume to a cleaned quartz slide. After identification of microtubules with immobilized Cy3-labeled motors, an ATP-containing solution (4 mM ATP) was washed into the chamber and the ensuing movement of the motor molecules was recorded on video tape. All motility assays, single and multiple motor microtubule gliding assays as well as processivity assays, were carried out at $22^{\circ}\text{C} \pm 1^{\circ}\text{C}$.

Analysis of single molecule experiment

Global bleaching constants of fluorescently labeled motors were determined from frame by frame analysis of large assemblies of surface- or microtubule-bound motors. The change of fluorescence intensity as a function of time was analyzed using an Argus 20 image processor (Hamamatsu Photonics, Hamamatsu, Japan). The intensity of individual fluorescent spots, either surface adsorbed or moving on a microtubule, was analyzed using the same method.

The speed of motor molecules translocating along microtubules was determined by calculating the distance using a calibration standard (Leica, Wetzlar, Germany) and dividing the distance traveled by the elapsed time. All data and statistical analysis was performed using Origin 4.0 (Microcal Software, Inc., Northampton, MA, USA) or routines contained in the S-Plus programming environment (Becker *et al.*, 1988).

Single molecule trapping assay

Biotinylation of latex-beads

50 μ l 1 μ m carboxylated latex beads were suspended in 200 μ l Na-Phosphate buffer (50 mM Na-phosphate, pH 7.2) and centrifuged for 15 min at 5000 rpm. This washing procedure was repeated three times. The beads were re-suspended in 3.7 mg EDC and biotin-XX-cadaverine were added and the solution was incubated for 30 min at RT or 1 h on ice. The beads were centrifuges for 15 min at 5000 rpm and re-suspended in 200 μ l Na.Phosphate buffer. The washing steps were repeated at least three better five times. Biotinylated beads could be stored in Na.phosphate buffer with 0.1% Azide and 4°C.

Streptavidin coating of biotinylated latex beads

12.5 μ l biotinylated beads were mixed with 175 μ l Phosphate buffer and centrifuged for 15 min at 5000 rpm. The beads were re-suspended in 100 μ l Phosphate buffer and 10 μ l 1M Glycin and 15 μ l 1 mg/ml Streptavidin was added. Streptavidin was allowed to bind for 20 min at RT or 1 hour on ice. The beads were washed 3 or better 5 times in 175 μ l phosphate buffer by repeated centrifugation. Streptavidin coated beads were sored at 4°C

Trapping assay

A solution of 1/100 diluted TMR-labeled Microtubules in 10 μ M Taxol I BRB80 was flowed in a standard assay chamber made using Poly-L-Lysin coated cover slips. The microtubules were allowed to bind for 10 min. The chamber was washed with 3 volumes 1 mg/ml Casein and incubated for 3 min. Then oxygen scavenger solution as described for standard gliding assays (BRB80 with 10 μ M Taxol, 2 mM ATP, 4 mM MgCl₂, 0.1 mg/ml glucose-oxidase, 0.08 mg/ml catalase, 1 mM DTT, 10 mM glucose, 50 U/ml Phosphocreatine kinase, 10 mM Phosphocreatine, 0.05mg/ml casein) containing 1/50 diluted beads sparsely coated with biotinylated motors was introduced. Assay chambers are sealed with wax. In the laser trapping microscope, single beads were captured and the stiffness of the trap was calculated, measuring the position-signal of the bead while moving the piezo-stage of the microscope at defined speeds. After calibrating the beads movement in the trap, the bead was brought above a horizontally attached microtubule. The bead was gradually lowered until interactionas occurred. Data were acquired for 128 s and stored on the hard drive for further analysis.

Data analysis

Data were analyzed in a custom-made program, that allowed to filter data, calculate the running variance of the position signal of the bead over time. Furthermore, stretches of the data trace could be selected for further analysis of the force velocity relation. Velocity of the bead movement in fragments of as little as 40 ms length was calculated as a linear regression of the positional data in this interval. The force was calculated from the mean displacement of the bead from the center of the trap as calculated as the mean position 300 ms before the event started. Minimal length of the selected fragments could be selected in order to allow adjustment of the regression to longer intervals at slower gliding speeds. Resulting data were plotted in a transient Force velocity diagram and could be appended to a specified ascii-file. Data of multiple events appended in a file were further analysed using Origin. The mean velocity and mean force of data points within 0.5 pN intervals was calculated. The data were plotted and data were fitted by a linear regression.

List of Figures

- Fig. I-1: Overall domain organization of kinesin
- Fig. I-1: Possible pathway of processive movement of conventional kinesin
- Fig. I-1: Docking the crystal structure of dimeric kinesin to the microtubule-lattice
- Fig. II-1: Single molecule gliding assays of Hkin and NKin
- Fig. II-2: Global bleaching behavior of Cy3 marked HKin and NKin motors
- Fig. II-3: Single molecule fluorescence processivity assays for HKin
- Fig. II-4: Single molecule fluorescence processivity assays for NKin
- Fig. II-5: Histograms of the run-lengths of HKin and NKin
- Fig. III-1: Sequence alignment and structural features of the neck of NKin
- Fig. III-2: Interaction of the Nkin motor head with the microtubule
- Fig. III-3: Partial Digestion of Tubulin controlled by SDS-PAGE
- Fig. III-4: Western-Blot analysis of a partial digestion of tubulin
- Fig. III-5: Histogram of run-lengths of NKin motors on digested microtubules
- Fig. III-6: Kymographs for HKin and NKin single molecule fluorescence assays
- Fig. III-7: Comparison of the ATPase-activity of NKin433 on digested and undigested microtubules
- Fig. III-8: Mant-ADP-Titration of dimeric NKin on digested and undigested microtubules
- Fig. III-9: Comparison of the rate of ADP-release of NKin 433 on digested and undigested microtubules
- Fig. III-10: Possible interactions of the E-hook with NKin-head
- Fig. III-11: Comparison of the ATPase-activity of NKin343 on digested and undigested microtubules
- Fig. III-12: Comparison of the rate of ADP-release of NKin343 on digested and undigested microtubules
- Fig. IV-1: Motors used in this study
- Fig. IV-2: Purification of NK433cys
- Fig. IV-3: Biotinylation procedure
- Fig. IV-4: Schematic view of the attachment of the motor to the bead
- Fig. IV-5: Representative traces of trapping studies
- Fig. IV-6: Force velocity diagram for HKin
- Fig. IV-7: Force velocity diagrams for NKin-Motors
- Fig. IV-8: Dependence of Stall forces on ATP concentration and Dependence of Force and initial speed on ATP concentration in NK433
- Fig. IV-9: Representative Force-Velocity diagram for Nk433 on digested microtubules
- Fig. IV-10: Force generated by NKin motors on digested microtubules does not depend on ATP-concentrations
- Fig. V-1: Sequence comparison of fungal and animal conventional kinesins
- Fig. V-1: Comparison of multiple motor gliding speeds
- Fig. V-1: Comparison of microtubule affinity purified motors
- Fig. M1: Schematic Illustration of the Prism-based TIRF-setup

List of Tables

- Table II-1: Comparison of the motile properties of HKin560cys and NKin480cys
- Table III-1: Comparison of the motile behavior of NKin on digested and undigested microtubules
- Table IV-1: Comparison of the motile behavior of biotinylated motor molecules in multiple molecule and laser trapping experiments
- Table V-1: Comparison of gliding speeds of the Neck-linker mutants measured in multiple motor gliding assays

Curriculum vitae

Name Lakaemper
First name Stefan

Address University of Michigan
Dept of Mechanical Engineering
1110 GG Brown
2350 Hayward
Ann Arbor, MI-48109, USA
lakaempe@engin.umich.edu

Date of birth February 2nd, 1974
Place of birth Gütersloh
Private Address Teutoburger Weg 26
33332 Gütersloh, Germany

School education 1980-1984 Overberg-Schule, Gütersloh
1984-1993 Ev. Stift. Gymnasium, Gütersloh

University education 1993-1999 Biochemistry/Diploma, University of Hannover, Germany
1995-1997 Human Medicine/Staatsexamen, MHH Hannover,

Degrees 05/1993 Allgemeine Hochschulreife (high school degree)
09/1997 Ärztliche Vorprüfung (preclinical exams)
05/1999 Diploma (Biochemie)

Scientific experience

Internships during university studies:

Internship at the Max-Planck-Institute for Experimental Endocrinology, Dr. Monica Marcus, Hannover, Germany, 08-09/1996

Internship at the INSERM, unité 159, Dr. Danielle Gourdji, Paris, Frankreich, 03-04/1997

Internship at the Institute for Biochemistry, Dr. Teruko Tamura-Niemann, MHH Hannover, Germany, 08-09/1997

Internship at the Departement of Anaesthesiology, Prof. Keith W. Miller, Massachussetts General Hospital, Boston, USA, 03-05/1998

Positions held

Research assistant at the Institute for Molecular and Cell Physiology at the Medical School Hannover (MHH), Germany, (Prof. Bernhard Brenner) in the group of Edgar Meyhöfer, Ph.D., 07/1999 - 08/2001

Research assistant at the Institute for Cell biology at the Ludwig-Maximilians-Universität in Munich, Germany (Prof. Manfred Schliwa), 09/2001 – to date

Visiting Scholar at the Department of Mechanical Engineering, University of Michigan, Ann Arbor, Michigan, USA (Prof Edgar Meyhöfer, Ph.D.), 05/2002 - to date

General research interest

My current research efforts are focusing on two aspects of molecular motors: 1. How do structural elements in motor molecules control and influence energy transduction and 2. What are the functions different biological motors in the cellular context.

Abstracts and Publications

NKin is a highly processive fungal kinesin, S. Lakämper, Kallipolitou A, Wöhlke A, Schliw M, Meyhöfer E, Poster at the Biophysical Meeting 2001, Boston, USA (Biophys. J., Vol 80(1); 570a (2001))

Unusual properties of the fungal conventional kinesin neck domain from *Neurospora crassa*., Kallipolitou A, Deluca D, Majdic U, Lakämper S, Cross R, Meyhofer E, Moroder L, Schliwa M, Woehlke G. EMBO J 2001 Nov 15;20(22):6226-35

Can we modify the processive behavior of Kinesins?, Lakämper S, Schliwa M, Meyhofer E, Poster at the Biophysical Meeting 2002, San Francisco, USA (Biophys. J., Vol 82(1); 62e, (2002))

Single fungal kinesin molecules move processively along microtubules. Lakämper S, Kallipolitou A, Woehlke G, Schliwa M, Meyhofer E, Biophys. J. March 2003, 84:1833-44

The E-hook of tubulin is essential for fast and effective coupling of the two heads of NKin, Lakämper S, Schliwa M, Meyhofer E, Poster at the SFB Meeting, 2002, München, Deutschland,

The E-hook of tubulin is essential for fast and effective coupling of the two heads of NKin, Lakämper S, Schliwa M, Meyhofer E, Poster at the Biophysical Meeting 2003, San Antonio, USA, (Biophys. J. 83(1);251, (2003))

Yearly talks at the meeting of the DFG-Priority Programme "Molecular Motors" from 1999-2002.

Literature

- Block, S. M., C. L. Asbury, J. W. Shaevitz, M. J. Lang. 2003. Probing the kinesin reaction cycle with a 2D optical force clamp. *Proc Natl Acad Sci U S A.* 100:2351-2356.
- Block, S. M., L. S. Goldstein, B. J. Schnapp. 1990. Bead movement by single kinesin molecules studied with optical tweezers. *Nature.* 348:348-352.
- Bloom, G. S., M. C. Wagner, K. K. Pfister, S. T. Brady. 1988. Native structure and physical properties of bovine brain kinesin and identification of the ATP-binding subunit polypeptide. *Biochemistry.* 27:3409-3416.
- Brady, S. T. 1985. A novel brain ATPase with properties expected for the fast axonal transport motor. *Nature.* 317:73-75.
- Coy, D. L., W. O. Hancock, M. Wagenbach, J. Howard. 1999a. Kinesin's tail domain is an inhibitory regulator of the motor domain. *Nat Cell Biol.* 1:288-292.
- Coy, D. L., M. Wagenbach, J. Howard. 1999b. Kinesin takes one 8-nm step for each ATP that it hydrolyzes. *J Biol Chem.* 274:3667-3671.
- Crevel, I., N. Carter, M. Schliwa, R. Cross. 1999. Coupled chemical and mechanical reaction steps in a processive *Neurospora* kinesin. *Embo J.* 18:5863-5872.
- Crevel, I. M., A. Lockhart, R. A. Cross. 1996. Weak and strong states of kinesin and ncd. *J Mol Biol.* 257:66-76.
- Crevel, I. M., A. Lockhart, R. A. Cross. 1997. Kinetic evidence for low chemical processivity in ncd and Eg5. *J Mol Biol.* 273:160-170.
- de Cuevas, M., T. Tao, L. S. Goldstein. 1992. Evidence that the stalk of *Drosophila* kinesin heavy chain is an alpha-helical coiled coil. *J Cell Biol.* 116:957-965.
- Endow, S. A. 1999. Determinants of molecular motor directionality. *Nat Cell Biol.* 1:E163-167.
- Foster, K. A., S. P. Gilbert. 2000. Kinetic studies of dimeric Ncd: evidence that Ncd is not processive. *Biochemistry.* 39:1784-1791.
- Foster, K. A., A. T. Mackey, S. P. Gilbert. 2001. A mechanistic model for Ncd directionality. *J Biol Chem.* 276:19259-19266.
- Gilbert, S. P. 2001. High-performance fungal motors. *Nature.* 414:597-598.
- Gilbert, S. P., M. L. Moyer, K. A. Johnson. 1998. Alternating site mechanism of the kinesin ATPase. *Biochemistry.* 37:792-799.
- Gilbert, S. P., M. R. Webb, M. Brune, K. A. Johnson. 1995. Pathway of processive ATP hydrolysis by kinesin. *Nature.* 373:671-676.
- Gittes, F., E. Meyhofer, S. Baek, J. Howard. 1996. Directional loading of the kinesin motor molecule as it buckles a microtubule. *Biophys J.* 70:418-429.
- Grummt, M., S. Pistor, F. Lottspeich, M. Schliwa. 1998a. Cloning and functional expression of a 'fast' fungal kinesin. *FEBS Lett.* 427:79-84.
- Grummt, M., G. Woehlke, U. Henningsen, S. Fuchs, M. Schleicher, M. Schliwa. 1998b. Importance of a flexible hinge near the motor domain in kinesin-driven motility. *Embo J.* 17:5536-5542.
- Hackney, D. D. 1992. Kinesin and myosin ATPases: variations on a theme. *Philos Trans R Soc Lond B Biol Sci.* 336:13-17; discussion 17-18.
- Hackney, D. D. 1994a. Evidence for alternating head catalysis by kinesin during microtubule-stimulated ATP hydrolysis. *Proc Natl Acad Sci U S A.* 91:6865-6869.
- Hackney, D. D. 1994b. The rate-limiting step in microtubule-stimulated ATP hydrolysis by dimeric kinesin head domains occurs while bound to the microtubule. *J Biol Chem.* 269:16508-16511.
- Hackney, D. D. 1995. Highly processive microtubule-stimulated ATP hydrolysis by dimeric kinesin head domains. *Nature.* 377:448-450.
- Hackney, D. D. 2002. Pathway of ADP-stimulated ADP release and dissociation of tethered kinesin from microtubules. Implications for the extent of processivity. *Biochemistry.* 41:4437-4446.
- Hackney, D. D., M. F. Stock. 2000. Kinesin's IAK tail domain inhibits initial microtubule-stimulated ADP release. *Nat Cell Biol.* 2:257-260.
- Hackney, D. D., M. F. Stock, J. Moore, R. A. Patterson. 2003. Modulation of Kinesin Half-Site ADP Release and Kinetic Processivity by a Spacer between the Head Groups. *Biochemistry.* 42:12011-12018.
- Hancock, W. O., J. Howard. 1998. Processivity of the motor protein kinesin requires two heads. *J Cell Biol.* 140:1395-1405.

- Hancock, W. O., J. Howard. 1999. Kinesin's processivity results from mechanical and chemical coordination between the ATP hydrolysis cycles of the two motor domains. *Proc Natl Acad Sci U S A.* 96:13147-13152.
- Henningsen, U., M. Schliwa. 1997. Reversal in the direction of movement of a molecular motor. *Nature.* 389:93-96.
- Hirokawa, N., K. K. Pfister, H. Yorifuji, M. C. Wagner, S. T. Brady, G. S. Bloom. 1989. Submolecular domains of bovine brain kinesin identified by electron microscopy and monoclonal antibody decoration. *Cell.* 56:867-878.
- Hirose, K., J. Lowe, M. Alonso, R. A. Cross, L. A. Amos. 1999. Congruent docking of dimeric kinesin and ncd into three-dimensional electron cryomicroscopy maps of microtubule-motor ADP complexes. *Mol Biol Cell.* 10:2063-2074.
- Howard, J. 1996. The movement of kinesin along microtubules. *Annu Rev Physiol.* 58:703-729.
- Howard, J. 1997. Molecular motors: structural adaptations to cellular functions. *Nature.* 389:561-567.
- Howard, J., A. J. Hudspeth, R. D. Vale. 1989. Movement of microtubules by single kinesin molecules. *Nature.* 342:154-158.
- Hua, W., J. Chung, J. Gelles. 2002. Distinguishing inchworm and hand-over-hand processive kinesin movement by neck rotation measurements. *Science.* 295:844-848.
- Hua, W., E. C. Young, M. L. Fleming, J. Gelles. 1997. Coupling of kinesin steps to ATP hydrolysis. *Nature.* 388:390-393.
- Huang, T. G., D. D. Hackney. 1994. Drosophila kinesin minimal motor domain expressed in Escherichia coli. Purification and kinetic characterization. *J Biol Chem.* 269:16493-16501.
- Hunt, A. J., F. Gittes, J. Howard. 1994. The force exerted by a single kinesin molecule against a viscous load. *Biophys J.* 67:766-781.
- Hunt, A. J., J. Howard. 1993. Kinesin swivels to permit microtubule movement in any direction. *Proc Natl Acad Sci U S A.* 90:11653-11657.
- Inoue, A., J. Saito, R. Ikebe, M. Ikebe. 2002. Myosin IXb is a single-headed minus-end-directed processive motor. *Nat Cell Biol.* 4:302-306.
- Inoue, Y., Y. Y. Toyoshima, A. H. Iwane, S. Morimoto, H. Higuchi, T. Yanagida. 1997. Movements of truncated kinesin fragments with a short or an artificial flexible neck. *Proc Natl Acad Sci U S A.* 94:7275-7280.
- Jiang, M. Y., M. P. Sheetz. 1995. Cargo-activated ATPase activity of kinesin. *Biophys J.* 68:283S-284S; discussion 285S.
- Jiang, W., M. F. Stock, X. Li, D. D. Hackney. 1997. Influence of the kinesin neck domain on dimerization and ATPase kinetics. *J Biol Chem.* 272:7626-7632.
- Kallipolitou, A., D. Deluca, U. Majdic, S. Lakammer, R. Cross, E. Meyhofer, L. Moroder, M. Schliwa, G. Woehlke. 2001. Unusual properties of the fungal conventional kinesin neck domain from Neurospora crassa. *Embo J.* 20:6226-6235.
- Karabay, A., R. A. Walker. 2003. Identification of Ncd tail domain-binding sites on the tubulin dimer. *Biochem Biophys Res Commun.* 305:523-528.
- Kikkawa, M., Y. Okada, N. Hirokawa. 2000. 15 A resolution model of the monomeric kinesin motor, KIF1A. *Cell.* 100:241-252.
- Kikkawa, M., E. P. Sablin, Y. Okada, H. Yajima, R. J. Fletterick, N. Hirokawa. 2001. Switch-based mechanism of kinesin motors. *Nature.* 411:439-445.
- Kinosita, K., Jr., R. Yasuda, H. Noji, S. Ishiwata, M. Yoshida. 1998. F1-ATPase: a rotary motor made of a single molecule. *Cell.* 93:21-24.
- Kirchner, J., S. Seiler, S. Fuchs, M. Schliwa. 1999a. Functional anatomy of the kinesin molecule in vivo. *Embo J.* 18:4404-4413.
- Kirchner, J., G. Woehlke, M. Schliwa. 1999b. Universal and unique features of kinesin motors: insights from a comparison of fungal and animal conventional kinesins. *Biol Chem.* 380:915-921.
- Klopfenstein, D. R., E. A. Holleran, R. D. Vale. 2002a. Kinesin motors and microtubule-based organelle transport in Dictyostelium discoideum. *J Muscle Res Cell Motil.* 23:631-638.
- Klopfenstein, D. R., M. Tomishige, N. Stuurman, R. D. Vale. 2002b. Role of Phosphatidylinositol(4,5)bisphosphate Organization in Membrane Transport by the Unc104 Kinesin Motor. *Cell.* 109:347-358.
- Kojima, H., E. Muto, H. Higuchi, T. Yanagida. 1997. Mechanics of single kinesin molecules measured by optical trapping nanometry. *Biophys J.* 73:2012-2022.
- Kozielski, F., S. Sack, A. Marx, M. Thormahlen, E. Schonbrunn, V. Biou, A. Thompson, E. M. Mandelkow, E. Mandelkow. 1997a. The crystal structure of dimeric kinesin and implications for microtubule-dependent motility. *Cell.* 91:985-994.
- Kozielski, F., E. Schonbrunn, S. Sack, J. Muller, S. T. Brady, E. Mandelkow. 1997b. Crystallization and preliminary X-ray analysis of the single-headed and double-headed motor protein kinesin. *J Struct Biol.* 119:28-34.

- Lakamper, S., A. Kallipolitou, G. Woehlke, M. Schliwa, E. Meyhofer. 2003. Single Fungal Kinesin Motor Molecules Move Processively along Microtubules. *Biophys J.* 84:1833-1843.
- Larson HJ. 1982. Introduction to probability theory and statistical inference: John Wiley and Sons, New York.
- Lehmler, C., G. Steinberg, K. M. Snetselaar, M. Schliwa, R. Kahmann, M. Bolker. 1997. Identification of a motor protein required for filamentous growth in *Ustilago maydis*. *Embo J.* 16:3464-3473.
- Lohman, T. M., K. Thorn, R. D. Vale. 1998. Staying on track: common features of DNA helicases and microtubule motors. *Cell.* 93:9-12.
- Ma, Y. Z., E. W. Taylor. 1997. Interacting head mechanism of microtubule-kinesin ATPase. *J Biol Chem.* 272:724-730.
- Masaike, T., E. Muneyuki, H. Noji, K. Kinosita, Jr., M. Yoshida. 2002. F1-ATPase changes its conformations upon phosphate release. *J Biol Chem.* 5:5.
- Mehta, A. D., R. S. Rock, M. Rief, J. A. Spudich, M. S. Mooseker, R. E. Cheney. 1999. Myosin-V is a processive actin-based motor. *Nature.* 400:590-593.
- Meyhofer, E., J. Howard. 1995. The force generated by a single kinesin molecule against an elastic load. *Proc Natl Acad Sci U S A.* 92:574-578.
- Miki, H., M. Setou, N. Hirokawa. 2003. Kinesin superfamily proteins (KIFs) in the mouse transcriptome. *Genome Res.* 13:1455-1465.
- Miki, H., M. Setou, K. Kaneshiro, N. Hirokawa. 2001. All kinesin superfamily protein, KIF, genes in mouse and human. *Proc Natl Acad Sci U S A.* 98:7004-7011.
- Mogilner, A., A. J. Fisher, R. J. Baskin. 2001. Structural changes in the neck linker of kinesin explain the load dependence of the motor's mechanical cycle. *J Theor Biol.* 211:143-157.
- Moller-Jensen, J., R. B. Jensen, J. Lowe, K. Gerdes. 2002. Prokaryotic DNA segregation by an actin-like filament. *Embo J.* 21:3119-3127.
- Naber, N., S. Rice, M. Matuska, R. D. Vale, R. Cooke, E. Pate. 2003. EPR Spectroscopy Shows a Microtubule-Dependent Conformational Change in the Kinesin Switch 1 Domain. *Biophys J.* 84:3190-3196.
- Noji, H., R. Yasuda, M. Yoshida, K. Kinosita, Jr. 1997. Direct observation of the rotation of F1-ATPase. *Nature.* 386:299-302.
- O'Connell, C. B., M. S. Mooseker. 2003. Native Myosin-IXb is a plus-, not a minus-end-directed motor. *Nat Cell Biol.* 5:171-172.
- Okada, Y., N. Hirokawa. 1999. A processive single-headed motor: kinesin superfamily protein KIF1A. *Science.* 283:1152-1157.
- Okada, Y., N. Hirokawa. 2000. Mechanism of the single-headed processivity: diffusional anchoring between the K-loop of kinesin and the C terminus of tubulin. *Proc Natl Acad Sci U S A.* 97:640-645.
- Ray, S., E. Meyhofer, R. A. Milligan, J. Howard. 1993. Kinesin follows the microtubule's protofilament axis. *J Cell Biol.* 121:1083-1093.
- Rice, S., Y. Cui, C. Sindelar, N. Naber, M. Matuska, R. Vale, R. Cooke. 2003. Thermodynamic properties of the Kinesin neck-region docking to the catalytic core. *Biophys J.* 84:1844-1854.
- Rice, S., A. W. Lin, D. Safer, C. L. Hart, N. Naber, B. O. Carragher, S. M. Cain, E. Pechatnikova, E. M. Wilson-Kubalek, M. Whittaker *et al.* 1999. A structural change in the kinesin motor protein that drives motility. *Nature.* 402:778-784.
- Rief, M., R. S. Rock, A. D. Mehta, M. S. Mooseker, R. E. Cheney, J. A. Spudich. 2000. Myosin-V stepping kinetics: a molecular model for processivity. *Proc Natl Acad Sci U S A.* 97:9482-9486.
- Romberg, L., D. W. Pierce, R. D. Vale. 1998. Role of the kinesin neck region in processive microtubule-based motility. *J Cell Biol.* 140:1407-1416.
- Romberg, L., R. D. Vale. 1993. Chemomechanical cycle of kinesin differs from that of myosin. *Nature.* 361:168-170.
- Rosenfeld, S. S., P. M. Fordyce, G. M. Jefferson, P. H. King, S. M. Block. 2003. Stepping and stretching. How kinesin uses internal strain to walk processively. *J Biol Chem.* 278:18550-18556.
- Rosenfeld, S. S., G. M. Jefferson, P. H. King. 2001. ATP reorients the neck linker of kinesin in two sequential steps. *J Biol Chem.* 276:40167-40174.
- Rosenfeld, S. S., J. Xing, G. M. Jefferson, H. C. Cheung, P. H. King. 2002. Measuring kinesin's first step. *J Biol Chem.* 277:36731-36739.
- Schafer, F., D. Deluca, U. Majdic, J. Kirchner, M. Schliwa, L. Moroder, G. Woehlke. 2003. A conserved tyrosine in the neck of a fungal kinesin regulates the catalytic motor core. *Embo J.* 22:450-458.
- Schief, W. R., J. Howard. 2001. Conformational changes during kinesin motility. *Curr Opin Cell Biol.* 13:19-28.
- Schnapp, B. J., T. S. Reese. 1989. Dynein is the motor for retrograde axonal transport of organelles. *Proc Natl Acad Sci U S A.* 86:1548-1552.
- Schnitzer, M. J., S. M. Block. 1997. Kinesin hydrolyses one ATP per 8-nm step. *Nature.* 388:386-390.
- Schoch, C. L., J. R. Aist, O. C. Yoder, B. Gillian Turgeon. 2003. A complete inventory of fungal kinesins in representative filamentous ascomycetes. *Fungal Genet Biol.* 39:1-15.
- Scholey, J. M., J. Heuser, J. T. Yang, L. S. Goldstein. 1989. Identification of globular mechanochemical heads of kinesin. *Nature.* 338:355-357.

- Seiler, S., J. Kirchner, C. Horn, A. Kallipolitou, G. Woehlke, M. Schliwa. 2000. Cargo binding and regulatory sites in the tail of fungal conventional kinesin. *Nat Cell Biol.* 2:333-338.
- Sellers, J. R. 2000. Myosins: a diverse superfamily. *Biochim Biophys Acta.* 1496:3-22.
- Sindelar, C. V., M. J. Budny, S. Rice, N. Naber, R. Fletterick, R. Cooke. 2002. Two conformations in the human kinesin power stroke defined by X-ray crystallography and EPR spectroscopy. *Nat Struct Biol.* 9:844-848.
- Song, Y. H., E. Mandelkow. 1994. Paracrystalline structure of the stalk domain of the microtubule motor protein kinesin. *J Struct Biol.* 112:93-102.
- Song, Y. H., A. Marx, J. Muller, G. Woehlke, M. Schliwa, A. Krebs, A. Hoenger, E. Mandelkow. 2001. Structure of a fast kinesin: implications for ATPase mechanism and interactions with microtubules. *Embo J.* 20:6213-6225.
- Steinberg, G., M. Schliwa. 1995. The *Neurospora* organelle motor: a distant relative of conventional kinesin with unconventional properties. *Mol Biol Cell.* 6:1605-1618.
- Steinberg, G., M. Schliwa. 1996. Characterization of the biophysical and motility properties of kinesin from the fungus *Neurospora crassa*. *J Biol Chem.* 271:7516-7521.
- Svoboda, K., C. F. Schmidt, B. J. Schnapp, S. M. Block. 1993. Direct observation of kinesin stepping by optical trapping interferometry. *Nature.* 365:721-727.
- Thorn, K. S., J. A. Ubersax, R. D. Vale. 2000. Engineering the processive run length of the kinesin motor. *J Cell Biol.* 151:1093-1100.
- Tomishige, M., D. R. Klopfenstein, R. D. Vale. 2002. Conversion of Unc104/KIF1A kinesin into a processive motor after dimerization. *Science.* 297:2263-2267.
- Tomishige, M., R. D. Vale. 2000. Controlling kinesin by reversible disulfide cross-linking. Identifying the motility-producing conformational change. *J Cell Biol.* 151:1081-1092.
- Tripet, B., R. D. Vale, R. S. Hodges. 1997. Demonstration of coiled-coil interactions within the kinesin neck region using synthetic peptides. Implications for motor activity. *J Biol Chem.* 272:8946-8956.
- Tucker, C., L. S. Goldstein. 1997. Probing the kinesin-microtubule interaction. *J Biol Chem.* 272:9481-9488.
- Vale, R. 2001. Guidebook to Cytoskeletal and Motor Proteins: Oxford University Press.
- Vale, R. D. 2003. The molecular motor toolbox for intracellular transport. *Cell.* 112:467-480.
- Vale, R. D., T. Funatsu, D. W. Pierce, L. Romberg, Y. Harada, T. Yanagida. 1996. Direct observation of single kinesin molecules moving along microtubules. *Nature.* 380:451-453.
- Vale, R. D., R. A. Milligan. 2000. The way things move: looking under the hood of molecular motor proteins. *Science.* 288:88-95.
- Vale, R. D., T. S. Reese, M. P. Sheetz. 1985. Identification of a novel force-generating protein, kinesin, involved in microtubule-based motility. *Cell.* 42:39-50.
- van den Ent, F., A. Lockhart, J. Kendrick-Jones, J. Lowe. 1999. Crystal structure of the N-terminal domain of MukB: a protein involved in chromosome partitioning. *Structure Fold Des.* 7:1181-1187.
- Venerables, Ripley. 1997. Modern applied S plus: Springer-Verlag, New York.
- Verhey, K. J., D. L. Lizotte, T. Abramson, L. Barenboim, B. J. Schnapp, T. A. Rapoport. 1998. Light chain-dependent regulation of Kinesin's interaction with microtubules. *J Cell Biol.* 143:1053-1066.
- Verhey, K. J., D. Meyer, R. Deehan, J. Blenis, B. J. Schnapp, T. A. Rapoport, B. Margolis. 2001. Cargo of kinesin identified as JIP scaffolding proteins and associated signaling molecules. *J Cell Biol.* 152:959-970.
- Verhey, K. J., T. A. Rapoport. 2001. Kinesin carries the signal. *Trends Biochem Sci.* 26:545-550.
- Visscher, K., M. J. Schnitzer, S. M. Block. 1999. Single kinesin molecules studied with a molecular force clamp. *Nature.* 400:184-189.
- Wade, R. H., F. Kozielski. 2000. Structural links to kinesin directionality and movement. *Nat Struct Biol.* 7:456-460.
- Wang, Z., M. P. Sheetz. 2000. The C-terminus of tubulin increases cytoplasmic dynein and kinesin processivity. *Biophys J.* 78:1955-1964.
- Wells, A. L., A. W. Lin, L. Q. Chen, D. Safer, S. M. Cain, T. Hasson, B. O. Carragher, R. A. Milligan, H. L. Sweeney. 1999. Myosin VI is an actin-based motor that moves backwards. *Nature.* 401:505-508.
- Wendt, T., A. Karabay, A. Krebs, H. Gross, R. Walker, A. Hoenger. 2003. A Structural Analysis of the Interaction between ncd Tail and Tubulin Protofilaments. *J Mol Biol.* 333:541-552.
- Woehlke, G., A. K. Ruby, C. L. Hart, B. Ly, N. Hom-Booher, R. D. Vale. 1997. Microtubule interaction site of the kinesin motor. *Cell.* 90:207-216.
- Woehlke, G., M. Schliwa. 2000. Directional motility of kinesin motor proteins. *Biochim Biophys Acta.* 1496:117-127.
- Yang, J. T., R. A. Laymon, L. S. Goldstein. 1989. A three-domain structure of kinesin heavy chain revealed by DNA sequence and microtubule binding analyses. *Cell.* 56:879-889.
- Yildiz, A., J. N. Forkey, S. A. McKinney, T. Ha, Y. E. Goldman, P. R. Selvin. 2003. Myosin V walks hand-over-hand: single fluorophore imaging with 1.5-nm localization. *Science.* 300:2061-2065.

Young, E. C., H. K. Mahtani, J. Gelles. 1998. One-headed kinesin derivatives move by a nonprocessive, low-duty ratio mechanism unlike that of two-headed kinesin. *Biochemistry*. 37:3467-3479.

Acknowledgements

First of all I would like to thank Prof. Dr. Dietmar Manstein for supervising my thesis from the distance; at times it was rather hard to localize me at all.

I am indebted for Prof-Dr. Manfred Schliwa's continuing support, not only while performing experiments in his laboratory, but also during difficult times of decision making.

I have to thank Prof. Dr. Bernhard Brenner for the possibility to work in his lab for the Diploma thesis and the first two years of this thesis.

Special thanks go to Prof. Dr. Edgar Meyhofer, who – apart from providing continuous scientific instruction - did everything possible to make moving from Germany to the United States smooth and comfortable. (...including the purchase of a Swiss Espresso machine!)

I would like to thank Dr. Günther Wöhlke for the year-long fruitful collaboration and the joy of being named the “Stefan La ... “ by his adorable daughter Lisa. I still have hope the swing is at least sometimes available for little Lennart.

I would like to thank the Imaging Core of the University of Michigan for allowing me to use their imaging software to construct kymographs.

During the last years I enjoyed the company of many wonderful colleagues in different laboratories: Dr. Christine Ruff shared many 5-minute-thoughts and -cigarettes with me on the bench outside the lab in Hannover! The members of Prof. Schliwa's lab in Munich for the friendly welcome and many tumultuous lunch breaks! Above all, I would like to thank Athina Kallipolitou, Kathrin Hahlen (“Ferchtich!”) and Friederike Schäfer, aka “Frieder Ike”, for help with protein-purifications and for the clones they provided. Dr. Lucia Driller for letting me know, that once you fall off the horse, you've got to get on immediately again! Christian Horn und Andreas Schneider for invaluable PC-support. Andrea Hestermann for sharing breakfast and impressions on books. My colleagues in Ann Arbor, Ming-Tse Kao and Harsha Nanjundaswamy, in Ann Arbor provided many interesting topics of conversation.

But above all I would like to thank my mother, Lore Lakämper, for supporting all my adventures and keeping the family together after my fathers death in 1988, and my partner Ludwig Gerns for his love and for bearing to be apart for such a long time! Without them and the support of the whole family this thesis would not have been possible. Thank you!